2004-04-19

Ultrasonic Beam Propagation in Turbulent Flow

Francis J. Weber
Worcester Polytechnic Institute

Ultrasonic Beam Propagation in Turbulent Flow

by

Francis J. Weber, Jr.

A Dissertation

Submitted to the Faculty

of the

WORCESTER POLYTECHNIC INSTITUTE

in Partial Fulfillment of the Requirements for the

Degree of Doctor of Philosophy
in
Mechanical Engineering

December 16, 2003

APPROVED:

_____
Dr. William W. Durgin, Major Advisor

_____
Dr. Hamid Johari, Co-Advisor

_____
Dr. Gretar Tryggvason, Department Chair

_____
Dr. Suzanne Weekes

_____
Dr. Julie Mullen

_____
Dr. John Sullivan, Graduate Committee Rep

ABSTRACT

This study was conducted to examine the effect of flow turbulence on sound waves propagating across a velocity field. The resulting information can be used to determine the potential for increasing the accuracy of an ultrasonic flowmeter, and understand the data scatter typically seen when using an ultrasonic flowmeter. A modification of the Ray Trace Method was employed which enabled the use of multiple rays in a very fine grid through a flow field. This technique allowed for the computation of the statistical variation of the propagation times for sound pulses traversing a flow field. The statistical variation was studied using two flow fields: 1) a uniform flow field with a superimposed vortex street and 2) an experimentally measured channel flow. The uniform flow field with a superimposed vortex street allowed for the examination of the effects of a large-scale flow structure on sound wave propagation, and for the verification of the analysis technique. Next by using the measured turbulent channel flow, as an example, the statistical variation of sound pulse propagation time was computed for flow likely to be encountered in actual flow measurement situations. Analysis was also conducted to determine the maximum allowable repetition rate of measurements with regard to the optimal time of flight measurements.

Both the propagation time of a sound pulse moving across a uniform flow field with superimposed vortex street, and the resultant computed flow were observed to vary at the same frequency of the vortex street. Further, the magnitude of the variations was proportional with the strength of the individual vortices in the vortex street. A sound pulse propagating back and forth across a measured turbulent channel flow, afforded individual time difference variation from the mean propagation time of up to 5%. It was shown that a minimum variation occurred when the sound pulses were transmitted at a 75 degree angle to the flow axis. It was also determined that the average speed of sound in a flow field affected the final flow measurements by decreasing the measured delta time difference between the upstream and downstream propagating sound waves, and therefore the measured flow. The width of the sound path also contributed to decreasing the variation of the individual measurements by integrating over a larger sound path. These findings suggest that turbulence in a flow field affects ultrasonic flowmeter measurements by creating differences in the propagation times of individual sound pulses. Thus, turbulence and large-scale flow structures can result in variations in volumetric flow rate determination made by an ultrasonic flowmeter system.

ACKNOWLEDGMENT

I would like to take this opportunity to thank numerous people and organizations without whose support this work would not have been possible. Many thanks go to Dr. Bill Durgin who allowed me the opportunity to study and pushed me to achieve my goals. Also his staff Gail Hayes and Nancy Hickman who juggled schedules to arrange the many meetings needed over the years. Thanks go to Barbara Edilberti and the staff in the Mechanical Engineering Department who provide the necessary support and the occasional ear. Many thanks go to the Alden Trust, which financially supported my quest for learning.

Many friends provided sounding boards for ideas, in particular Bob Till, who listened to my ideas and allowed me to develop them into useable thoughts and provide much friendship along the way.

Of course none of this work would have been possible without the support of my family. My mother, Marilyn, and father, Frank Sr, gave me as much support as a mom and dad can while I was growing up. They taught me that education was the backbone of a full life, and were always there to encourage me to seek my dreams. Finally, my biggest thank you goes to my wife Tracy and children, Emily and Daniel, whose unquestioning love and support made a difficult journey as painless and enjoyable as possible.

TABLE OF CONTENTS

LIST OF FIGURES

LIST OF TABLES

NOMENCLATURE

A	Wave Amplitude
A’	Spatial Derivative of Wave Amplitude
D	Diameter of Pipe
a	Streamwise distance between individual vortices
c	Speed of Sound
$\bar{c}$	Average Speed of Sound
c_o	Reference sound velocity
f	frequency of vortex street
h	Distance from streamwise axis to individual vortices
$\hat{i}$	Unit vector in ‘x’direction
$\hat{j}$	Unit vector in ‘y’direction
L	Length of Sound Propagation Path
n	number of vortices from reference point
$\hat{\mathbf{n}}$	unit vector
n’	spatial derivative of index of reflection
N	Number of counts
P	Sound Path
$\vec{\mathbf{P}}$	Vector Sound Path
$\vec{r}$	unit vector in direction of sound ray
Re	Reynolds Number
s	streamwise distance from reference point to vortex core
$\vec{s}$	arbitrary unit vector
S	$\prod_i (x - x_i)$ Product taken over all subscripts i
S’	Derivative of S
T	Total time
T_{avg}	Average Time
t	Time
t’	Time fluctuation
u	Instaneous Flow Velocity in 'x' or Streamwise Direction
v	Instaneous Flow Velocity in 'y' or Spanwise Direction
w	Instaneous Flow Velocity in 'z' or Spanwise Direction
U	Velocity
U	Velocity in 'x' or Streamwise Direction
V	Velocity in 'y' or Spanwise Direction
W	Velocity in 'z' or Spanwise Direction
u'	Turbulent Velocity in 'x' or Streamwise Direction

v'	Turbulent Velocity in 'y' or Spanwise Direction
w'	Turbulent Velocity in 'z' or Spanwise Direction
$\bar{\mathbf{u}}$	Spatial Average Velocity in 'x' or Streamwise Direction
$\bar{\mathbf{v}}$	Spatial Average Velocity in 'y' or Spanwise Direction
$\bar{\mathbf{w}}$	Spatial Average Velocity in 'z' or Spanwise Direction
$\vec{v}$	Velocity vector of moving fluid
y	distance from streamwise axis to reference point
X	Axial Length between Transducers
α	angle of attack
β	Beam Width
Δ	Delta
Γ	Vortex Strength
λ_o	wavelength
η	Smallest Eddy Size
ν	Kinematic Viscosity
ρ	Fluid Density
τ_w	Allowable Transmission Delay
ϕ	Angle Between Local Wave Normal Vector and Wave; Wave front location $\equiv c_o t$
θ	Angle Between Sound Path and Mean Flow Path Axis
ψ	Angle Between Ray Vector and Wave
φ	wave front position
∇	Gradient
μ	Refractive index of the fluid
ϑ	Instantaneous Velocities
Υ	population mean; or overall mean
χ	individual measurement.
$^\circ$	Degree

Subscripts

1	Location 1 - Send Transducer
2	Location 2 - Receive Transducer
abs	absolute

descriptive markings

bold	vector
$\hat{}$	unit vector
$\vec{}$	vector
$\bar{}$	Spatial Average

1 Introduction

1.1 Motivation

Accurate measurement of fluid flow rate in a conduit system is critical in process control and custody transfer of fluids of high economic value. In pharmaceutical manufacturing and petrochemical processing, multiple chemicals must be mixed in precise proportions to guarantee quality and maintain stoichiometry. In custody transfer, accurate measurement becomes an economic necessity. For example, oil and gas are bought by pipeline companies and sold after transport. Measurement inaccuracy has a huge economic cost because of the large amount of product transferred.

Flow in closed conduit pipelines is measured by one of several basic methods, local velocity, volume, and mass flow[73]. While mass flow is typically more desirable for many applications, volume flow is easier to measure directly. In a volume flow measurement, the fluid volume passing through a cross-section per unit time is determined, whereas the mass flowrate is the fluid mass per unit time. Mass flowrate accounts for the changes in density of a fluid with temperature and is important in controlling the result of chemical reactions such as thrust from a jet engine. Volumetric flowmeters can be used to determine the mass flow rate if a separate density determination is available[73]. Although mass flow is typically the desired flow quantity, the usual flow measurement is volumetric. If a mass flow measurement is made using a combination of volumetric flowrate and density, then the number of uncertainties is increased.

There are many types of flowmeters each with its own strengths and weaknesses. Direct mass flow is typically measured using a calibrated spring device or a vibrating tube device. Direct mass flow systems typically involve moving parts, which are subject to wear and must be periodically serviced. In contrast, volumetric flowmeters, which predominate the market, usually have no moving parts and thus require less service over the device's lifetime. Examples of volumetric flowmeters include pressure drop devices such as orifice plates and venturi-meters. Additional volumetric meters include rotameters, anemometers, and acoustic meters. The acoustic meter, which is a comparatively new technology, uses the principles of sound propagation to measure average velocity within a volume. Typically, acoustic meters have no protrusions into the flow field and, in fact, can be installed on the outside diameter of a pipe. The acoustic meter is ideal for use in a pipeline when pressure losses cannot be tolerated, shear stresses would damage the fluid, or high accuracy is required.

Acoustic flowmeters measure local flow velocities,[73] and operate by sending a pulse of sound diagonally across the flow in a pipeline.[32] The average fluid velocity in the pipeline, along that path, either speeds up or slows down the sound pulse depending on whether the pulse was transmitted with the flow or against the flow. The amount of increase or decrease of the sound pulse propagation time across the flow field is proportional to the average velocity of the fluid along the sound path. So, if the sound pulse is launched in a single direction, and the crossing time is compared to a no velocity condition, the average velocity along the path can be found. However, finding the

crossing time in a no flow condition is not usually practical. By launching the sound waves in two opposing directions across a flow field and comparing the time difference between the counter-propagating waves, otherwise known as the Δt, the integrated velocity along the path can be found directly from the propagation times, the Δt's, and path geometry.[73] A spatial averaging scheme or quadrature integration is typically used to compute the average velocity of the flow in the pipeline using the average along one or more paths.

Ultrasonic flowmeter technology was brought into commercial applications in the late 1960's and 1970's.[24,31] At the time, it was understood that the mean velocity profile was an important variable with regard to the accuracy of the flow measurement. The mean velocity profile varies from one flow system to another, making prediction of accuracy difficult from system to system. In order to attempt to increase accuracy of ultrasonic flowmeter systems from application to application and in particular those with disturbed velocity profile conditions, various multi-path systems and quadrature integration techniques have been the focus of research and development.[9] Additionally, the electronic control portions of the ultrasonic flowmeters have received a great deal of study over the past 20 years or so. The thrust of this work has been to produce stable timing intervals to allow determination of the Δt measurements on the order of a nanosecond.

Ultrasonic flowmeter accuracies have remained unchanged at approximately 1%[31,32,50] with claims of accuracies in the range of 0.25% to 0.1%[9] for many years. This is despite

dramatic improvements in the stability and computational power of electronics over the past 10 to 15 years mainly driven by significant advances in semi-conductor circuitry. To achieve claimed accuracies, many commercial ultrasonic flowmeters employ some degree of averaging methodology in concert with some type of quadrature integration techniques, as well as system geometry and sound pulse transmission strategies. While these various methods may work for specific flow systems, it is not usual for ultrasonic flowmeter system uncertainties to exceed the expected uncertainty. When individual Δt realizations are examined, individual variations can be as much as 5% [38] from the mean value. It is clear that despite all the research into ultrasonic flowmeter electronics, geometric configurations, and data manipulations, there exists some underlying phenomenon that is not properly understood or accounted for in these types of flowmeters which is causing unwanted flow velocity variations from the mean.

1.2 Outline of Work

The goal of this research is to investigate the effect of flow turbulence on ultrasonic wave propagation. It is known that the non-ideal flows lead to significant errors in flowmeter readings. The present research is intended to identify the dependence of the propagation time of a sound pulse on turbulence, and to improve performance of ultrasonic flowmeters in attaining accurate flow measurements.

A brief overview of the dissertation is presented here. In Chapter 2, a detailed review is given on the past research in the area of acoustic flowmeters development. Special attention is paid to the mathematical modeling of ultrasonic flowmeters. Accuracy issues are discussed and prospects for improving ultrasonic flowmeters are evaluated. An overview of the work presented to date is followed by the objectives and approach stated for the present work.

To study the effect of turbulence on sound wave propagation, the ray trace method was chosen as a numerical approach. Chapter 4 contains a review of the literature on recent developments in applications of the ray trace method. Mathematical formulation of the ray trace method along with the application to the particular problem of waves propagating in an inhomogeneous random media is presented.

In Chapter 5, a mathematical formulation of flowmeter equations that accounts for turbulent fluctuations is introduced. In order to demonstrate the effect of turbulent flow qualitatively, the output data of ultrasonic flowmeters collected from different experimental setups such as turbulent channel flow,[38,43] circulation flow about a stationary airfoil[8], flow around a closed circuit in an empty wind tunnel[8] are plotted for demonstration purposes.

In Chapter 6, the assumptions that are customarily made for this class of problems being studied are discussed. The magnitude of the effects of these assumptions on ultrasonic flowmeter output is shown.

Chapter 7 is devoted to the discussion of the methodology for which the research is based. A new, Modified Ray Trace Method was developed to numerically model the propagation of acoustic waves through a turbulent fluid. The numerical code employed two flow fields: vortex street in a uniform flow field, and experimentally obtained (PIV) data structure of a turbulent flow in a channel. Details of these two model flows are also presented in Chapter 7. Additionally, the verification of the Modified Ray Trace Method is discussed in this chapter.

Results obtained using the Modified Ray Trace Method on a uniform flow field with superimposed vortex street, are presented in Chapter 8. The problem of a pair of sound waves propagating across a uniform flow field with a superimposed vortex street was first solved numerically by using a piece-wise numerical integration method, the results of this calculation are presented and used as a benchmark for validation of the Modified Ray Trace Method. The Modified Ray Trace Method was then used to study the effect of a large scale flow structure, such as a vortex street, on the propagation of an acoustical wave in terms of travel time difference, Δt, as a function of sound speed, sound beam width, vortex strength, and a uniform flow angle.

Chapter 9 contains the results from the validated Modified Ray Trace Method applied to the experimental PIV velocity data. The effects of the turbulence were studied in terms of propagation time differences as a function of sound speed, sound beam width, and the angle between the uniform flow and the sound path.

1.3 Hypothesis

It is hypothesized that the variation in the individual transit times of ultrasonic pulses can be caused by the variations of the mean flow velocity, thereby causing flowmeter inaccuracies. It is further hypothesized that the variations in individual transit times of ultrasonic pulses are caused by naturally occurring turbulence in a flow system. This study tested these hypotheses first by using a modification of the Ray Trace Method to study how a sound pulse propagates through large-scale periodic flow disturbances such as a vortex street. From this study, the variation in propagation time of the sound pulse could be computed and then compared to piece-wise numerical integration solutions. After determining the effect of a vortex street on the propagation time of a sound pulse, a similar method of study was used to calculate the statistical propagation times of ultrasonic pulses through a measured turbulent channel flow. In both studies, four quantities of the sound pulse or flow field were varied: the angle of the sound to the field, the temperature of the flow, and therefore, the speed of sound, the sound beam width, and in the uniform flow with superimposed vortex street the angle of the flow was varied by several degrees, and the strength of the vortices in the vortex street was varied.

2 Review of Ultrasonic Flow Metering

2.1 Ultrasonic Flowmeters - Historical Perspective

Sound has been used as a metrology tool for hundreds of years. The understanding of the relationship between thunder and lightning allowed people to determine the approximate distance of a thunderstorm as well as the direction of approach. In the 1940's, the United States Navy developed sonar capability to passively listen for and actively find and follow submarines and ships. By listening for sounds emanating from vessels, the Navy could determine the location of ships. Resultant from military sonar research, it was discovered that sound can also be used to determine the average flow within a flow field. [24]

Acoustic or ultrasonic flowmeter development began in the 1950's as a joint venture between government and private industries.[24] The effort was directed towards the accurate measurement of large volumes of water flowing through channels and dams. The Department of Water Resources, the U.S. Geological Survey, and the U.S. Army Corps of Engineers along with Raytheon Manufacturing Company began to develop an acoustic velocity flowmeter in 1957. [24] The general design and operation of these early acoustic flowmeters was similar to present designs, in that sound was sent through a flow field and the propagation time was measured. In the mid-1960's, Westinghouse Electric Corporation began designing acoustic flowmeters for placement in canals and a pipeline along the California Aqueduct.[24,9] Westinghouse's contribution to flowmeter design was the replacement of the acoustic hydrophones previously used in acoustic flowmeters with

crystals embedded in a transducer assembly. These crystals generated very high frequency or ultrasonic waves versus lower frequency sonic sound waves so that system accuracy was increased.[31,32,33] Higher frequencies allowed for better timing accuracies since these early devices utilized zero crossing detection of received pulses.

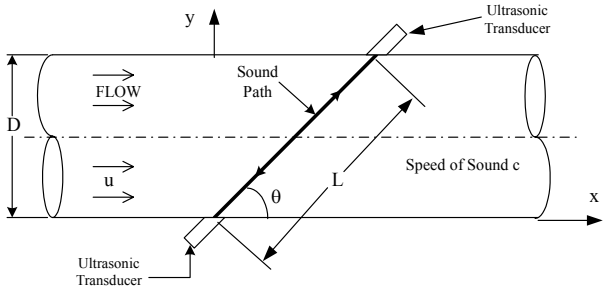

Figure 2-1 Schematic of Ultrasonic Setup

In the 1960's and 1970's, development work continued on ultrasonic flowmeter systems primarily for application to flow in large conduits and open channels.[24] These flowmeters were based upon the same acoustic techniques developed in the 1950's. Figure 2-1 shows a schematic of a typical simple ultrasonic flowmeter setup. That is two ultrasonic transducers are placed facing each other on opposite sides of a pipe or channel, at a given angle, θ, to the axis of the flow. [3] The straight line path between the sensors is known as the sound path. The angle of the sound path to the flow axis is generally set between 30° and 65° depending on the available spacing and accuracy requirements. [3,31,32,33] By launching a sound wave packet similar in shape to Figure 2-2,[4] and measuring the time lapse for zero crossing of the acoustic signal, typically the first zero crossing, between launch and receive, an integrated flow velocity can be determined

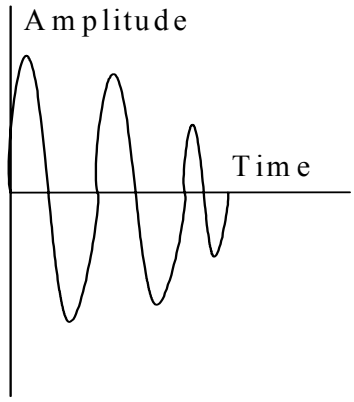

Figure 2-2 Sketch of a Typical Sound Wave Pulse

along the sound path. Many of the systems for these large conduits and open channels use a single path setup, in which the sound path is manually or semi-automatically moved around in an attempt to determine an average flow profile.[31]

Sound can be used to measure general fluid motion in other circumstances. For instance, in a study performed by Munk in 1986, a method to determine ocean currents and temperatures via a sonic method was developed.[44] In this work, Munk used data from several experiments in which very low frequency sound was sent across ocean basins. From these experiments, it was shown that the average temperature and velocity profiles in the ocean could be determined by measuring the time of travel in the forward and reverse directions. This arrangement may be considered a very large scale application of a sonic flowmeter device, where the largest scale of the turbulence is on the order of the size of an ocean basin.

2.2 Acoustic Properties in Turbulence - Historic Perspective

Sound propagation through a random media is an important and much studied subject. It is understood that turbulence affects sound propagation through fluids, and, has been discovered, the effect must be quantified to determine the behavior of ultrasonic flowmeters. One strategy of investigation is to follow the sound path through a turbulent flow field. Rayleigh, who developed the generalized Ray Trace Method for following a sound wave in a fluid was among the first people to study the effect of turbulence on

sound propagation.[53] In the 1950's, a series of researchers worked on the question of sound propagation with relation to sonar devices for locating objects in or on the oceans. Kornhauser, applied the Ray Trace Method in a more general sense to allow for moving fluids and inhomogeneous media.[23] Mintzer studied the refraction and reflection of sound waves moving through an inhomogeneous medium in 1953. [39,40,41] These researchers showed how sound propagated through fluids on a large scale such as in the ocean or the atmosphere.

Lipkens and Blackstock performed experiments involving sound propagation through turbulent flow fields.[29] The experimental setup consisted of a spark generator, a receiver, and a timing device to measure the elapsed time of travel of the sound from the spark generator to the receiver. Two basic sets of tests were performed in these experiments. The first set of tests consisted of sending sound waves through a turbulent field of constant size and varying intensity. The second set of tests consisted of sending the sound across a turbulent field of constant intensity but varying distances. The sound parameters measured in Lipkens and Blackstock's[29] work were pressure rise times and peak pressure distributions. The authors concluded that both turbulent intensity and propagation distance affected sound passage through a turbulent field.

Schmit and Tilman [59] performed a series of experiments in which the phase angle of sound waves were examined for an ultrasonic wave traveling through a turbulent wake. Based on the phase shift of the sound wave, they were successfully able to analyze the magnitude

of turbulent motion in the direction of the sound wave propagation, as well as circulation of vortices in the wake. They were able to provide further conclusions as to the general structure of the turbulent flow.[59]

2.3 Ultrasonic Theory of Operation

There are several basic ultrasonic flowmeter applications in use, including the time of flight flowmeter[73], the Doppler shift flowmeter[73], and the correlation flowmeter.[12,72] Doppler shift ultrasonic flowmeters send out a signal, and capture the Doppler shift of the signal reflected by particles in the flow. In this method, the ultrasonic signals reflected back to the receiver from particles in the flow are shifted slightly in frequency, which is proportional to the particle velocity. The correlation flowmeter uses a device to perturb the flow and then attempts to correlate the disturbed travel time signal to the average velocity in the flow.

In the time of flight flowmeter technique, an ultrasonic pulse is launched from a first transducer and the elapsed time required for the pulse to arrive at a second transducer placed upstream or downstream from the transmitter is measured. In most cases, the transmitter and the receiver then change roles and the pulse is sent in the opposite direction. The difference between the upstream and downstream propagation time, Δt, can be directly related to an integrated mean fluid velocity as will be seen in a later section. To determine average velocity in a flow, several assumptions are required, such as a constant path length, L, a constant speed of sound, c, and a mean velocity profile, $u = f(y)$,

for a coordinate system as shown in Figure 2-1. Finally, to determine the mean flowrate in a system from this integrated mean velocity, a velocity profile must be assumed for the fluid in the system, from which the system flow can be inferred.

2.3.1 Basis of Time of Flight Flowmeter Operation in Literature

If the time required for ultrasonic waves to propagate between two transducers in a flow condition is compared with the time required in a second flow condition, the change in the integrated flowrate between the conditions is detected. If one of these conditions is a no flow condition, then the average flowrate in the other condition can be determined. This ability to determine the average flow in a system results from the fact that sound is carried along with the fluid in which it is propagating. Thus, a sound wave propagating with the flow will have an absolute velocity of

$$U_{abs} = \bar{c} + \bar{u}, \qquad \textbf{(1)}$$

where $\bar{c}$ is the local average speed of sound and $\bar{u}$ is the spatial average velocity of the flow along the sound path. While for a sound wave propagating against a flow, the absolute speed is

$$U_{abs} = \bar{c} - \bar{u}; \qquad \textbf{(2)}$$

therefore, the wave velocity described in Equation 2 will be slower than the velocity described by Equation 1, as viewed from a stationary reference.

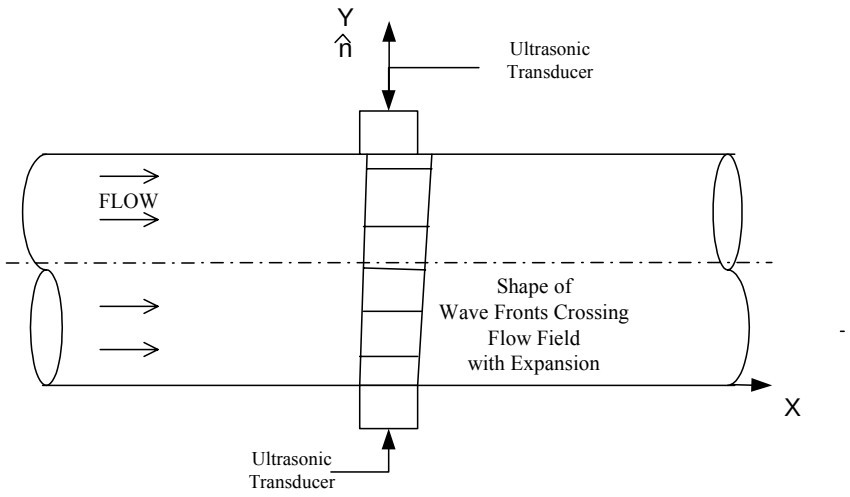

Figure 2-3 Sketch of a Wave Front Crossing a Uniform Velocity Field; Note as the Wave Front Crosses the Field, it is Convected Downstream by the Velocity and Spreads Slightly(not to scale)

Typically, the sound waves used to measure mean flowrate in a system are in the ultrasonic range because the high frequency and short wavelengths facilitate accurate measurement of the transit time for the sound pulse across the flow.[31,32,33] The ultrasonic sound waves are generated using piezoelectric transducers, which can act as both transmitter and receiver. The sound generated by these transducers is similar to a piano key being struck with the damper on, that is a short heavily damped intense pulse is generated. The transducers used in flow-metering devices are designed to produce a relatively flat wave front, which propagates in a directional beam through the fluid and spreads at a half angle of approximately 3°, [8] as shown in Figure 2-3. As the beam propagates across a velocity field, it interacts with the local velocities and can be deflected from its original path, sped up, or slowed down by these interactions.

2.3.2 Time Required for Sound Wave to Propagate Across a Flow Field

2.3.2.1 Perpendicular Sound Path

Figure 2-4 shows a geometry in which sound is sent directly across a pipe in the 'y' direction, this is a special circumstance and is shown here for example. If there is a uniform non-turbulent flow along the axial, or 'x', direction of the pipe, it may be assumed that the velocity of fluid would have no effect on the speed of propagation in the 'y' direction. The only effect on the sound wave is in the 'x' direction, and is the bending of the sound wave downstream in the direction of the flow; which, in several references, is ignored.[24, 31,32,33] Therefore, if the speed of sound is assumed to be uniform across the flow, it is possible to compute the time required for the sound wave to cross the flow shown in Figure 2-4 by using the relation:

$$dt = \left(\frac{d\vec{P}}{\bar{c}} \right) \cdot \hat{\mathbf{n}}, \qquad \textbf{(3)}$$

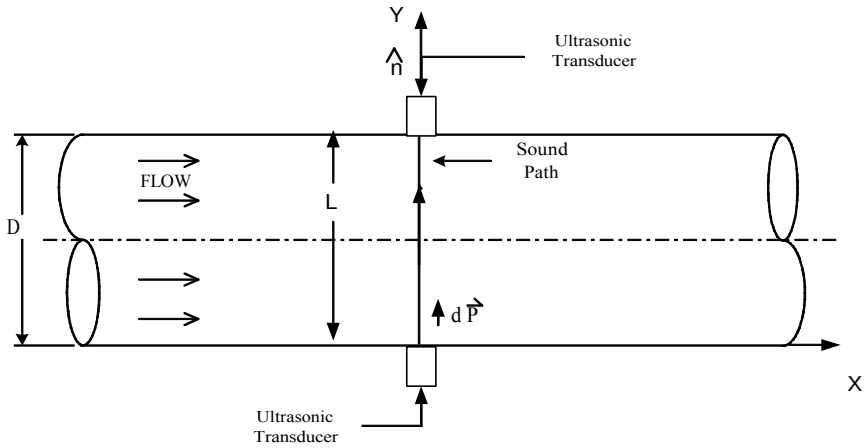

Figure 2-4 Geometry for Sound Waves Launched Perpendicular to Mean Flow

where: $\vec{P}$ is the vector along the sound path, and t is the time of propagation. Also, $\bar{c} = \frac{1}{L}\int_0^L c\,dx$ is the spatial average speed of sound along the sound path. Since $\hat{\mathbf{n}}$ is parallel to the sound path, integrating over time and the path length, L yields:

$$t = \int_0^L \frac{dP}{\bar{c}} \tag{4}$$

where P is now just the path, finally arriving at

$$t = \frac{L}{\bar{c}} \quad \Rightarrow \quad t = \frac{D}{\bar{c}}, \tag{5}$$

because the sound path is perpendicular to the flow.

2.3.2.2 Angled Sound Path

While it is easy to calculate the time required to cross a flow field perpendicular to the axis, it is slightly more difficult to calculate the time to cross at an angle. The reason is that velocity of the fluid along the sound path must be accounted for. In Figure 2-5, the sound wave is depicted as being introduced into the flow field at an angle, θ. The time to cross the pipe to the receiver is then[14,73]

$$dt = \left(\frac{d\vec{\mathbf{P}} \cdot \hat{\mathbf{n}}}{c + \vec{\mathbf{V}} \cdot \hat{\mathbf{n}}} \right), \tag{6}$$

where $\vec{v}$ is the total velocity vector. By integrating over time and path length, and using Figure 2-5 where the flow is assumed to be parallel to the x axis so there is no transverse velocity in the y direction, or $v = 0$, one arrives at

$$t = \int_o^L \left(\frac{dP}{c + u\cos\theta} \right), \tag{7}$$

where u is the velocity magnitude in the x direction. Again assuming $u = \bar{u}$, and $c = \bar{c}$, to be constants in both time and space, and integration of Equation 7 yields[14,73]

$$t = \frac{L}{\bar{c} + \bar{u}\cos\theta}, \tag{8}$$

where: $\bar{u} = \frac{1}{L}\int_0^L u\,dx$ and $\bar{c} = \frac{1}{L}\int_0^L c\,dx$

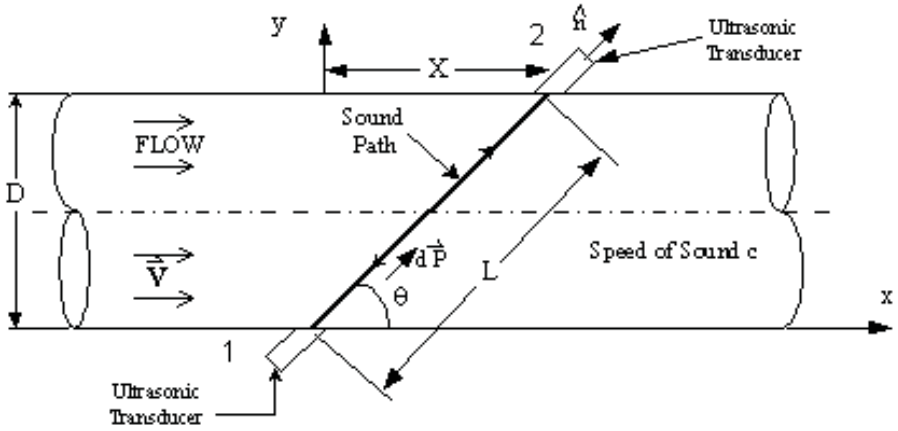

Figure 2-5 Typical Geometry for an Ultrasonic Flowmeter Angled to the Flow

The spatially averaged fluid velocity was assumed to be constant along the sound path to perform the integration. This assumption and its effects will be discussed at length later in this work.

To arrive at Equation 8, two basic assumptions are made in literature. The first is that the flow is uniform. The second assumption is that the speed of sound is constant or has an average value throughout the fluid. These assumptions average the flow both temporally, and spatially, because the velocity is computed over a constant time and averaged over the path length, L. Therefore, Equation 8, extensively used as a flowmeter equation is best used for ideal flow conditions. However, the presence of secondary flows is known to cause significant metering inaccuracies.[74] So the identification of the effects introduced by non-ideal flows is crucial for accurate flow measurements.

2.3.3 Computation of Velocity by Ultrasonic Flowmeters in Literature

Using Equation 8 for upstream and downstream propagating pulses yields the respective time for the sound pulse to propagate in each direction. For the downstream time (from location 1 to 2), t_{12}, is:[14,73]

$$t_{12} = \frac{L}{\bar{c} + \bar{u}\cos\theta}, \tag{9}$$

and upstream(from location 2 to 1) takes time t_{21}:[14,73]

$$t_{21} = \frac{L}{\bar{c} - \bar{u}\cos\theta}. \quad \textbf{(10)}$$

Note the inherent assumption of a constant sound path length, L. Equations 9 and 10 can be used to evaluate explicitly the expression for the average velocity $\bar{u}$.

There are several methods for computing velocity once the time for an acoustic wave to propagate upstream and downstream is measured. By solving Equations 9 and 10 for $\bar{c}$ yields

$$\bar{c} = \frac{L}{t_{21}} + \bar{u}\cos\theta. \quad \textbf{(11)}$$

and

$$\bar{c} = \frac{L}{t_{12}} - \bar{u}\cos\theta, \quad \textbf{(12)}$$

Again the speed of sound is typically assumed to be constant, so that equating Equations 11 and 12 and solving for $\bar{u}$ leads to[17,73]

$$\bar{u} = \frac{L}{2\cos\theta}\left[\frac{1}{t_{12}} - \frac{1}{t_{21}}\right], \quad \textbf{(13)}$$

or

$$\bar{u} = \frac{L^2 \tan\theta}{2D}\left[\frac{\Delta t}{t_{12}t_{21}}\right]. \quad ^{4} \qquad \textbf{(14)}$$

This equation represents the axial velocity averaged along the sound path in terms of the propagation times, but requires accurate knowledge of the path length between the transducers, L, and the angle, θ. Other equations[29] are developed through a similar method; however, several of which eliminates the angle from the formulation, these are:

$$\bar{u} = \frac{L^2}{2\sqrt{\left(L^2\text{-}D^2\right)}}\left[\frac{t_{21} - t_{12}}{t_{21}t_{12}}\right], \quad ^{30} \qquad \textbf{(15)}$$

and

$$\bar{u} = \frac{L\,\Delta t}{2T_{avg}^2 \cos\theta}, \quad ^{24} \qquad \textbf{(16)}$$

where $T_{avg} = \frac{t_{12}+t_{21}}{2}$ is the average propagation time. These equations are similar in form to Equations 13 and 14, but the unknown path and diametrical lengths, and sound path angles between the ultrasonic transducers are handled differently.

The second basic derivative starts again with Equations 9 and 10 and by defining:

$$\Delta t = t_{21} - t_{12} \qquad \textbf{(17)}$$

Substitution of Equations 9 and 10 into Equation 17 produces :[24,31,32]

$$\Delta t = \frac{2\bar{u}\,L\cos\theta}{\bar{c}^2 - \bar{u}^2\cos^2\theta} \qquad \textbf{(18)}$$

Now because $\cos\ominus \leq 1$ and assuming[31,32] $\bar{u}^2 << \bar{c}^2$, equation 18 is usually approximated as

$$\Delta t \approx \frac{2\bar{u}L\cos\theta}{\bar{c}^2} \tag{19}$$

and solving for $\bar{u}$ produces:[14,31,32,33]

$$\bar{u} = \frac{\Delta t}{2L\cos\theta}\bar{c}^2. \tag{20}$$

This development requires knowledge of the speed of sound, sound path geometry, and time differences between the upstream and downstream propagating sound pulses in the fluid media being measured.

2.3.3.1 Conclusions from Literature Review

All of these derivations have the basic assumptions that u, c, and L are constants across the velocity measurement volume. The net effect of these assumptions is to produce a spatially and temporally averaged velocity across the velocity measurement volume. These developments do not allow for variations in velocity and sound speed along the sound path. An additional problem is the assumption of constant path length. In order to understand the data scatter observed in usual flowmeter output it is necessary to derive a more general expression not restricted by such assumptions. Then by determining if the data scatter of the flowmeter output is within the scatter expected due to naturally

occurring turbulence in the flow system, the hypothesis that the variation in individual transit times of ultrasonic pulses is caused by this turbulence can be demonstrated.

2.4 Computation of Flow from Velocity

Once the integrated $\bar{u}$ is found using Equations 13 -16, and 20, the total flow in a system is found by integrating the $\bar{u}$ found over the area of the pipe,

$$Q = \int \bar{u}\, dA. \qquad \textbf{(21)}$$

This equation may be solved in several ways, either by assuming that $\bar{u}$ is constant over the entire area, or alternatively, that multiple paths can be used to determine the flow. A commonly used integration method using multiple paths is Gaussian Quadrature. This method was first used by Westinghouse with ultrasonic flowmeters and has been used since by several ultrasonic flowmeter manufacturers. [9] Numerical quadrature techniques attempt to perform an accurate integration without having to make use of scaling factors. [9] A typical application of the Gaussian Quadrature method is to use a 4-path setup as shown in Figure 2-6. The Gaussian Quadrature integration technique allows the flow in a pipe to be integrated without knowing the actual velocity profile in the pipe. By measuring the flow velocities at specific points in a pipe or channel, the velocity profile can be integrated so that the flow can be computed.[45,46] The velocity profile is approximated by

$$\int_{-1}^{1} f(y)dy = \sum_{i} w_i f(y_i), \qquad \textbf{(22)}$$

where w_i is a weighting coefficient defined by

$$w_i = \int_{-1}^{1} \frac{S(y)}{(y - y_i)S'(y_i)} dy \qquad \textbf{(23)}$$

and $S(y) = \prod_i (y - y_i)$. To use Equation 23, a velocity must be measured at a location y and modified by the weighting coefficient w. These coefficients are tabulated in numerous references and a partial list of the y positions and coefficients, w, are listed in Table 2-1. [45,46] To use the Gaussian Integration technique on the system diagramed in Figure 2-6, the sound paths should be located at ±33.998% of the radius and ±86.114% of the radius [45,46] measured from the centerline of the pipe. Then after measuring the velocities at these locations, the inner velocities are multiplied by 0.65215 and the outer velocities by 0.34785. Summation of the weights and velocities results in the integrated velocity across the pipe.

For velocity profiles of greater than 2i+1, [45,46] the integration error will be due to terms of order higher than 2i+1. An additional error source is that the y position of the function is computed as shown to 10 decimal positions and should be a point velocity; however, the ultrasonic beam used to determine the velocity has a finite diameter over which it averages velocities. Also, it is averaging the velocities encountered along the x direction, making the point velocity incorrect.

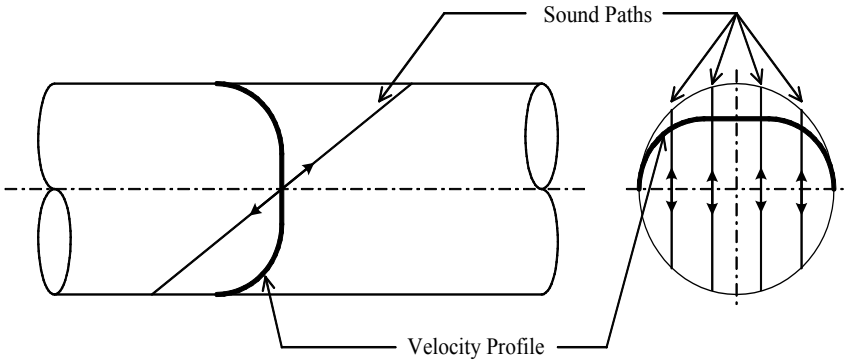

Figure 2-6 Sketch of Layout for Multiple Path Flowmeter

The number of paths in an ultrasonic flowmeter should vary significantly as the potential for flow distortions increase. For instance, if a pipe flow is long and straight with a well-developed velocity profile, similar to those profiles measured in the literature by Nikuradse, Reichardt, and others,[57,70] only one ultrasound path may be needed for a reasonable measurement. However, if the measurement location is not in a long straight pipe, but instead is located downstream of any number of piping configurations, more paths are needed to reduce the uncertainty of the assumed velocity profile in the pipe. If a swirling flow is suspected, it may be necessary to place ultrasound paths in an 'x' configuration at each chordal location to account for the swirl. Although placing more sound paths in the flow increases accuracy, the complexity of the meter increases rapidly. Also, one is limited by physical constraints, such as transducer size and potential for cross-talk, to the number of paths placed in smaller pipes. Finally, each sound path will still have the same problems relative to computing the velocity at a particular location. That is, what is the velocity at the location, what does the data fluctuation indicate, and

finally how might one use the measured data to better determine the mean flowrate in the pipe.

Table 2-1 Gaussian Integration Locations and Coefficients [46]

n	$\pm y_i$	w_i
2	0.5773502691	1
3	0	0.8888888888
	0.7745966692	0.5555555555
4	0.3399810435	0.6521451548
	0.8611363115	0.3478548451
5	0	0.5688888888
	0.5384693101	0.4786286704
	0.9061798459	0.236926885

2.5 Review of Accuracy Issues in Ultrasonic Flowmeters

Claims are made that ultrasonic flow measurement methods in accuracies between 0.1%[24,9] to 2%.[31,32,33] Some sources[9, 31,32,33] report that there is no need to calibrate an ultrasonic flowmeter if the required accuracy is no greater than 1% in a straight pipeline. There are, however, several generally recognized important sources of error in ultrasonic flowmeter systems. The first error source is line velocity errors including such things as installation errors, errors resulting from variations of temperature, pressure, or acoustic signal strength, and fluid cross-flow errors.[31,32,33] These errors affect the calculation of the average velocity along a sound path. Typically the way in which these errors are eliminated is by systematically measuring path length, temperature, pressure and carefully evaluating all of the electronics used to power the flowmeter.

The other important groups of errors are known as integration errors. These errors are the result of improperly integrating the total flow based on the measured points. This error has two basic sources, first the degree to which the flow profile along the propagation path in the system is known; second, the temporal and spatial variation of this flow profile across the section. For example, if a system does not have a well-developed flow profile, and only one sound path is used, the total integrated flow may not be indicative of the actual mean flowrate. There are two standard methods to eliminate these errors. The first is to add more paths to the flowmeter, thus providing more data for evaluation of the velocity profile, and the second is to calibrate the meter in a piping arrangement similar to that in which it will be installed.

To determine flow from the mean velocity, as computed using Equations 13 - 16, and 20, a velocity profile must be assumed. The velocity profile assumption is the weak point when computing the mean flowrate using flowmeters, including the ultrasonic flowmeters.

Velocity profiles are by nature extremely hard to predict accurately. In well-behaved flows, those that are not separated or do not have a large swirl, the velocity profile may be predicted by using the law of the wall of turbulent flows.[57,70] However, these profiles vary with Reynolds number, necessitating a variable empirical factor to compute flow. By examining and understanding the velocity field characteristics one may make better decisions about the characteristics of the velocity profile, in turn achieving higher accuracy of the flow measurement. Most research on the subject of ultrasonic flowmeters,

as it turns out, has centered on determining the aforementioned empirical factors as a constant or average value rather than as a variable.

2.6 Prospects for Improving Ultrasonic Flowmeter Accuracy

The generally recognized line velocity errors are the easiest errors to correct from the fluid mechanic viewpoint; these errors are quantities which on the surface appear to be easily measured or controlled. Two errors in path length are not easily measured, these are the curvature of the path due to velocity, and path length due to turbulence. Both of these errors result in a longer than accounted for sound path. The curvature of the path results from the sound being "swept" downstream of the intended path. The path increase due to turbulence is caused by the random nature of fluid turbulence speeding up and slowing down the sound in the path, the result of which is a "crooked" path similar to the one sketched in Figure 2-7.

The errors associated with acoustic signal strength and timing accuracy are a function of the electronics and transducers in the flowmeter. These errors have traditionally been the focus of many ultrasonic flowmeter developments. It is now thought and has been observed by the author that many of the electronics issues have been resolved to the point where other issues involving fluid mechanics have become more important with respect to the errors produced by the flowmeter electronics.

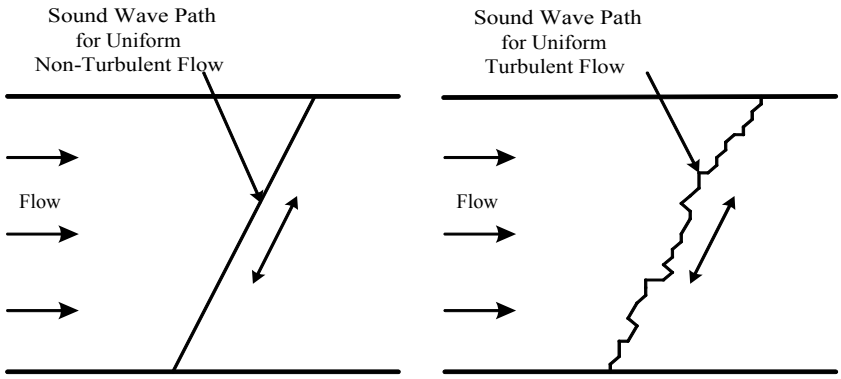

Figure 2-7 Magnified Examples of a Sound Path in a Flow: a) Non-Turbulent or Average Velocity Used; b) Instantaneous Velocities Used

The other major source of error, the integration error, has also been focused on quite rigorously. As previously described, the integration error is associated with the uncertainty of the velocity profile within the pipe. Additionally, integration errors can result from line velocity errors, as the integration can only be as accurate as the average velocity measured along a sound path.

The usual method to reduce or eliminate integration error is to attempt to measure more line velocities within a flow field as discussed in Section 2.3. In the 1970's, it was standard practice to move the transducer setup so that the sound path could be shifted within the flow system.[58,65] The disadvantage here is when the flow within the system is not at a steady state, the individual line velocities will not be at the same flowrate and will cause erroneous data to be input into the integration technique. However, for long term averages, or well-behaved flows this method of moving the sound path can be quite

effective, especially as the number of sound paths is increased. As an alternative to moving the sound paths around, multiple sound paths can be used to help determine the velocity profile in the system. The number of paths installed is limited only to the size of the flow system and expense. With different numbers of sound paths, different methods of integration are used to find the average flow in a system from the line velocities.

More recently, some focus has returned to reducing errors in the line velocity. Two recent papers dealing with this subject were published by Mattingly and Yeh. [38,73] Contained in both of these papers are discussions of the appropriate method for applying different velocity profiles to the flow in a pipe to determine the final flow. Mattingly and Yeh concluded that the velocity profile chosen may cause as much as a 4-5% error in the measured versus actual mean flowrate.[73]

3 Problem Statement and Supporting Assumptions

Chapter 1 introduced the hypothesis that the individual Δt realization variations produced by an ultrasonic flowmeter are due to the turbulence present in nearly all flows of interest. To better test this hypothesis, the variation in the data output from an ultrasonic flowmeter must be understood. However, evidence that turbulence produces fluctuations in flowmeter outputs is not readily available. As shown in Chapter 2, typical equations used to compute the output of an ultrasonic flowmeter assume that the flow velocity, speed of sound, and path length are all constant in the flow during the time of measurement. Additionally, the flowrate output by most flowmeters is usually smoothed by mechanical or electronic averaging techniques incorporated into the process so direct comparison to other flowmeters does not provide insight into the data scatter seen with ultrasonic flowmeters. For instance, pressure drop meters, such as venturi and orifice, have spatial and mechanical averaging built into the method. The measurements are over a relatively large area, and small pressure changes must be transmitted over a distance to the pressure transducers and are modified by viscous damping along the way; therefore small pressure perturbations are not recorded.

Ultrasonic flowmeters differ from other flowmeters in that the individual sound pulses travel fast enough, relative to the flow time scales, to allow for an assumption of frozen flow for each pulse. By using this assumption, it can be demonstrated that a sound propagation time may be increased or decreased by the overall effect of all the

instantaneous velocities (turbulence) in a velocity field. This increase or decrease in the sound propagation time occurs because the turbulent flow velocities cannot be assumed to be random, but rather have some spatial correlation. Only in the limit of hypersonic flow, $u>>c$ can the flow be randomly averaged along the path, because the flow velocities will no longer be correlated to each other during the time of the sound propagation. Individual realizations, on the other hand, can be considered independent and random as long as they are sufficiently separated in time. Therefore, it is necessary to develop an understanding of the effect of the instantaneous turbulent velocities on the propagation time of a sound pulse.

The time dependent nature of turbulent flows only allows for the discreet measurement of the instantaneous velocity field. Present measurement technology is not capable of continuous whole field measurement at high acquisition rates. Heretofore, ultrasonic flow measurement technology has relied on the assumption that only average flow velocities play a significant role in the propagation time of an acoustic wave. This assumption was used because it was thought that the average velocities were the only significant contributor to the Δt measurements of a typical ultrasonic flowmeter, so little attention has been paid to the instantaneous velocities in a flow field. This assumption regarding fluid flow average velocities is thought to be incorrect due to the relative high sound speed with respect to low fluid velocity ($u<<c$), because of this high sound speed flow may be assumed to be frozen during the propagation time of the sound wave. This assumption will be discussed fully in Chapter 6.

This research examines the effect of flow turbulence on sound waves propagating across a velocity field. The resulting information can then be used to determine affect on the accuracy of an ultrasonic flowmeter, and understanding the data scatter typically associated with ultrasonic flowmeters.

3.1 Objectives and Approach

The primary goal of the research is to investigate the influence of the turbulence on acoustic wave propagation. Numerical modeling forms the body of the dissertation. The following objectives are stated:

1. Develop a numerical model (multiple/Modified Ray Trace Method on a very fine grid) that allows computation of the statistical variation of propagation times for sound pulse propagating through the turbulence. The model is based on the flowmeter equation that takes into consideration turbulent fluctuations of the velocity.

2. Validate the numerical code using benchmark results obtained from the piece-wise numerical integration method applied to the problem of a sound waves contra-propagating in a uniform flow field with a superimposed vortex street.

3. Examine the effect of large scale flow structures on sound wave propagation using the uniform flow field with a superimposed vortex street as a flow field employed by the numerical code. Demonstrate the effect of turbulence in terms of the first and higher

moments of the propagation time difference for up and downstream moving waves as a function of

a. Temperature change (sound speed change),

b. Width of a sound beam,

c. Sound path angle with respect to the mean flow,

d. Vortex strength.

4. Use experimentally measured PIV data from a turbulent channel flow to compute the statistical variation of sound pulse propagation times as a function of

a. Temperature change (sound speed change),

b. Width of a sound beam,

c. Sound path angle with respect to the mean flow.

4 Ray Trace Method

In order to determine the effect of flow turbulence on the propagation time of a sound wave, and to estimate the error in measuring the velocity along a sound path, the Ray Trace Method is chosen as a numerical approach.[27] By breaking the path of the sound wave into ever smaller segments, it is possible to include the effects of local variations in temperature and velocity on the sound wave propagation. It is not necessary that the segments be infinitesimal, but an argument will be made that the steps should be on the order of the size of the Kolomogrov scaled, the smallest scale, eddies. Using the Ray Trace Method and accounting for these turbulent eddies in the flow provides an indication as to the amount of data scatter expected from a flowmeter. This in turn will allow a better statistical analysis of the flow field, thereby allowing a better determination of the mean flowrate. In addition, the Ray Trace Method was used to examine the problem of how a pulse of sound propagates through a flow structure such as a vortex.

4.1 Use of Ray Trace Method

The Ray Trace Method utilizes vector analysis to determine the path that a particle, or in this case a "point" of sound, will propagate through a velocity field. To use the Ray Trace Method, the sound pulse is modeled with a vector and the flow field is modeled with a second vector. These vectors are added together using simple vector addition to obtain a resultant sound pulse travel vector.[53]

To start the analysis, a measuring volume within which a sound pulse propagates is created. This volume has the dimensions of the diameter of the ultrasonic transducer and length of the sound path. All fluid velocities within this volume at the time of sound propagation will affect the sound wave front as it propagates between the two transducers. One simplifying assumption made here, and throughout the rest of this study, is that the sound wave does not spread as it propagates. This assumption simplifies the calculation of the sound pulse path by eliminating the spreading that occurs as the pulse propagates. However, for short distances, the spreading of the sound pulse is minor compared to the distance traveled this will be discussed further in Chapter 6. To determine the effects on the sound wave pulse as it propagates through the measuring volume, multiple thin lines, or rays, connected at the head were used to simulate the finite width beam. Using the Ray Trace Method on each ray it was possible to get an idea of how the sound wave pulse distorts while propagating through a velocity field. This distortion could cause the receiving transducer to register an early receive, resulting in an incorrectly computed velocity.

Other researchers have used the Ray Trace Method in their research on sound propagation, including L' Esperance[27] used the Ray Trace Method to determine how sound propagates in the atmosphere. The study included examinations of atmospheric absorption, refraction, and turbulence. While there were limitations and simplifications imposed, such as the use of a constant or a linear sound speed gradient, the majority of the comparisons made between the ray tracing algorithm and experimental work showed good agreement.

An additional article by Raspet et.al.,[54.] applied sound impedance to the Ray Trace Method. Again, there was good agreement between the model and a fast field program. This held true even though some criteria of the Ray Trace Method were violated. Equation 24 describes the criteria under which the ray trace algorithm is valid[14,27,55]:

$$\lambda_o n' << \mu^2 \approx 1 \quad \text{and} \quad \lambda_o \frac{A'}{A} << 1. \tag{24}$$

Where n' = spatial derivative of index of refraction and A'= spatial derivative of wave amplititude. In words these equations represent the speed of sound and amplitude of the wave cannot change significantly over one wave length.

4.2 Derivation of Ray Trace Method

The motion of a discontinuity, such as a sound pressure wave, through a fluid medium can be described by the eikonal equation. The generalized eikonal equation defines the edge of a shock or discontinuity propagating through either a static or dynamic fluid.[23] Based on this definition the eikonal equation can be used to define the Ray Trace Method, which also models the motion of an acoustic wave. The general eikonal equation is derived from the equations of motion and continuity [13,69] which are shown in Equations 25 and 26:

$$\rho \frac{D\vec{U}}{Dt} = -\nabla P \tag{25}$$

$$\frac{D\rho}{Dt} = -\rho \nabla \cdot \vec{U} \tag{26}$$

where viscous effects of the fluid are ignored. Viscosity in the fluid medium results in sound, this absorption is in general small[25] and can be ignored, this assumption is

discussed in Chapter 6. The small effect of viscosity on sound propagation in a fluid is a consequence not only of the smallness of the viscosity coefficient, but also of the smallness of all quantities which undergo a change during the sound propagation. Also, pressure and density of the sound wave (assumed to be isentropic) are related via the relation

$$\bar{c}^2 = \left(\frac{\partial p}{\partial \rho}\right)_s . \qquad \textbf{(27)}$$

If φ is the wavefront location, then the evolution of φ is described by the eikonal equation as shown by Heller:[13]

$$\left|\nabla\varphi\right|^2 = \mu^2\left(1 - \frac{\vec{\mathbf{u}}\cdot\nabla\varphi}{c_o}\right)^2 , \qquad \textbf{(28)}$$

where μ is the refractive index of a fluid, and c_o is the reference sound velocity. The eikonal equation approximates the propagation of an acoustic wave in the limit of the high frequency short wavelengths, such as ultrasonic waves. Additionally, the wavelength must be short relative to the rate of change in the speed of sound in a medium as described in Equation 24. In conclusion, since an acoustic wave front is a weak shock, it may be described using Equation 28.

In the case of motionless fluid, ie $\vec{\mathbf{u}} = 0$ Equation 28 reduces to:

$$\left|\nabla\varphi\right|^2 = \mu^2 = \left(\frac{c_o}{\bar{c}}\right)^2 . \qquad \textbf{(29)}$$

Since $\nabla\varphi$ describes the positional change in the wave front, Equation 29 indicates that the wave front propagates and expands normal to itself in still media. If the fluid media is moving, the wave motion is described as:

$$v_{front} = \bar{c} + \vec{u} \cdot \hat{n} \tag{30}$$

where

$$\hat{n} = \frac{\nabla\varphi}{|\nabla\varphi|}, \tag{31}$$

is a unit vector in the wave propagation direction. Now introduce a phase shift Ω between undisturbed media and media where the turbulence is present, as the following

$$\Omega = \omega t - k_o \varphi, \tag{32}$$

where ω is a sound frequency and $k_o=\omega/c_o$ is a wave number and the physical setup is shown in Figure 4-1. The right hand side of Equation 28 may be rewritten as remembering: $\vec{u} = u\hat{i}$; $\vec{u} \cdot \hat{n} |\nabla\varphi| = \vec{u} \cdot \vec{p} = u\cos\theta |\nabla\varphi|$

$$|\nabla\varphi| = \mu \left(1 - \frac{\vec{u} \cdot \nabla\varphi}{c_o} \right) = \frac{1}{\bar{c}} \left(c_o - u \cos\theta |\nabla\varphi| \right). \tag{33}$$

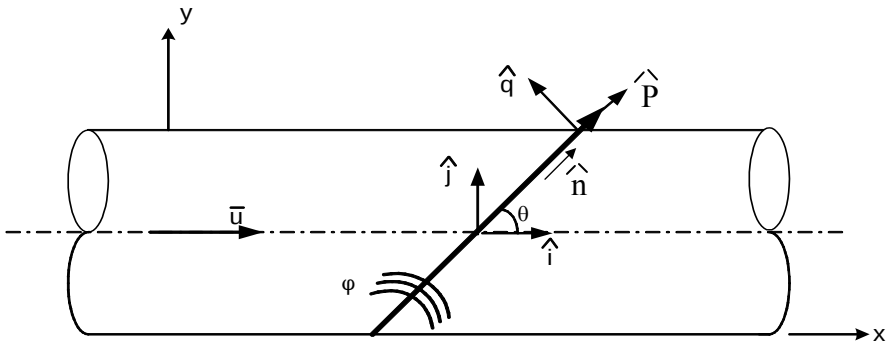

Figure 4-1 Setup for Acoustic Wave Propagation in One Direction

Solving for $|\nabla\varphi|$ yields

$$|\nabla\varphi| = \frac{c_o}{\bar{c} + u\cos\theta}. \tag{34}$$

Using Equation 32 with a constant Ω

$$\frac{d\Omega}{dx} = \omega\frac{dt}{dx} - k_o\frac{d\varphi}{dx} = 0 \Rightarrow \frac{dt}{dx} = \frac{k_o}{\omega}\left(\frac{c_o}{\bar{c} + u\cos\theta}\right). \tag{35}$$

Therefore, the flowmeter equation for the sound waves propagating upstream is obtained by rearranging Equation 35

$$\frac{dx}{dt} = \bar{c} + \bar{u}\cos\theta, \tag{36}$$

or

$$dt = \frac{dx}{\bar{c} + \bar{u}\cos\theta}. \tag{37}$$

For sound waves propagating in the opposite direction, Equation 37 becomes

$$dt = \frac{dx}{\bar{c} - \bar{u}\cos\theta}. \tag{38}$$

Finding a direct solution for an eikonal equation in an inhomogeneous medium in general is difficult.[23] However, by using Snell's law to obtain an ordinary differential equation which describes wave normals, several solutions may be found. The generalized form of Snell's law as shown by Kornhauser[23] is:

$$\left(\frac{d}{d\vec{s}}\right)\left(f\vec{i}_x \cdot \hat{n}\right) = f\vec{s} \cdot \left(\frac{\partial \hat{n}}{\partial x}\right) + \vec{s} \cdot \hat{n}\left(\frac{\partial f}{\partial x}\right) \tag{39}$$

where $\vec{s}$ is an arbitrary unit vector. This equation is most useful if the right-hand side

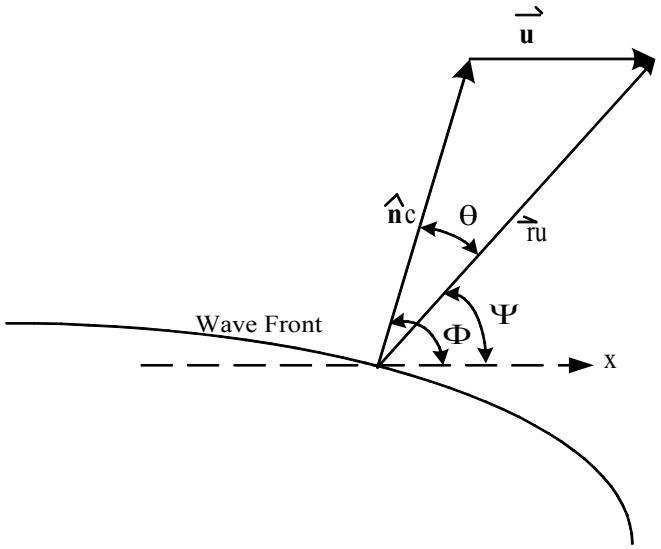

Figure 4-2 Sketch of Ray Trace Geometry

goes to zero, at which time the left side can immediately be integrated yielding a constant quantity in the direction of $\vec{s}$. The right-hand side goes to zero in three cases: 1. Stationary fluid, 2. Wave normals in a moving media, and 3. Rays in a moving media. All three cases were discussed at length by Kornhauser[23]; however, the case involving rays in a moving media is the most applicable to this research. Figure 4-2 demonstrates this relationship, and can be stated mathematically as:

$$\hat{\mathbf{n}}c + \vec{\mathbf{u}} = \vec{\mathbf{r}}u. \tag{40}$$

In a moving fluid, the arbitrary unit vector $\vec{s}$ is set in the same direction as the sound ray, $\vec{r}$, $\vec{s} = \vec{r}$, and rearranging Equation 40

$$\vec{\mathbf{r}} = \frac{\left(\hat{\mathbf{n}}c + \vec{\mathbf{u}}\right)}{u}. \tag{41}$$

Also defining f as $f = \nabla\varphi = c_o / \left(\overline{c} + \vec{u} \cdot \hat{n}\right)$, the right-hand side of Equation 39 becomes:

$$f\,\vec{\mathbf{r}} \cdot \frac{\partial \hat{\mathbf{n}}}{\partial x} + \vec{\mathbf{r}} \cdot \hat{\mathbf{n}} \frac{\partial \mathbf{f}}{\partial x} = f u^{-1} v_{front} \cdot \frac{\partial \hat{\mathbf{n}}}{\partial x} - f\,u^{-1} v_{front} \cdot \frac{\partial \hat{\mathbf{n}}}{\partial x} = 0. \tag{42}$$

Equation 42 then becomes:

$$\frac{\partial}{\partial \vec{\mathbf{r}}}\left(\left(\frac{c_o}{\overline{c} + \hat{\mathbf{n}} \cdot \vec{\mathbf{u}}}\right)\cos\Phi\right) = 0; \tag{43}$$

therefore,

$$\left(\frac{c_o}{\overline{c} + \hat{\mathbf{n}} \cdot \vec{\mathbf{u}}}\right)\cos\Phi = \text{cons tan t} \tag{44}$$

indicating that $f = \frac{c_o}{\bar{c} + \hat{\mathbf{n}} \cdot \vec{\mathbf{u}}}$ is constant along a ray. Although Kornhauser continues the derivation, for this work it is assumed that the time step used is small enough such that $\vec{\mathbf{u}}/c_o$ and wave speed $f = c_o/\left(c + \hat{\mathbf{n}} \cdot \vec{\mathbf{u}}\right)$ are constant during the time step. It should be noted that Equation 44 is constant along the normal to the wave front. The direction of the actual ray is found by relating the angle of the wave normal and the local velocity which includes the angle θ. It follows that if the step-size is small enough that neither the speed of sound nor the fluid velocity changes over the step, if f and $\vec{\mathbf{u}}/c_o$ constants. This is consistent with the L'Esperance conditions in Equation 24 and leads to the conclusion that for a turbulent flow, step-size must be smaller than the smallest eddy size, which is considered to be the Kolomogrov scale eddy. A similar result may be obtained using Rayleigh analysis from 1938. [53] By applying the small step-size, one may conclude that the fluid velocity along each step in the Ray Trace Method does not change radically during an individual step maintaining the L'Esperance condition. This allows the Ray Trace Method to properly integrate the velocities along the sound path.

As stated above, a time step must be chosen such that the ray length is smaller than the smallest eddy, or Kolomogrov scale. By invoking this rule, the L'Esperance conditions from Equation 24 are satisfied. In addition, time step-size must also allow for sufficient precision to measure the expected Δt's. For example, if the expected Δt's are on the order of 1 ns, then the time step must be less than that to record a time difference between the

two propagating waves and even smaller in order to achieve a reasonable resolution. Table 4-1 compares the approximate size of typical Kolomogrov eddies[66] in a flow of water in an approximate pipe diameter of 0.15 m, and a step-size based on a time step 10 times smaller than the expected Δt. A time step, t, is chosen and multiplied by the sound speed and the velocity to get a vector for each, then the vectors are added together to obtain the resultant vector, mathematically:

$$\Delta t\left(\overline{c}_i + \overline{u}_i\right) = P_i \tag{45}$$

where subscript i = x, y, z, and P is the path length. To obtain an algorithm for the Ray Trace Method, one separates the terms of the equation, rearranges, and integrates:

$$\begin{aligned} x &= \int_0^t (\overline{c}_x + \overline{u})dt, \\ y &= \int_0^t (\overline{c}_y + \overline{v})dt, \\ z &= \int_0^t (\overline{c}_z + \overline{w})dt. \end{aligned} \tag{46}$$

In the work reported herein, only a one or two-dimensional analysis was used, so only the first two equations of the system in Equation 46 are used. In the next chapter, a software program is described which makes use of this set of equations to compute the path the sound front takes across several different velocity fields.

Table 4-1 Comparison of Step-size Necessary for Δt to be Determined and Kolomogrov Eddy Size in a Flow with an Average Water Flow Velocity of 3.05 m/sec and Pipe Diameter of 0.15m.

Kolomogrov Eddy	2.2 μm
Time Step-size Used in Research	0.1 ns
Typical Ray Length Used in Research	0.1 μm

5 Sound Propagation Time Fluctuations

5.1 Transit Time Fluctuations Related to Turbulence

The sound pulse propagating across a flow field, in effect, integrates the fluid velocities so that the average speed of the pulse propagation will be the speed of sound in the fluid plus the integrated effect of the local flow velocities. The total propagation time will vary about the mean propagation time. Figure 5-2 illustrates this phenomenon for three sound paths. On the plot, there is velocity versus time traces at seven separate locations shown across a numerical simulation of a turbulent flow field(courtesy of Moser); Figure 5-1 is a schematic of the setup.[43] For discussion purposes, three example ultrasonic paths are indicated by vertical dashed lines. In this example, the sound is propagating perpendicular to the flow so that, there is no average velocity in the sound travel direction. It would be

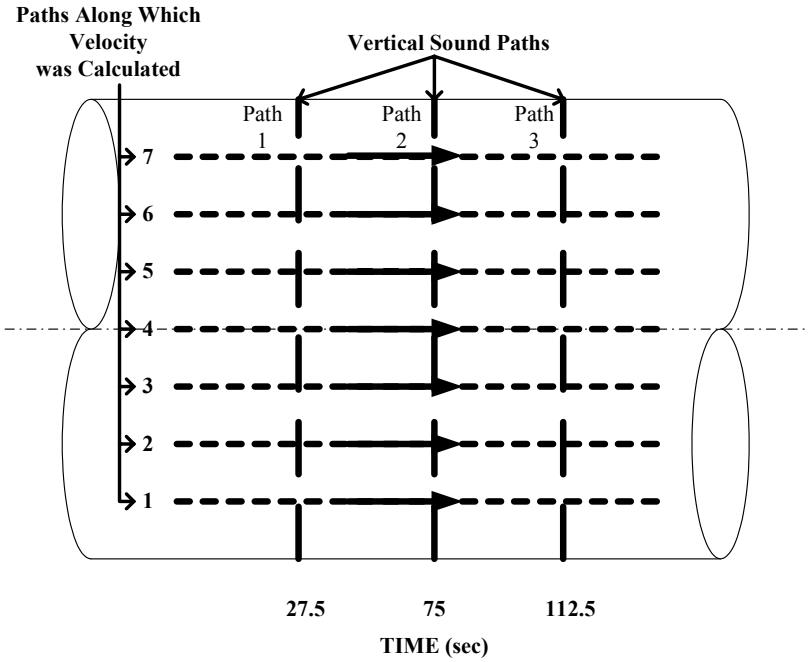

Figure 5-1 Schematic of Turbulent Channel Flow Setup Shown in Figure 5-2

expected, then, that the propagation time will always be defined by Equation 3; however, due to turbulence, there are small velocity perturbations in the direction of the sound propagation. As the sound pulse propagates, it will be sped up and slowed down by these velocity perturbations or turbulent velocities as compared to the mean transit speed. For example, along the first path in Figure 5-2, path 1, by visual inspection, a sound pulse would first be sped up, then for the next several time increments, the flow velocity contribution would be near zero. Finally, near the last two increments speed of the pulse will be increased again. The final result is that the pulse propagation time will be shorter than the mean. Along the second line, 2, it appears the propagation time will be closer to the mean. Along the last path, 3, however, the propagation time would be much longer than the mean. So, as can be seen in this very simple visual example, sound pulse propagation time can be altered by instantaneous velocity fluctuations on a spatial basis. Remember that this flow field is assumed to be frozen, this is an assumption discussed at length in Chapter 6.

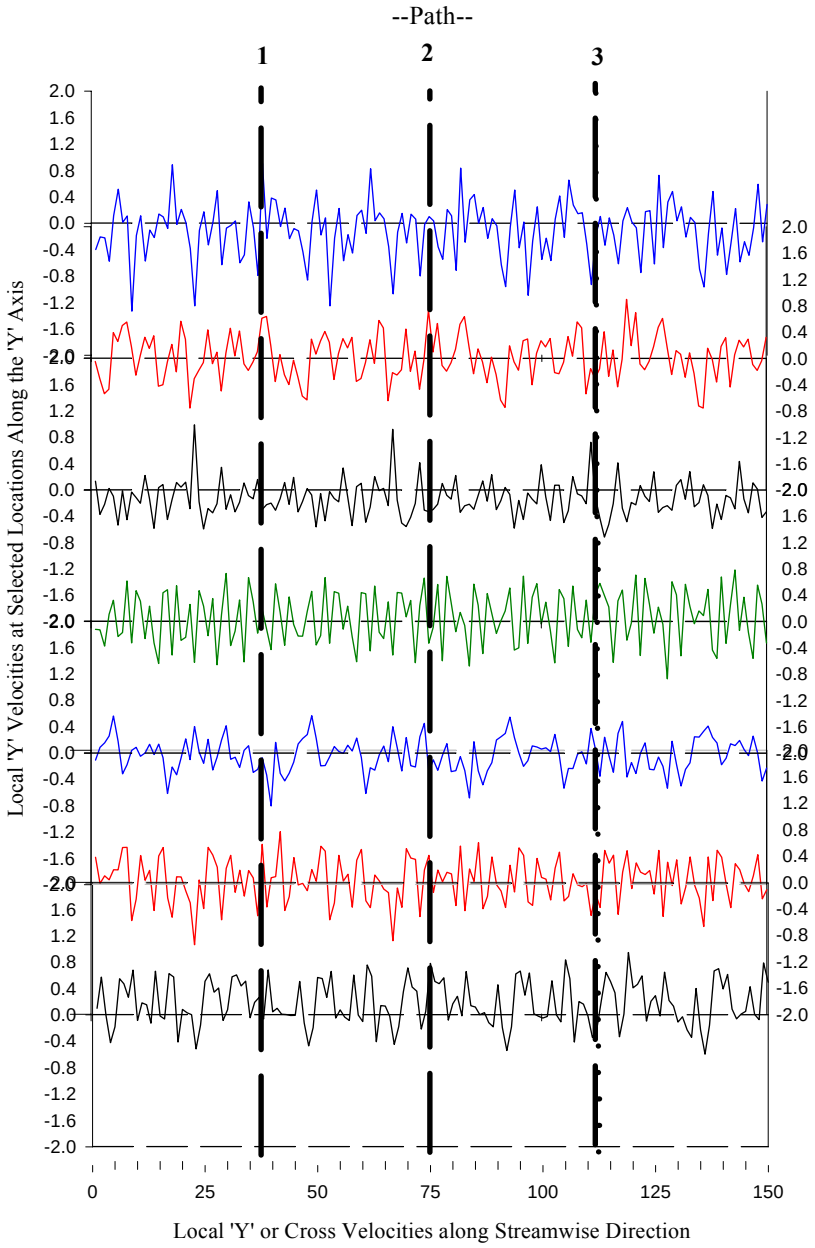

Figure 5-2 Velocity Plots at 7 Locations Across a Turbulent Channel Flow for 3 Paths. [43] The Dashed Lines Represent Propagation Paths Across the Channel for Sound Waves. The Sum of all Velocities Along the Path Afforded a Propagation Time Which May Be Slightly Shorter or Longer than the Expected Mean Propagation Time. Velocity Plots Courtesy of Moser.

5.2 Discussion of Ultrasonic Flowmeter Output Fluctuations

Although little work has been done to date to quantify the effect of instantaneous values of turbulent velocities on the propagation time of a sound pulse propagating in a turbulent field, there are nevertheless, some data that indicate a problem exists. Since the individual realizations of transit time measurements are separated in time, it should be expected that each realization will randomly vary from the expected mean because the correlation data from typical turbulent flows indicates that the velocities at a point become temporally uncorrelated very quickly.[66] Figure 5-3(courtesy of Mattingly) for example, is data collected from the flow laboratory at the National Institute of Standards and Technology (NIST), and shows time series data from three different flowmeters, two ultrasonic meters

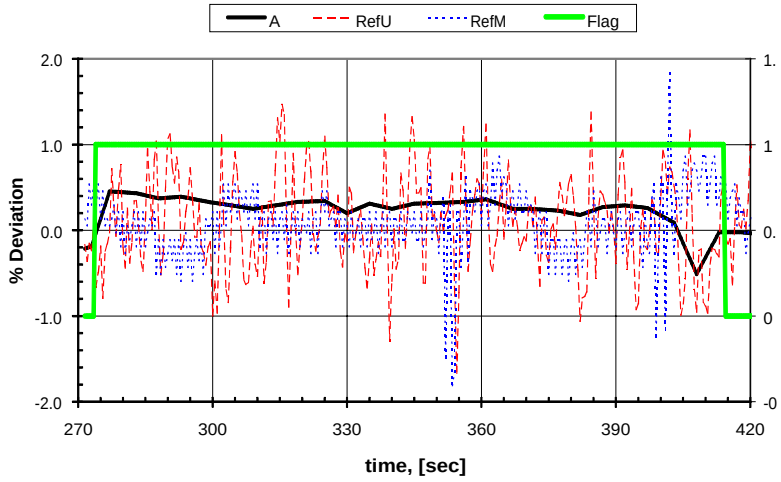

Figure 5-3 Data Scatter as Measured in a Flowmeter at the NIST Flow Laboratory; Real-Time Data Record Plotted as a Percent of Deviation from the Temporal Mean Values During a Single Collection Run. The Red Dashed Lines Represent Data from a Reference Ultrasonic Meter, and the Black Line Represents Data from an Ultrasonic Meter Being Calibrated. The Blue Line is an Installed Magnetic Meter used as a Reference. Courtesy of Mattingly, NIST.

and a magnetic meter.[38] One of the ultrasonic flowmeters was used as a reference flowmeter and shows approximately a 1% scatter about the mean. These data points represent an approximate one second average of data taken at approximately 15 Hz.[37] Therefore, the individual data points plotted on this graph are already the average of approximately 15 points and show a substantial variance. The second ultrasonic flowmeter was tested against the reference meter and shows less data scatter, but indicates an average flow for the period that was in error by as much as 0.5% with a positive bias for most of the period. The averaging technique for this device is proprietary. Finally, the output from the reference magnetic meter indicated scatter of approximately 1%. The data scatter reported using the reference meter indicates that the average velocity flowing through the device was not a constant, but, varied significantly on a short-term basis.

In a second example, research conducted separately by Desabrais and Weber at WPI used an ultrasonic technique to directly measure circulation about an object in a wind tunnel.[6,40] In both cases, data scatter was a problem when attempting to analyze the experimental results. Desabrais used the geometry shown in Figure 5-4, to measure the circulation about a stationary airfoil in a wind tunnel. The sound path was a closed path around the airfoil. Measurements taken without an airfoil, Figure 5-5, and with an airfoil in place, Figure 5-6 are shown with several time series of Δt data. In Figure 5-5, the data are plotted as Δt versus sample number at several different speeds in the wind tunnel. The samples were taken at a rate of 15 Hz, so each was approximately 0.067 seconds apart. The measured Δt would be expected to be zero since the measurements were made in a

closed path, which enclosed no sources of vorticity, but as can be seen in Figure 5-5, there was variation of Δt.

The data shown in Figure 5-6 was measured on a path enclosing an airfoil and, therefore, enclosed a vorticity source. Because airfoils generate circulation within a flow, and by having the airfoil enclosed within a sound path, a finite circulation would be expected. The data shown in this figure represent the airfoil at different angles of attack under steady state conditions, and should have resulted in constant Δt's at varying magnitudes as the angle of attack varied. It is clear from Figure 5-6 that the result was a mean Δt with substantial variation; however, there is data scatter on each time series which could be attributed to turbulence in the tunnel boundary layer or in the wake of the airfoil. These results are inconclusive because the scatter due to the electronic noise of the

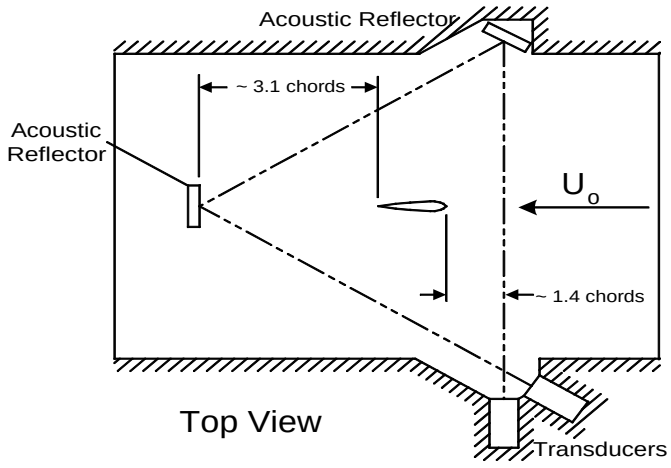

Figure 5-4 Wind Tunnel Geometry Used by Desabrais to Directly measure Circulation about a Stationary Airfoil. Courtesy of Desabrais.

instrumentation used may have been as significant as the scatter due to turbulence.

The fluctuations of measured transit times or differential times, Δt, by ultrasonic flowmeter systems seem to originate from the velocity fluctuations of the turbulent flow

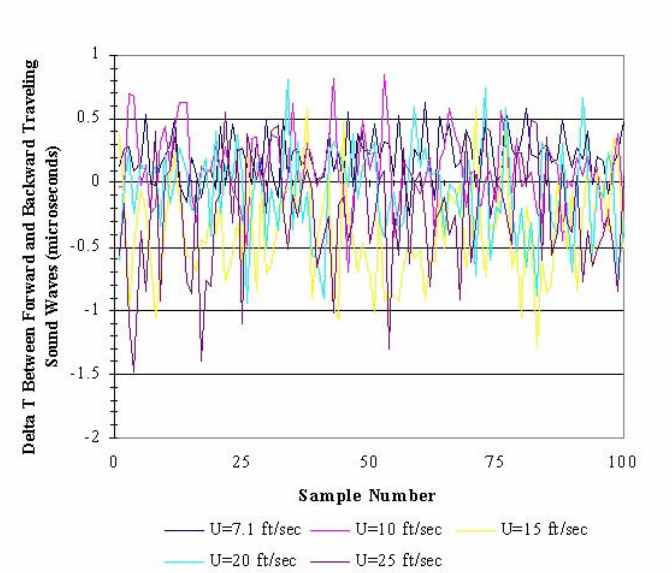

Figure 5-5 Measurements of Δt Around a Closed Circuit in an Empty Wind Tunnel as Diagrammed in Figure 5-4. Courtesy of Desabrais.

being measured. These Δt fluctuations stem from the fact that the sound waves employed in an ultrasonic system travel much faster than the fluid and, therefore, are greatly affected by the spatial correlations. As discussed in Section 5.1, sound waves propagating through a particular region integrate the instantaneous velocities, higher and lower than the mean, resulting in a slightly advanced or retarded travel time of an individual sound wave. The difference between forward and reverse propagating waves, Δt, varies from the mean by some amount related to the integrated turbulent velocities encountered.

In conclusion, as a turbulent flow is being measured, Δt will vary as a result of the cumulative turbulent intensities encountered by the sound wave. If the intensity of the turbulence being encountered is large, it is expected that the Δt fluctuations will increase, and as the turbulence intensities decrease the Δt scatter will decrease until no scatter is detected, i.e. laminar flow. Additionally, it may be possible to differentiate homogenous turbulence from flows in which large scale structures exist. All of this has implications on the velocity profile in the pipe, and therefore, the accuracy of the measured flow.

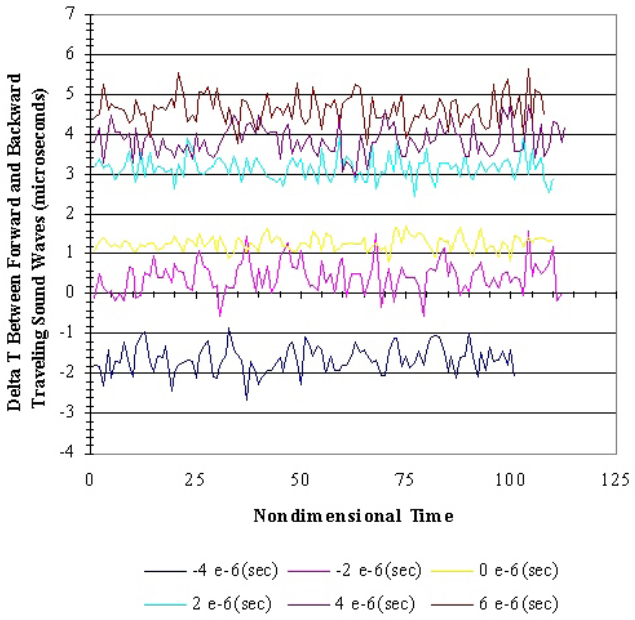

Figure 5-6 Measurements of Circulation about an Airfoil in a Steady State for Several Angles of Attack. The Setup is Diagrammed in Figure 5-4; α = Angle of Attack of Airfoil. Courtesy of Desabrais.

5.3 Mathematical Formulation of Flowmeter Equation Including Turbulence

As previously discussed, the time for a sound pulse to propagate is not a single average time, but rather a combination of an average time plus a variable fluctuating time component. A standard approach to analyzing turbulent flows takes this same form, and is known as Reynolds decomposition. Using this technique, flow velocities are assumed to be of two parts, the mean velocity and a fluctuating component:

$$\begin{aligned} u &= \bar{u} + u', \\ v &= \bar{v} + v', \\ w &= \bar{w} + w', \end{aligned} \tag{47}$$

where each equation represents velocities in a Cartesian coordinate system; x, y, and z. In a pipe or channel flow, the coordinate system is typically arranged so that the mean flow along the pipe or channel is aligned with the x-axis. Using the Reynolds decomposition technique, the fluctuation of the propagation time of a sound wave across a flow field may be computed, by breaking the propagation time into mean and fluctuating parts. For example, if the acoustic path is parallel to the flow, the propagation time in a new mathematical description (including turbulence) is

$$t = \int_0^L \frac{dx}{\bar{c} + \bar{u} + u'}. \tag{48}$$

Backing up several steps, starting with Equation 6 reprinted here as Equation 49,

$$dt = \left(\frac{dP}{c + \vec{V} \cdot \hat{n}} \right). \tag{49}$$

Now expanding $\frac{1}{\bar{c} + \left(\vec{U} \cdot \hat{n} \right)}$ in a series for small u/c yields:

$$\frac{1}{\bar{c} + \left(\vec{U} \cdot \hat{n} \right)} \approx \frac{1}{\bar{c}} \left(1 - \frac{\left(\vec{U} \cdot \hat{n} \right)}{\bar{c}} + \frac{\left(\vec{U} \cdot \hat{n} \right)^2}{\bar{c}^2} + \ldots \right), \tag{50}$$

which by neglecting $\frac{\left(\vec{U} \cdot \hat{n} \right)^2}{\bar{c}^2}$ and higher order terms since $\frac{\left(\vec{U} \cdot \hat{n} \right)}{\bar{c}} << 1$ leads Equation 49 to:

$$t \approx \frac{1}{\bar{c}} \int_0^L \left(1 - \frac{\bar{u}}{\bar{c}} - \frac{u'}{\bar{c}} \right) dx \tag{51}$$

Simplifying:

$$\frac{1}{\bar{c}} \int_0^L \left(1 - \frac{\bar{u}}{\bar{c}} - \frac{u'}{\bar{c}} \right) dx = \frac{L}{\bar{c}} \left(1 - \frac{\bar{u}}{\bar{c}} \right) - \frac{1}{\bar{c}} \int_0^L \left(\frac{u'}{\bar{c}} \right) dx \tag{52}$$

finally

$$\frac{L}{\bar{c}} \left(1 - \frac{\bar{u}}{\bar{c}} \right) - \frac{1}{\bar{c}} \int_0^L \left(\frac{u'}{\bar{c}} \right) dx = \bar{t} + t'. \tag{53}$$

So the time, t, for crossing a fluid flow in which velocity, u, is a function of $\bar{u}$ and u' is a function of $\bar{t}$ and t'.

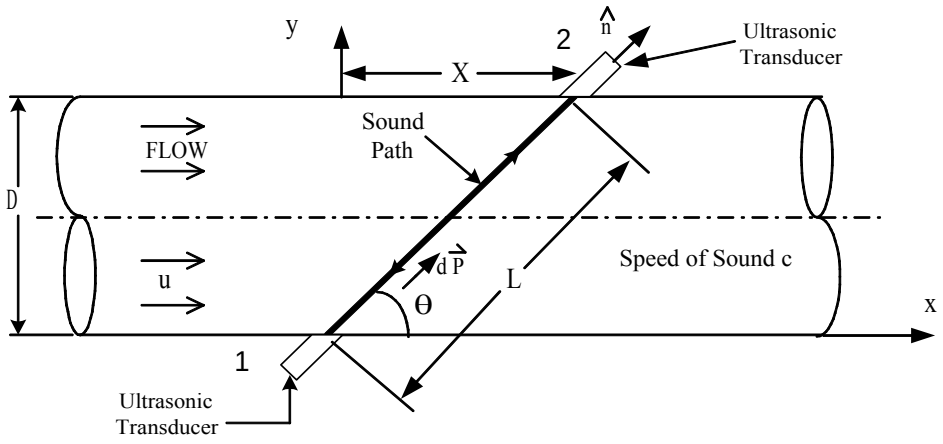

Figure 5-7 Typical Geometry for an Ultrasonic Flowmeter Angled to the Flow

As shown directly and indirectly by Lipkens[29], NIST[38], Weber[68], and Desabrais[8], varying turbulence levels cause the crossing time for sound in a turbulent field to vary. Heretofore, turbulence has not been included in the basic equations developed in the literature for ultrasonic flowmeters. If turbulence could be accounted for mathematically, it would be possible to better quantify the accuracy of such a flowmeter. Using Figure 5-7 (a reprint of Figure 2-5) shows:

$$dt_{12} = \frac{dP}{\bar{c} + \left(\vec{U} \cdot \hat{n}\right)} \qquad \textbf{(54)}$$

where $\vec{U} = u\hat{\mathbf{i}} + v\hat{\mathbf{j}} + w\hat{\mathbf{k}}$.

again by neglecting $\frac{\left(\vec{U} \cdot \hat{n}\right)^2}{\bar{c}^2}$ and higher order terms from Equation 50 since $\frac{\left(\vec{U} \cdot \hat{n}\right)}{\bar{c}} << 1$

leads Equation 54 to:

$$dt_{12} \approx \frac{1}{\bar{c}}\left(1-\frac{\left(\vec{U}\cdot\hat{n}\right)}{\bar{c}}\right)dP. \qquad \textbf{(55)}$$

Using the geometric relationships in Figure 5-8, the relationships $u=\bar{u}+u';\ v=\bar{v}+v';\ w=\bar{w}+w',$ and finding the dot product to integrate Equation 55, results in

$$t_{12} \approx \frac{L}{\bar{c}}-\frac{1}{\bar{c}^2}\int_0^L\left(\left(\bar{u}+u'\right)\cos\theta+\left(\bar{v}+v'\right)\cos\alpha+\left(\bar{w}+w'\right)\cos\beta\right)dP. \qquad \textbf{(56)}$$

Now for the derivation for a sound pulse propagating in the opposite direction:

$$\frac{d\vec{P}}{dt_{21}}\cdot\hat{n}=\left(\bar{c}-\vec{u}\right)\cdot\hat{n}, \qquad \textbf{(57)}$$

Resulting in

$$t_{21} \approx \frac{L}{\bar{c}}+\frac{1}{\bar{c}^2}\int_0^L\left(\left(\bar{u}+u'\right)\cos\theta+\left(\bar{v}+v'\right)\cos\alpha+\left(\bar{w}+w'\right)\cos\beta\right)dP. \qquad \textbf{(58)}$$

Now, the difference between the time of flights for sound pulses propagating upstream and downstream is

$$\Delta t=\frac{2t_o}{-\bar{c}\,L}\left(\int_0^L\bar{u}dP+\int_0^L u'dP\right)\cos\theta-\frac{2t_o}{\bar{c}\,L}\left(\int_0^L\bar{v}dP+\int_0^L v'dP\right)\cos\alpha-\frac{2t_o}{-\bar{c}\,L}\left(\int_0^L\bar{w}dP+\int_0^L w'dP\right)\cos\beta \qquad \textbf{(59)}$$

rearranging

$$\frac{-\overline{c}\,\Delta t\,L}{2t_o} - \int_0^L u'_P dP = \int_0^L \overline{u}_P dP, \qquad \textbf{(60)}$$

where u'_P is the fluctuating velocity component along path P and $\overline{u}_P$ is the mean velocity component along path P. Now assuming that the average velocities in the 'y' and 'z' directions are zero, Equation 60 becomes

$$\frac{-\overline{c}\,\Delta t\,L}{2t_o} - \int_0^L u'_P dP = \left(\int_0^L \overline{u} dP\right)\cos\theta. \qquad \textbf{(61)}$$

where there can still be fluctuating velocities in all three directions. For the case of a uniform flow,

$$\overline{u} = \frac{-\overline{c}\,\Delta t}{2t_o \cos\theta} - \frac{\int_0^L u'_P dP}{L}, \qquad \textbf{(62)}$$

which, when simplified, is Equation 20 modified by turbulent velocities in each direction. The difference between Equation 20 and Equation 62 is that Equation 62 properly accounts for the velocity fluctuations of turbulent flow, resulting in the determination of the average velocity temporal fluctuations in terms of fluctuating velocity component. The accurate measurement of flow velocity requires a full understanding of the velocity fluctuations of the flow field being examined. Conversely, these measurements afford a better understanding of the velocity fluctuations.

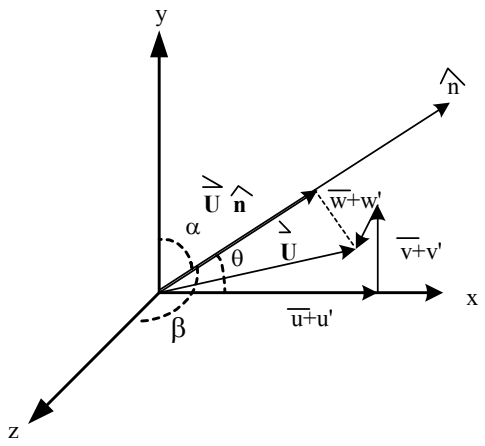

Figure 5-8 Velocity Vectors in a Flow (General)

6 Discussion of Assumptions

In order to test the premise of this dissertation, numerous assumptions have been made to create a simple model. This model can then be defined, mathematically resolved, and applied to increasingly complex scenarios. This chapter reviews these assumptions and discusses the resulting effects.

6.1 Speed of Sound Relative to Flow Velocity

This research assumes that the speed of sound is much greater than the flow velocity, $u<<c$, which is also assumed in literature.[14] This assumption is valid until the velocity increases to a point where the flow field reaches a fraction of that required for supersonic conditions. A calculation of the error, as the velocity or Mach number, M, increases, can be made using Equation 50. For M = 0.05, the error using Equation 50 will be 0.25%, and for M = 0.1 the error will be 1%. The ultrasonic flowmeter will still work, but the derivation of the controlling equations will change and the Δt behavior will no longer be linear with flowrate. Overall, this is a reasonable assumption since the error for a Mach number of 0.05 is a quarter percent.

6.2 Sound Attenuation

Sound typically attenuates as it travels along a path. For example, it becomes more and more difficult to hear someone speak as the distance between the speaker and the listener

increases. For this work, it was assumed that the sound will traverse the flow at reasonable power levels such that the sound pulse will propagate over the entire path. Attenuation of sound is strongly frequency dependent, so as the frequency increases, the power must be increased accordingly. The accuracy of a flowmeter is dependant on frequency, for example, long wavelengths will propagate long distances, but will result in a less accurate measurement. Higher frequencies or shorter wavelengths are more desirable from an accuracy point of view, but are more highly absorbed by the media, requiring more power. However, depending on the system, a frequency can be found which optimizes the length of the sound wave for the required traverse distance.[35] This assumption has no practical effect on the data reported here as the power needed to allow the sound to be received has no effect in the analysis.

6.3 Sound Beam Diameter

Two types of transducers are used for flow measurement applications. The first type is a high frequency flat transducer which typically includes appropriate impedance matching and acoustic lenses such that only a 3° or 4° spread[8] is produced. The second type of transducer is a high frequency of hemispherical design, which produces a spherical wavefront that radiates as if produced by a point source. With both types, it is assumed that some small bundle of sound rays will have enough power (Section 6.2) to directly reach the receiving transducer. In this work, a planar wave front is assumed to be used and that it does not spread. Several effects occur because of these assumptions, first it is

important that a sufficient beam diameter be present such that the entire beam is not swept past the receiver at the highest flow velocities. This assumption can be enforced in three ways, first the beam width can be adjusted wider if the beam is being swept past the receive transducer. Also, the transducer can be reoriented so that the sound path is at a slightly steeper angle. A second effect of this assumption is that no portion of the sound beam which would have spread beyond the original diameter would arrive at the receive transducer first. If this were to occur, the time of flight would be shorter causing the Δt to be different. This effect is not likely to affect this analysis since the portion of the sound which spreads would have to take a longer curved path to reach the receive transducer.

6.4 Time Step-size

From the discussions in Chapter 4 the time step must be small enough to assume constant sound and fluid flow velocities during the time step. This assumption ensures that the vector addition of the sound velocity and fluid velocity vectors used constant velocity vectors during a step. By using constant velocity vectors, a more precise result can be computed. The step-size used was based on two requirements, first the size had to be small enough to ensure the flow velocities did not change significantly during each step. The high speed of the sound relative to the fluid allows the approximations in the derivations in Section 4.2 and 5.3 to be held. The second step-size requirement was that the step be small enough to produce a stable result.

A calculation of the Kolmogrov sized eddy [66] in a flow with an Re = 100,000 indicates an eddy size of 27μm so that the step-size of 0.1μm used in this work meets the requirement. In all cases analyzed, the fluid was assumed to be water with M < 0.01. The end result of choosing a small step-size is that it allowed the flow velocities to be constant during a time step and the resolution of the computation to be stable.

6.5 Frozen Flow Assumption

The frozen flow assumption in fluid mechanics can be applied to a flow field for short periods of time to hold the fluid velocities constant during a calculation. Proper application implies that during the calculation, the flow would not radically change from its 'frozen' state.

6.5.1 Reason for Frozen Flow Assumption

Several techniques exist for determining the Δt between the forward and reverse propagation times of the sound waves in a time of flight type ultrasonic flowmeter. Generally, the techniques vary from one where both waves propagate in opposite directions simultaneously to multiple waves propagating in one direction then reversing to the other direction. The flowmeters using the simultaneous technique assume that to get the most accurate flow velocity, one must ensure that the sound waves are propagating across the flow field at the same time. On the other-hand, the meters which send several sets of waves first in one direction and then in the opposite direction, assume the flow

field has an average constant value. These particular meters cannot resolve time varying flow with precision.

It is sometimes assumed that sound waves sent simultaneously in opposite directions in time-of-flight meters results in more accurate flow measurements. However, there is a problem with this assumption making the problem more difficult than necessary as illustrated in the diagram shown in Figure 6-1. Here the system is shown as a straight line system; however, in reality, the wave front sweeps downstream and stays with the fluid particles that started out within the straight measurement volume. So, when sound waves are launched simultaneously, the fluid particles and local flow patterns at the beginning of one sound propagation path are not the same as the particles at the end of the opposite propagating sound path particularly in turbulent flows, even when the sound waves are launched simultaneously. The remaining parts of this Section 6.5 will discuss the actual limitations needed to be placed on the system with regard to sound wave launch times.

6.5.2 Description of Frozen Flow Assumption

To enable one to start an analysis of sound propagating across a turbulent flow field using actual turbulent velocity data, an assumption about the flow field must be made. Since, for most applications, the speed of sound is very much greater than the fluid velocities, it is reasonable to invoke the frozen flow assumption. Frozen flow means that during the

passage of acoustic waves, the fluid velocities in the flow field remain fixed during the entire propagation time.

As discussed, in time-of-flight type ultrasonic flowmeters, sound propagating in both directions along the acoustic path is used to make the velocity measurements. The difference in these propagation times, Δt, is proportional to the average velocity along the path as described in Chapter 4. It has been postulated that an accurate velocity measurement requires forward and reverse propagating sound waves to go through the same fluid particles, and therefore fluid structures. Thus, ultrasound must be launched at the same moment in opposite directions along the measurement path and then each transducer becomes a receiver. In this method, the sound waves propagate through the same fluid structures at the center of the path, but at both ends the sound waves are not actually in the same fluid packets. However, due to the relative differences between the speed of sound and speed of the fluid flow, it is possible to determine if a fluid packet moves entirely out of the sound path between the arrival of two oppositely propagating sound waves. If sound speed is high and the path not too long the fluid will not move much during the sound wave propagation time, hence frozen flow. To use the frozen flow assumption, one must decide when it applies, and for how long the assumption is valid.

6.5.3 Validity of Frozen Flow Analysis

The smallest eddies in a turbulent flow occur at the Kolomogrov scale. The size of these eddies can be approximated using the relation[66]

$$\eta = L\left(\frac{1}{Re}\right)^{3/4}. \qquad \textbf{(63)}$$

where:

$\eta \equiv$ smallest eddy size

$L \equiv$ length scale

$D \equiv$ flow length scale

$Re \equiv \frac{\bar{u}\, D}{\upsilon}$

Using this relationship, the length scales for eddies in four flow fields, 2 each in air and water, have been computed and compared with the results shown in Table 6-1. The comparisons are for air flowing at 3.05m/sec, and 30.5m/sec and water flowing at 0.305m/sec, and 3.05m/sec, which are reasonable velocities for each fluid. In addition to the Kolomogrov eddy size being computed, the number of Kolomogrov eddies which can fit within the diameter of a typical sized sound path can be determined. For water with the flow conditions computed and typical sound path size, between 500 and 2900 eddies can fit within the sound path. For air, the sound path is larger due to lower frequency ultrasound being used, so more eddies can fit in the sound path, calculated to be between

1500 and 8700 eddies. The largest eddy size in a pipe flow would be approximately ¼ pipe diameter[66] in a turbulent pipe flow or 38 mm in these cases. Therefore, there is a large range in the number and sizes of eddies in the measurement volume. As long as there are "many" Kolomogrov scale eddies in the entire measurement volume, it is assumed that differences in propagation time for the sound waves will cancel the effects of individual vortices. Each small eddy has an effect on the sound wave, but because of the high number eddies and the randomness of the eddies, the "law of large numbers" can be invoked[6]. By invoking this law, the many small random variations are canceled, leaving only the larger eddies to affect the velocity computation. The logical question now is what size eddies will affect the sound wave passage.

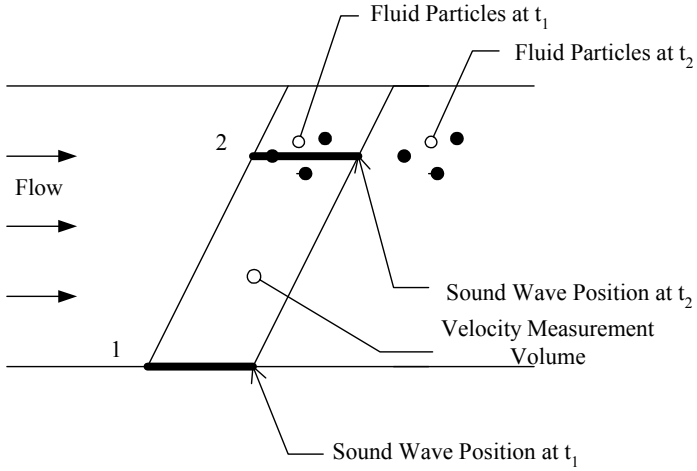

Figure 6-1 Sketch of Velocity Measuring Volume; Ultrasonic Sound Wave Launched at Location 1 and Time t_1; Ultrasound Wave at Location 2 and Time t_2

In the case where there are few eddies of a size, the law of large numbers no longer applies. Thus, given larger eddies, the planar wavefront will warp as shown in Figure 6-2, because of the positive and negative distortion of the rays. This effect will begin to be observed as the eddy size approaches the beam width size. When the characteristic length scale of the eddies grows to approximately two times the beam width,

$$L \approx 2\beta , \tag{64}$$

where β is the beam width, the eddy seems to have an effect on the sound wave front. To cause the greatest effect on sound wave passage, the eddy centerline should just be entering the measuring volume as the sound wave passes it. The relative velocity resulting from the combination of the axial and vortex flows will be in the '-y' direction and '+x' direction, downward and to the right, as depicted in Figure 6-3. However, if the return sound wave passes the eddy after its center crosses through the volume, the velocity field will be in the opposite direction. For this case, the measured Δt will be completely different than the average Δt with no vortices passing through velocity measurement volume.

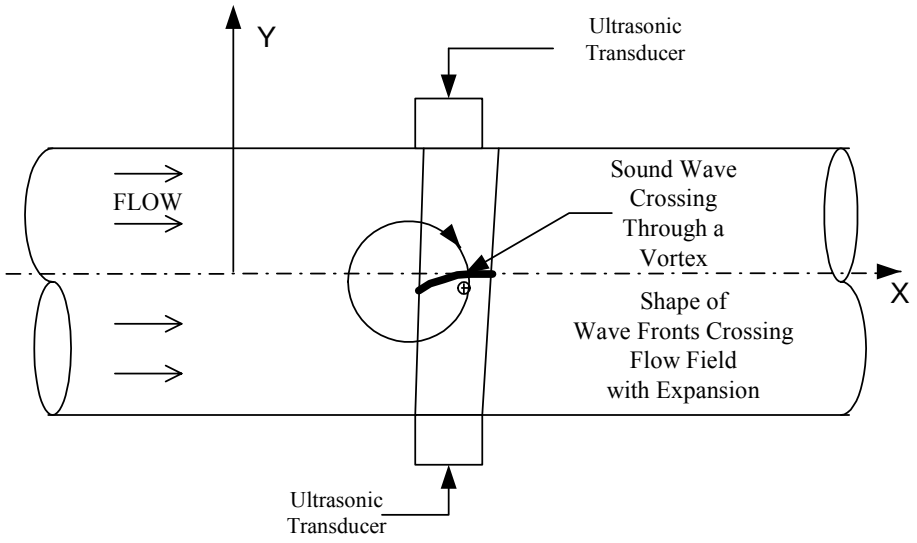

Figure 6-2 Sketch of Sound Front Warping as it Passes Across a Vortex Centered within the Velocity Measurement Volume

Table 6-1 Characteristic Eddy Size for Varying Reynolds Numbers

Fluid	Velocity (typ) (m/sec)	Characteristic Length Scale in Flow (mm)	Kolomogrov Eddy Size (typ) (μm)	Diameter of Transducer (typ) (mm)	Number of Eddies in Diameter of Transducer
Air	3.05	152	16.4	25.3	1542
	30.5	152	2.9	25.3	8724
Water	0.305	152	12.2	6.4	524
	3.05	152	2.2	6.4	2909

To eliminate the problem of the vortex centerline crossing all the way across the measuring volume an assumption that 50% of the fluid in the sound path at the time of transmission of one of the sound waves is still in the straight line sound path at the time of transmission of the second sound wave. Due to this assumption, we can expect negligible differences in the characteristics of the fluid velocities over which the sound waves

propagate. So if the volume of fluid particles change is limited to 50% of the volume, the maximum allowable path length can be calculated. Also by using this assumption, the minimum pulse repetition rate required to insure that both the upstream and downstream sound waves propagate through the same velocity field can be determined. The time for the sound wave to propagate across the pipe is,

$$t_s = D/\overline{c}\,. \qquad \textbf{(65)}$$

The time for the fluid to propagate through measurement volume is

$$t_f = D/\overline{c}\,. \qquad \textbf{(66)}$$

Table 6-2 presents results of calculations for the distance an average fluid particle travels during the transit time of a sound wave across a 0.305 meter velocity field, this distance is

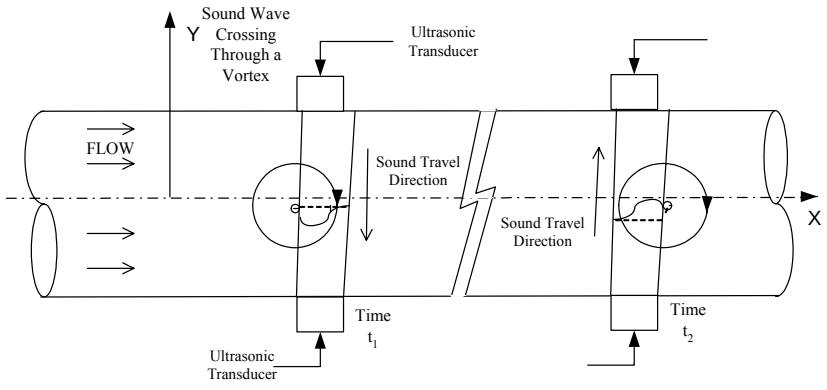

Figure 6-3 Comparison of the Effect by a Vortex Twice the Size of the Velocity Measurement Volume Width on Oppositely Propagating Sound Waves. The Dashed Line Represents an Unaltered Sound Wave Front while the Solid Curved Line Represents the Effect of the Vortex on the Sound Wave Front

then compared to a selected beam width. Additionally, a maximum sound path length can was computed based on a single sound wave propagating across a velocity field,

$$L = \left(\frac{\beta}{2v} \right) \bar{c}, \tag{67}$$

assuming an average fluid particle is allowed to travel half a beam width. Finally, an allowable delay was calculated between receiving a signal and transmitting the return signal,

$$\tau_w = \frac{\beta}{v} - \frac{2D}{\bar{c}}. \tag{68}$$

As can seen in Table 6-2, for an average velocity of 30.5 m/sec in either air or water, a fluid particle will travel approximately 100% of the beam width with just one sound pulse crossing the pipe diameter. This indicates that the beam will be swept downstream of the transducer. In order to make measurements in these fluid velocities, the beam width should be increased by approximately a factor of two. However, for an average velocity of 3.05 m/sec in either fluid, a fluid particle will only move approximately 10% of the sound beam width, and as can be seen, there is a delay permitted before the second signal is sent. In this case, the frozen flow assumption as defined is satisfied.

The time, τ_w, is the minimum pulse rate between receiving a sound wave and launching the opposite sound wave, while ensuring that the return wave is still within the original domain of fluid particles. All these computations were based on a 30.5 cm path length in

air and water at standard temperature and pressure. For the case of air, the beam width was chosen to be 25.3 mm, and in water the beam width was chosen to be 6.4 mm. Fluid velocities used in these computations were 3.05 and 30.5m/sec for air and .305 and 3.05m/sec for water. It is noted that at the highest velocity shown in each fluid no time delay can be tolerated, necessitating the need for simultaneously launched sound waves. But for the lower velocities shown, some reasonable delay between the launching the opposing waves can be tolerated without breaking the assumption that 50% of the fluid particles must remain in the measurement volume.

6.5.4 Frozen Flow Assumption Conclusions

It is concluded, using the frozen flow assumption that the analyses performed in this work and in the actual operation of a typical flowmeter that the sound waves can be sent sequentially from each side of a typical flow. Allowing this assumption means that the typical flowmeter application electronics and transducers can be simplified. The reason for this simplification is that sound waves do not need to be generated simultaneously at each transducer, and the transducer ring down time, defined as the time required for the transducer to finish resonating, can be longer. Since this is how most flowmeter applications operate, the analysis presented in this work will be more representative of actual hardware. All further discussions and analyses in this work assume the frozen flow, and also assume that the sound pulses are sent sequentially; that is, the pulses are sent first from one direction then in the reverse direction. Additionally, wait time between the receiving of the first sound pulse and the launching of the second pulse is short enough to

ensure no more than 50% of the fluid particles in the sound propagation path are exchanged at the time the second sound pulse is received.

Table 6-2 Estimates of Validity of Frozen Flow Assumption

	Air	Water
Distance Fluid Particles will Travel During Propagation of a Sound Wave		
Flow Velocity = 30.5 m/sec	26.8mm(105% Beam Width)	6.0mm(99% Beam Width)
Flow Velocity = 3.05 m/sec	2.68mm(11% Beam Width)	0.6mm(10% Beam Width)
Flow Velocity = 0.305 m/sec	0.268mm(1%Beam Width)	0.06mm(1% Beam Width)
Maximum Length of Sound Propagation Path		
Flow Velocity = 30.5 m/sec	143 mm	155 mm
Flow Velocity = 3.05 m/sec	1.43 m	1.55 m
Flow Velocity = 0.305 m/sec	14.3 m	15.5 m
Allowable Delay Between Receiving the First Signal and Transmitting the Second Signal		
Flow Velocity = 30.5 m/sec	0 seconds	0 seconds
Flow Velocity = 3.05 m/sec	2.4 milliseconds	0.6 milliseconds
Flow Velocity = 0.305 m/sec	39 milliseconds	10 milliseconds

7 Methodology

Restating the hypotheses presented in Chapters 1 and 3, the variations in the individual transit times of ultrasonic pulses represent variations from the mean flow velocity, thus causing perceived flowmeter inaccuracies. Further, the variations in individual transit times of ultrasonic pulses are caused by naturally occurring turbulence in a flow system. In order to determine the effect of a turbulent flow field on the passage of acoustic waves, a systematic approach was developed to analyze the effect of velocity fields on the propagation time of ultrasonic pulses. Initially, a simple flow field was chosen which would provide a varying velocity and allow Equation 6 to be solved using a piece-wise numerical integration method. This allowed all the variables to be known over short discrete distances along the sound propagation path. A flow field providing these characteristics is a vortex street superimposed on a uniform flow. By using this particular flow field, it was possible to determine an exact representation of the flow and calculate a varying Δt for the sound waves propagating upstream and downstream.

A computational Ray Trace Method was then used to analyze the same flow field, this Modified Ray Trace Method was designed to follow five rays across the flow field using equal time steps. The local flow and sound velocities were calculated at each ray position for every time step. The superposition principle was used to compute the local velocity vector and the Ray Trace Method was used to determine the ray path. Therefore, both the

increase in path length over a straight line as well as turbulent velocity affects are calculated.

After using the computational method to determine the Δt's, comparisons could be made between the two methods, proving the veracity of the computational approach. After verifying the code, the simplified vortex street flow was replaced with a PIV measured turbulent flow field, and a similar analysis was conducted.

In the simplified flow analysis, the velocity field at each step for each ray was computed. An important variable to consider when analyzing the difference between the upstream and downstream propagation times was the time step. Because the difference between the upstream and downstream propagating pulses was approximately five orders of magnitude smaller than the time required for the sound pulse to propagate across the flow field, the step-size had to be at least the same order of magnitude of these expected Δt's. When the simplified flow field was replaced by the PIV measured flow field, the same time constraints were required. The major difference between the simplified flow field and the PIV measured flow field was that the simplified flow field was continuous while the PIV field was defined by discrete points. Due to this difference, a spatial interpolation procedure had to be implemented to fill in the coarse velocity grid and produce the resolution necessary for the required step-size. The interpolation allowed for the very fine time steps required to determine a difference between the forward and reverse propagating

sound waves. The interpolation performed between the grid points was a linear interpolation between the four surrounding data points. The assumption is that the velocities vary linearly between the data points and that the variations of these velocities are smooth.

7.1 Ray Trace Method

7.1.1 Single Ray

In a standard Ray Trace Method, the ray is an infinitesimal line representing the sound pulse direction. As discussed in Section 4.0, using standard vector analysis, the sound pulse vector and the local flow velocity vector can be combined to obtain a resultant vector. In this way, the path a sound pulse takes to cross a flow field may be calculated. Since the ray representing the sound is infinitely thin, the path of the ray will only be affected by flow velocities along the path of the ray. The single path approach allows examination of the effects of flow on the propagation of a sound wave. However, since a sound pulse from an ultrasonic flowmeter is a coherent front of finite diameter, the single Ray Trace Method does not provide insight as to how a fluid structure affects the sound pulse. For example, will part of the sound pulse arrive ahead of the rest of the pulse because it is warped by fluid flow structures.

7.1.2 Multiple Rays

In order to simulate the interaction of fluid structures with a finite diameter pulse, multiple ray traces were used, hereafter referred to as the "Modified Ray Trace Method." The rays were positioned close enough together as to allow the assumption of a straight line connecting each ray at a specific time step. In this research, five rays were used to represent a sound pulse allowing the pulse to be divided into quarters. This simulation of a sound pulse was then used to examine effects of flow parameters on the propagation times of the upstream and downstream propagating sound waves.

A parameter of interest was the shape of the sound pulse, see Figure 6-2 for example, as it would determine which "part" of the sound pulse reached the receiver first. To examine this shape, a line drawn through the head of each ray was assumed to describe the shape of the pulse as it crossed through a flow field. As a sound pulse crosses a flow field, the local fluid velocities alter the shape of the pulse. For example, if the sound pulse crossed directly over the middle of a vortex, one side of the pulse would be "warped" up while the other side "warped" down. This warping of the pulse will persist through the remainder of the flow field, unless it is further altered by another vortex, and will cause one side of the pulse to reach the receiving transducer before the other side, resulting in early detection. An early detection would cause one of the times in Equation 17 to be smaller than that which is based on the mean velocity, resulting in an incorrect value of Δt. The Modified Ray Trace Method was also used to determine the deviation of the sound pulse from a straight path as well as the impingement location on the

receiving transducer. Since a curved path results in the sound pulse front being convected further downstream than anticipated, it is possible that the pulse could completely miss the receiving transducer. The curved path also results in a longer sound path than typically anticipated, affecting computation of the average velocity in the sound path, as well as the speed of sound calculation.

7.2 Computer Simulation

Due to the complexity of following five rays through a varying flow field, a computer code was developed to follow the rays and compute the flow velocity at each ray, a flow chart for the code is shown in Figure 7-1. To obtain the computational results, the sound wave propagation direction was chosen, the receiving and transmitting transducer locations were defined, and the time step was chosen, which would result in a "reasonable" time resolution. The choice of time step-size will be discussed in a later section. For each time increment, the velocity in the x-y plane, at the start point of each of the 5 rays was computed using[15]

$$U_{tot} = u + \left\{ \frac{\Gamma}{2\pi r} \left(1 - e^{\frac{-r^2}{4vt}} \right) \right\}. \qquad \textbf{(69)}$$

In the case of the uniform flow superimposed with a Rankine combined vortex street, the uniform flow velocity was added to the velocities induced at the ray origin by each of the individual vortices in the vortex street. Since this calculation was performed for each of the five rays in the system, each ray had a slightly different flow velocity. These flow

velocities were then added to the sound velocity for each ray, and this total velocity was multiplied by the time step-size to find the distance the ray was displaced. After each ray was incremented, the steps were repeated starting with the calculation of the 'x' and 'y' velocities at the new positions. This continued until one of the five rays was received by the receiving transducer on the opposite side of the pipe.

The sound wave front was considered to have been received when any one of the rays intersected the plane of the receiving transducer. The number of steps to traverse the pipe or channel were counted, and when the signal was received, the total number of steps required was multiplied by the time step-size to determine the time required for the sound to propagate across the flow field. After the downstream sound wave front was received, a new wave front was launched in the opposite direction and the same procedure followed. After the upstream signal was received, the downstream propagation time was then subtracted from the upstream propagation time to obtain the Δt. The program saved the time of flights in both directions, the distances traveled in both directions and the Δt's, for later use in data reduction schemes.

The simulation program was quite flexible. Basic quantities such as the fluid properties and the speed of the uniform flow in the 'x' and 'y' directions could easily be varied, as well as the strength of the individual vortices in the vortex street. Additionally, the temperature of the flow, and therefore the speed of sound, the beam width, and the time step taken could easily be specified. Time step-size was important to ensure the results

were stable and well resolved. That is, the data remained the same for smaller time steps once the program reached a certain limiting time step-size.

7.3 Flow Fields

In this research two major types of simulated flow fields were employed. The first was a vortex street in a uniform flow field, the second was a PIV generated data structure of a turbulent flow in a channel. These flows are discussed below.

7.3.1 Vortex Street in Uniform Flow

In order to gain a qualitative understanding of the effect of varying velocities on the magnitude of Δt's measured by an ultrasonic flowmeter, a simple flow field in which the propagation time of the sound pulse varied with time was computed. Such a velocity field can be computed using the superposition of a uniform flow and potential vortices with viscous cores, Figure 7-2, in the form of a vortex street, as shown by Schaefer and Eskinazi.[56] A vortex street is often used to represent vortices being shed from alternating sides of a bluff object in a uniform flow. The use of this flow field in the analysis provided useful insight as to how a real vortex street may affect the measurements of an ultrasonic flowmeter. In addition, as discussed in Section 7.0, since this flow field could be described along discreet points, it allowed for a comparison to the computational solution, thereby verifying the Modified Ray Trace Method. Mathematically, a vortex street is a simple summation of potential flows which easily lends itself to analysis via a

piece-wise numerical integration solution or by numerical procedure. The velocity induced in the 'y', or cross-stream direction is given by:[56]

$$v_{iv} = \frac{\Gamma_o}{2p}\sum_{\pm n=0}^{k}\left[\left\{\pm(-1)^{|n|}\frac{|n|a \mp s}{\left[|n|a \mp s\right]^2 + \left[y-(-1)^{|n|}h_n\right]^2}\right\} * \left\{1-\exp\left[\frac{\left(-\left[|n|a \mp s\right]^2 + \left[y-(-1)^{|n|}h_n\right]^2\right)}{4\upsilon\left[(x-s+na)/2af\right]}\right]\right\}\right]. \quad \textbf{(70)}$$

where:

Γ = circulation strength of individual vortices

n = number of vortices from reference point

a = streamwise distance between individual vortices

h = distance from streamwise axis to individual vortices

s = streamwise distance from reference point to vortex core

y = distance from streamwise axis to reference point

f = frequency of vortex street

p = reference position from start of vortex street

x = distance along streamwise axis

υ = viscosity of fluid.

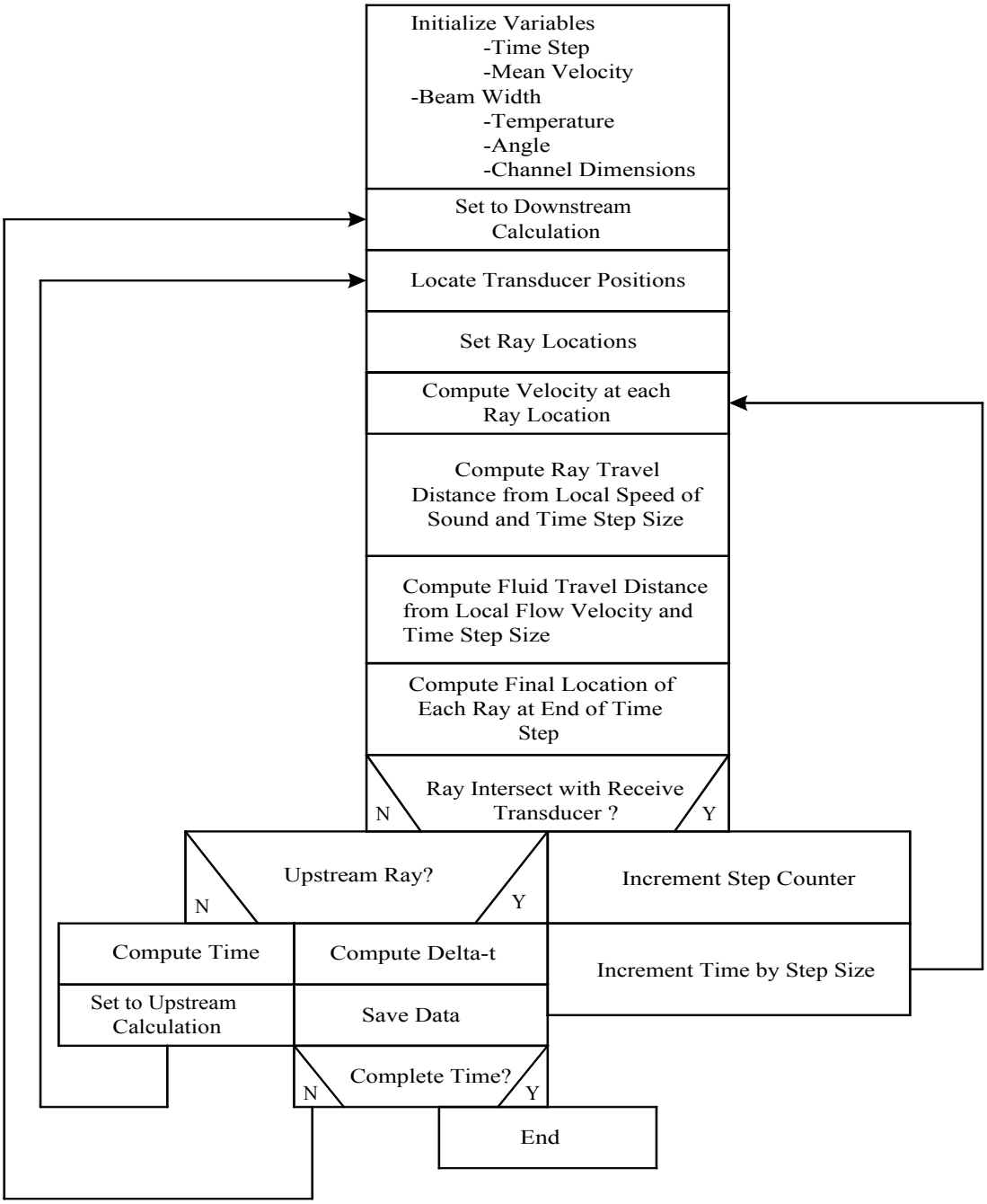

Figure 7-1 Flow Chart for Modified Ray Trace Method Computer Program

Note that the viscosity of the fluid is used in the relationship in Equation 70. By using the fluid viscosity, the vortices were allowed to age with time which enabled a better representation of the vortex street because the vortices downstream of the measurement location will be slightly less influential on the velocities at the measurement location than those vortices upstream of the measurement location. Additionally, Equation 70 builds in the properties of the vortex core, such as velocity going to zero at the center of the core.

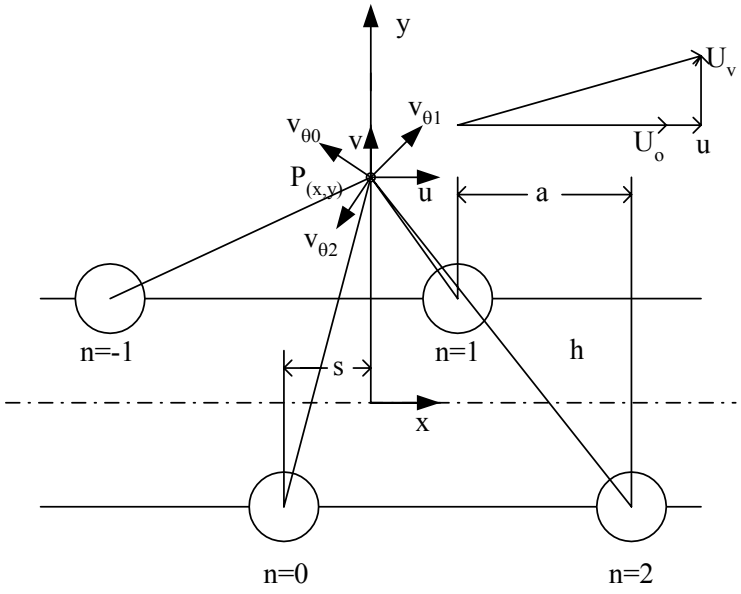

Figure 7-2 Diagram of Vortex Street Showing How a Point Velocity is Computed Relative to Vortices in a Vortex Street.

The velocity in the 'x' or streamwise direction was the uniform flow velocity plus the velocity in the 'x' direction induced by the vortices in the vortex street. The flow model geometry is depicted in Figure 7-3. The perpendicular line between the ultrasonic transducers is the reference line on which Equation 70 was applied to compute 'y'

direction velocities induced by the vortex street. The Δt was defined as shown in Equation 17

$$\Delta t = t_{up} - t_{dn}. \tag{71}$$

To start, the t_{up} and t_{dn} were determined by summing each segment distance divided by the speed of sound and y velocities induced by each vortex in the street

$$t_{up} = \sum_{i=0 \text{ to } N} \left(\frac{\frac{D}{n}}{c + v_{iv}} \right), \tag{72}$$

and

$$t_{dn} = \sum_{i=0 \text{ to } N} \left(\frac{\frac{D}{n}}{c - v_{iv}} \right), \tag{73}$$

where: n = number of segments the sound path is divided into and where N = Number of vortices. What Equations 72 and 73 indicate is that the time required to propagate in one direction or the other along a known sound path is determined by summing each small path segment divided by the total of the velocity induced by the vortex street added to or subtracted from the speed of sound.

Since the vortex street was constructed of viscous core vortices, there was decay in vortex strength with time. In order to track this decay, a time scale had to be set up for

the vortices; the time scale for each individual vortex started at the center of the bluff body as shown in Figure 7-3. The sound path was located approximately 10 body diameters downstream of the actual bluff body.

As the individual vortices of the vortex street passed through the path of the sound beam, the time required for sound to cross the flow field was either shortened or lengthened depending on the direction of propagation of the sound wave relative to the rotation of

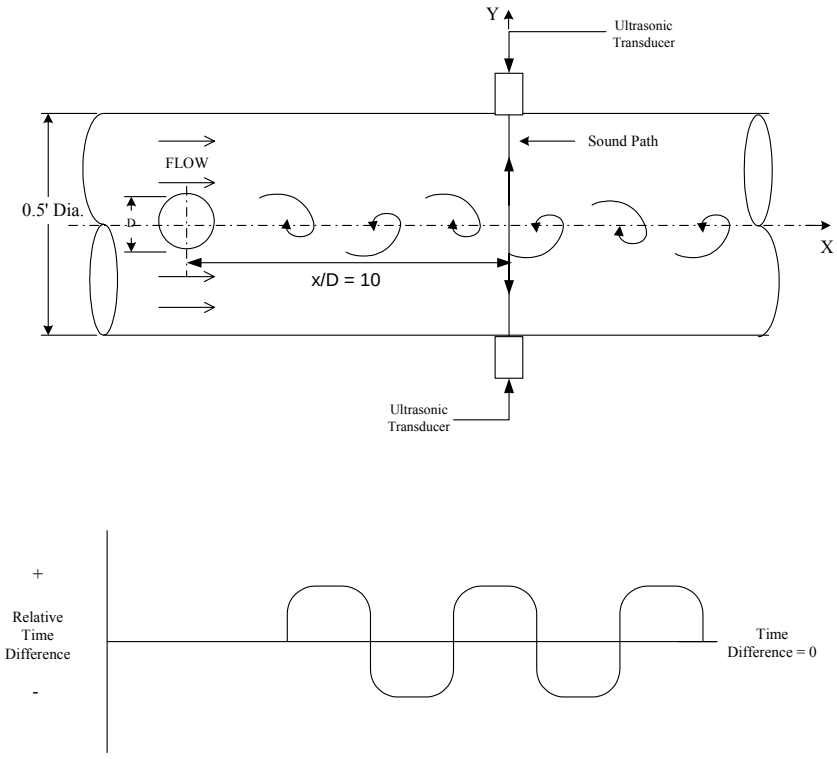

Figure 7-3 Geometry of Potential Flow Model Superimposing Vortices on a Uniform Flow

the vortex. Since ultrasonic flowmeters compute flowrate based on the difference between the upstream and downstream propagation times of the sound wave, large fluid structures, such as vortices, seem to affect accuracy by imparting data fluctuations.

7.3.2 PIV Measured Turbulent Flow

The final part of the study utilized turbulent flow data obtained from PIV measurements. In this portion of the work, a set of PIV data was used to determine the velocity at each location along the ray. After testing the Modified Ray Trace Method program on the vortex street flow, the same program was adapted for application to a PIV measured flow field.

The PIV technique typically uses an asynchronous laser sheet and cameras to determine the magnitude and direction of a velocity flow field. The technique produces a near instantaneous two-dimensional grid of velocity vectors for a flow. In this way, a flow field can be frozen and various analyses can be performed on the field. The PIV data is a set of discrete 'x' and 'y' measured velocities from a specific area of the turbulent flow field. The advantage of using the PIV technique is that all the velocities within a defined area are measured simultaneously. To obtain the 2-D velocity grid used in the PIV technique, the flow field is broken up into many overlapping areas. The velocities within each small area are measured and then averaged, resulting in a single velocity vector for the area. The resultant PIV data are discretized, making it necessary to interpolate between the individual points to produce the continuous field required, as discussed in Section 7.0, for this study. Typically, PIV systems will take data at rates nearing 15 Hz.

The PIV channel flow data used in this investigation was obtained from Dr. Kenneth Kiger of the University of Maryland. The channel used to obtain the data was 4 cm wide by 6 cm high, and 4.87 m long. The test location was approximately 420 cm downstream

of the entrance to the channel. The Reynolds number based on channel width was approximately 23,000. The velocity fields were measured at 15 Hz for approximately 51sec thereby obtaining approximately 768 velocity fields. A grid of 122 points spanwise by 67 points streamwise was used in obtaining the velocity data. To produce as dense a grid as possible within the limitations to the PIV system, the grid overlaid slightly more than ½ the channel and was sized at 2.2 cm by 2.2 cm, giving a grid spacing of approximately 0.18 mm spanwise and 0.32 mm streamwise.

7.4 Verification of the Modified Ray Trace Method

In order to verify the Modified Ray Trace Method, a piece-wise numerical integration scheme was used to compute the effect on the Δt, and therefore, the velocity calculation. As depicted in Figure 7-4, a vertical line was established within the vortex street. Along this vertical line 61 points were established, 30 on each side plus the centerline, at each point the 'y' direction velocity could be calculated with Equation 70. The velocities are summed along the line with the induced velocities of the vortex street calculated at each point. The induced velocities are both added and subtracted from the sound velocity and a time to travel from one side to another is computed. The Δt along this line could then be computed. The line is then moved upstream and a new Δt is calculated, this process continues from the centerline of one vortex to a second vortex, n=1 and n=2 shown in Figure 7-2. The results of this piece-wise numerical integration are discussed in Section 8.2.

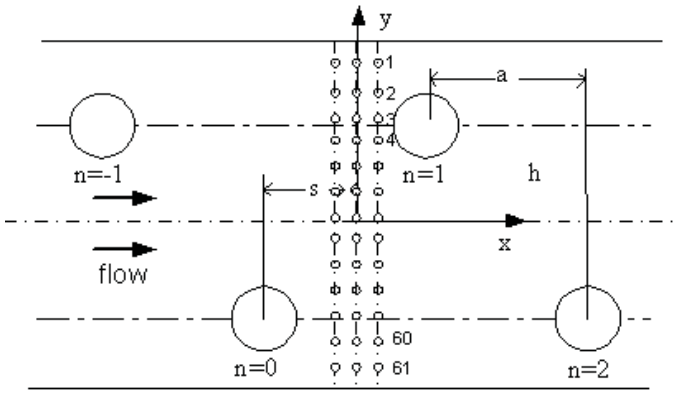

Figure 7-4 Setup for the Piece-wise Integration Scheme

8 Results for the Vortex Street Flow Fields

The Modified Ray Trace Method described in Chapter 7, was used to determine the propagation characteristics of coherent sound pulses though flow fields. Initially, a simple flow field which lent itself to a piece-wise numerical integration solution was chosen for analysis. This simple field was a vortex street superimposed on a uniform flow. Initial analysis was done by inspection, followed by an exact solution to the problem, for the case of a single ray crossing the flow field perpendicularly. Next, the Modified Ray Trace Method was applied, which by use of multiple rays allowed for analysis of a finite sound beam pulse in the simplified flow field. The results were compared to each other to ensure all three methods agree. When the methods agreed, the Modified Ray Trace Method was then used to analyze a number of different flow conditions and sound path variations.

8.1 Estimation of Δt via Inspection

It is not difficult to qualitatively determine the effect of a vortex on the propagation time of a sound wave moving perpendicular to a fluid flow. As a vortex street passes through the sound beam path, the time difference, Δt, between the upstream and downstream propagation times will vary depending on the location of the closest vortex core relative to the sound path. As depicted in the sketch shown in Figure 8-1, when a vortex with clockwise motion is located to the left of the sound path, the measured Δt will be positive.

As a vortex core passes through a sound path perpendicular to the main flow direction, Δt will pass through zero as there is no net velocity in the 'y' direction. As the vortex core continues to propagate to the right of the sound path, the Δt becomes negative, but as the next vortex moves closer to the sound path, the opposite will occur, since the next vortex in a vortex street has a counterclockwise motion. The temporal variation of Δt appears to be a periodic sequence of square waves because the relative fluid motion in the 'y'

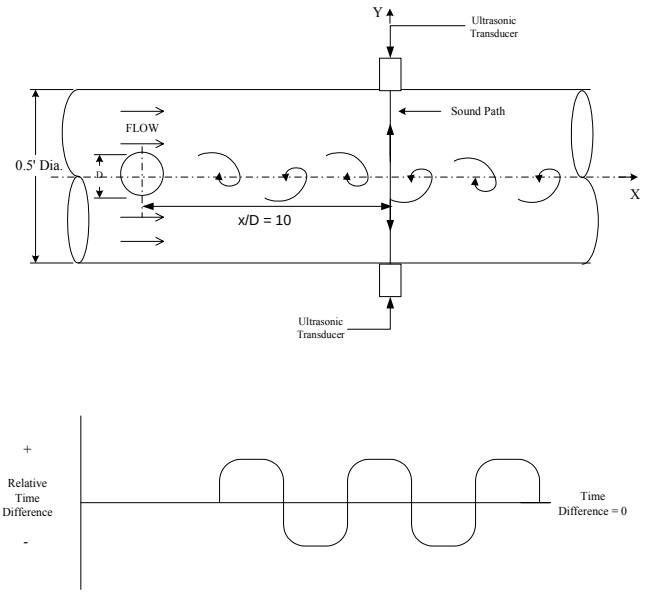

Figure 8-1 Geometry of Potential Uniform Flow Model Superimposed with Free Vortices, and Sketch of Δt.

direction starts at zero when the center of the vortex core coincides with the acoustic beam. The Δt quickly increases as the edge of the core approaches. As the sound wave propagates through the inviscid region of the vortex, the individual Δt realizations return to zero. However, simultaneously, the next vortex causes the Δt realizations to return to an absolute maximum. Therefore, the interaction of these two vortices should cause the Δt to remain at or near the absolute maximum until the second vortex core crosses the

sound path. The signal will then cross zero rapidly and become an absolute maximum again, Figure 8-1. This pattern repeats itself as long as the vortex street crosses the sound path of an ultrasonic flowmeter. If the vortex did not contain an irrotational outer region and was composed entirely of a rotational core, the signal shape would be a saw tooth pattern as depicted in Figure 8-2. In this pattern, the maximums and minimums would be nearly half-way between the individual vortex cores.

This analysis by inspection was quite simple and assumed the sound waves propagating in a straight line, meaning that a sound wave front is not allowed to be bent or curved off the straight line path between the transducers by the velocity of the fluid. In addition, the

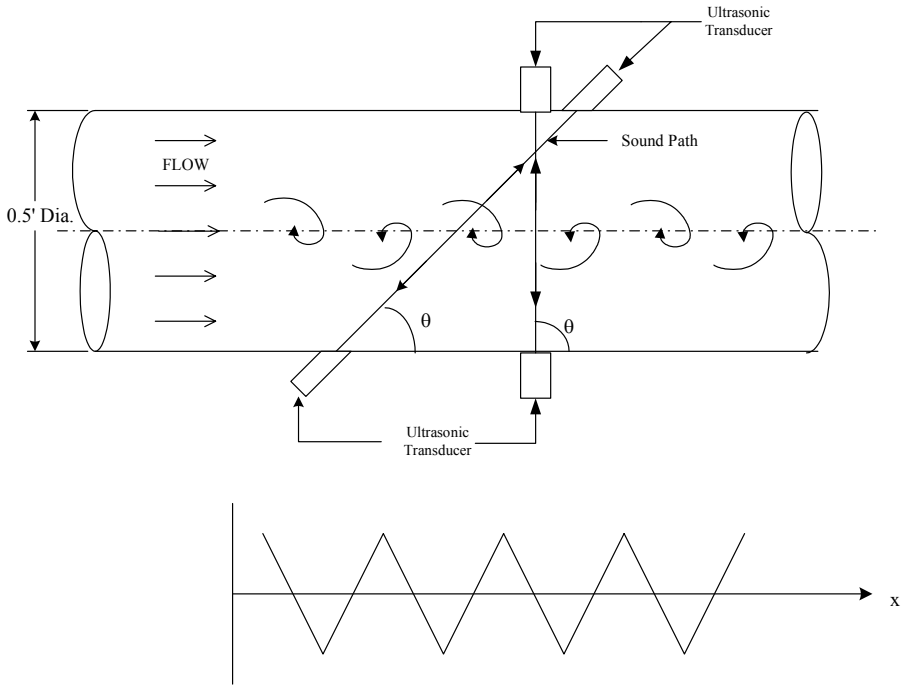

Figure 8-2 Geometry of Potential Flow Model with Superimposed Rotational Vortices, and Sketch of Δt.

assumption used an infinitely thin ray to perform the analysis, which, as was discussed in Section 7.1.1, does not allow for the examination of the interaction of a finite width sound beam pulse with a flow structure such as a vortex street.

8.2 Computation of Δt via Piece-wise Numerical Integration Method

The problem of a pair of sound waves propagating perpendicularly in opposite directions across a uniform flow field with a superimposed vortex street, Figure 8-1, can be computed using a piece-wise numerical integration method (which is discussed in Section 7.3.1), from Equation 70. The results of these calculations are shown in Figures 8-3 and 8-4. Figure 8-3 is a plot of the results of an integral computation for a single set of variables, while Figure 8-4 represents the same data compared to two other computations

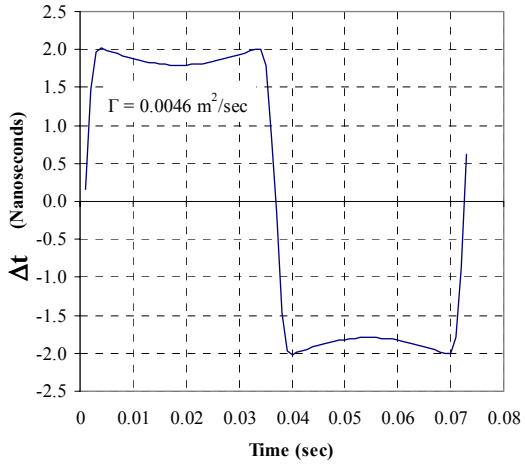

Figure 8-3 One Dimensional Analysis of Sound Waves Propagating Back and Forth on a Perpendicular Path, as Shown in Figure 8-1, Across a Uniform Flow with a Vortex Street Superimposed. This Represents the Expected Δt Between the Wave Propagating in Opposite Directions.

for different vortex strengths, Γ. The vortex street, as discussed in Section 7.3.1, was modeled using viscous core vortices and was first modeled using this method by Schaefer and Eskinazi.[56] In Figures 8-3 and 8-4, the difference in propagation time between the two sound waves propagating in opposite directions, a single Δt realization, is plotted together with Δt realizations from other discrete time steps. The velocity field was "frozen" for the entire calculation, and the perpendicular reference line or sound path, shown in Figure 8-1, moved in the negative 'x' direction between each discrete realization. For these computations, the variables were set at magnitudes that one may find in a typical 6 inch pipe with water flowing. The uniform flow was set at 3.048 m/sec, the vortex strength, Γ, was set at 0.009 m^2/sec, and the oscillation frequency was 21cycles/sec. In addition, a cross-stream separation of the vortices can be defined, based on the diameter of the bluff body creating the vortex street. The Strouhal number, St, was set to 0.21 based on a typical value for a high Reynolds number flow,[51] but can be varied if desired. Knowing the St number, one can then determine the period of the Δt time series realization plot; for example, for a free stream velocity of 3.048 m/sec and a bluff body diameter of 2.29 cm, the expected vortex shedding period would be 35.7 milliseconds. The Γ chosen is representative of a typical Γ strength in a vortex street. The y direction velocities induced by the vortex street are computed using the relation by Schaefer and Eskinazi,[56] Equation 70. This relation allowed the vortices to 'age' as they moved downstream from the bluff body. The sound path is located such that the transducer nearest to the bluff body was 10 diameters downstream from the body as

shown in Figure 8-1. The age of each vortex is important because as the individual vortices move downstream viscous losses cause the vortices to spread altering the measured Δt. The 10 diameter downstream location was chosen as it is within the region considered to have well developed vortices in a vortex street wake behind a bluff body in a cross-stream.[56] This well developed region continues downstream far enough to allow the upstream location of the transducers to remain the same while the downstream transducer was moved, but the sound path between the two transducers remains within the well developed region.

In Figure 8-3, it may be noted that the Δt realization signal is similar to the result sketched in Figure 8-1 obtained by "inspection". The major difference between these two

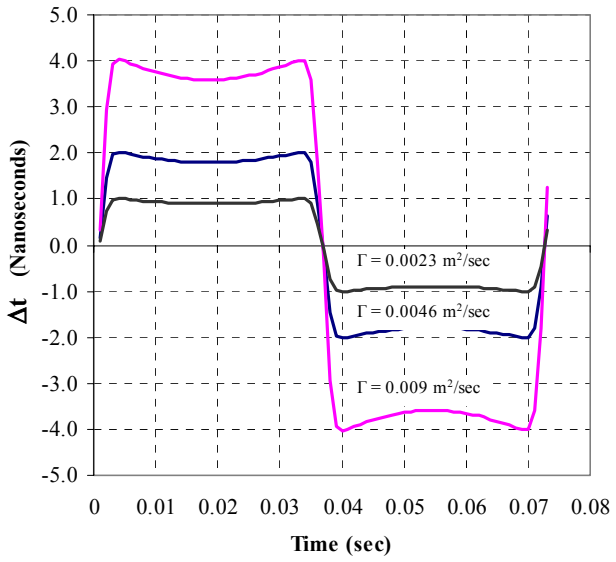

Figure 8-4 One Dimensional Analysis of Sound Waves Propagating in Opposite Directions Across a Uniform Flow with a Superimposed Vortex Street. Each Line Represents a Different Vortex Strength, Γ.

figures, 8-1 and 8-3, is that after the individual Δt realizations reach the local absolute maximum, the time series of realizations curves slightly back to the Δt origin in 8-3, as opposed to staying at the maxima in 8-1. The reason the time series of Δt realizations exhibit this behavior, instead of staying constant as found in the "inspection" solution, has to do with the decay of the vortex velocities as they vary inversely with the radius. In other words, the velocity decay from the previous vortex is faster than the velocity rise of the next vortex. This 1/r velocity decay represents the irrotational portion of the vortex. It is noted that the period of each vortex crossing the sound path is approximately 35.7 milliseconds matching the passage time computed based on the 2.29 cm bluff body in a flow with an average velocity of 3.048m/sec.

The effect of the strength of the vortices, Γ, on the computed Δt was calculated using the piece-wise numerical integration method and is shown in Figure 8-4. In Figure 8-4, similar Δt profiles result for three different vortex strengths; Γ= 0.0023, 0.0046, 0.009 m^2/sec. It was observed that doubling the vortex strength of the individual vortices resulted in an approximate doubling of the individual Δt realization variation. In other words, doubling the vortex strength doubled the maximum Δt observed. This behavior should be expected since induced velocity is directly proportional to Γ, and Δt is directly proportional to velocity as was described by Equations 13 - 16, and 20.

8.3 Computation of Δt Using the Modified Ray Trace Method

8.3.1 Software Development

Computer simulation of contra-propagating sound waves in a flow field, using the Modified Ray Trace Method, was used to examine the effects of four primary variables, speed of sound, c, beam width, β, vortex strength, Γ, and flow angle, α. The Modified Ray Trace program was tested using dimensional values and flow conditions which were the same as those used in the piece-wise numerical integration to allow for validation of the results obtained to those obtained by the analyses in Sections 8.1 and 8.2. The simulations were initially conducted using sound waves which were allowed to propagate perpendicularly to the uniform flow. The basic geometry, shown in Figure 2-5, was a pipe which had uniform flow set to 3.05m/sec in the 'x' direction and no flow in the 'y' and 'z' directions. The fluid simulated was water flowing in a channel at 20°C, which would have a sound speed of 1,483 m/sec. While it is understood that a real flow in a pipe or channel would have a boundary layer, the boundary layer was not used here so that the effect of just a flow disturbance such as one generated by a bluff body could be examined.

Using a simulated bluff body set 10 body diameters ahead of the nearest transducer, a vortex street that would have been formed was set up in the uniform flow. The vortices in the vortex street were simulated to be of different strengths, but Γ was set to $0.0046 m^2/sec$ for initial computations; this quantity was chosen based on expected vortex

strength in a flow of water at 3.05m/sec. The Γ chosen allowed direct comparisons of the results generated by these simulations to previous results. The Strouhal number was set to the expected value of a reasonably high Reynolds number flow (above 500 [71]), that is 0.21.

8.3.1.1 Convergence and Stability of Program

Initially the time step-size was varied to determine the optimum value, based on run time and resolution. As the time step-size was reduced, two things occurred, first the program took much longer to run, and second, the data produced finer resolution results. Figure 8-5 shows the result as the time step was reduced. With time steps of 100 and 10 nanoseconds, the Δt realization was found to be zero. The reason for the Δt = 0 seconds was because the Δt realizations for this system were on the order of 1 to 2 nanoseconds,

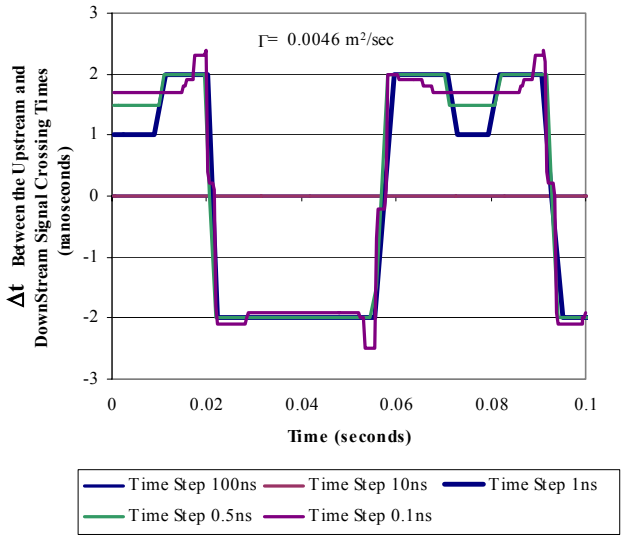

Figure 8-5 Comparison of Different Time Steps for the Simulation Program. Sound Propagation Path Perpendicular Uniform Path.

as shown Figure 8-3 where the Δt versus time had a magnitude of +/-2 nanoseconds smaller than these step-sizes. In Figure 8-5 for a time step-size of 1 nanosecond, the individual Δt realizations time series jumps back and forth between +/-2 nanoseconds with some intermediate jumps to +/-1nanosecond. When the time step was further decreased to 0.1 nanoseconds, the resolution of the resultant data approaches the time series of data predicted by the piece-wise numerical integration, shown in Figures 8-3 and 8-4. The time series still had discontinuities because of the finite step-size; however, further reduction of the step-size would smooth the time series. At a time step of 0.1 nanoseconds, the time required to run the program and obtain the desired amount of data was approximately 4 days with available computer equipment. To obtain a finer resolution, the program run time would increase significantly. For example, at a time step-size of 0.05 nanoseconds, the run time for the simulation increased to 8 days. It was decided to forgo a finer resolution for the sake of obtaining more information.

8.3.1.2 Comparison to Previous Results

The results from the Modified Ray Trace Method and the piece-wise integrated solution were compared to determine whether or not the two methods resulted in the similar answers, the comparison is depicted in Figure 8-6. As can be seen, the two time series follow nearly identical traces, the main difference is the resolution of the Modified Ray Trace Method. In Figure 8-7, the vortex strengths were the same as in the piece-wise integration method, that is $\Gamma = 0.0023, 0.0046, 0.009 m^2/sec$. Not only are the shapes and

amplitudes of the time series curves similar, but the amplitudes of the Δt's follow the same pattern of doubling with a doubling of the Γ. In addition, the magnitudes of the Δt's for the simulation were within a few percent of the Δt's computed in the piece-wise numerical integration, Figure 8-8. In general, the Δt resulting from the simulation was slightly larger than the Δt calculated using the piece-wise numerical integration. The slight difference between the results shown in Figure 8-8 was the result of the computer simulation taking into account the 'x'-component velocities in the simulations causing the sound paths to be slightly curved while the integral solution sound path was not allowed to curve. These comparisons lead to the conclusion that the Modified Ray Trace simulation program worked correctly, and provided results that were similar to the piece-wise numerical integration results. More importantly, the simulation program was expected to provide reasonable results when the sound wave was launched at an angle to the flow.

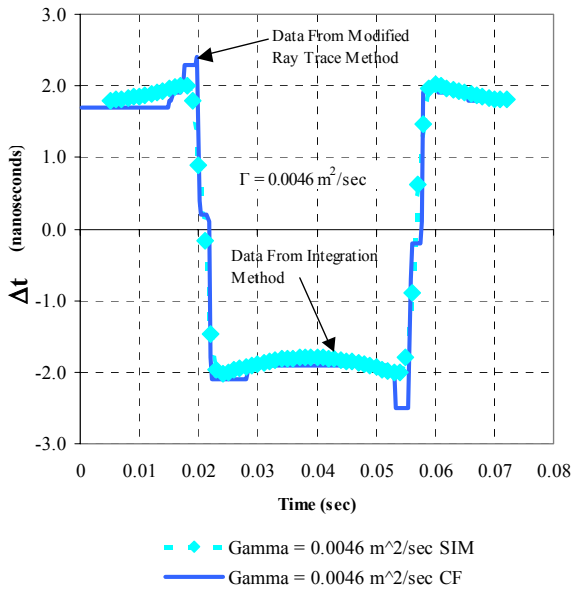

Figure 8-6 Comparison of Modified Ray Trace Results with the Solution from the Integral Solution.

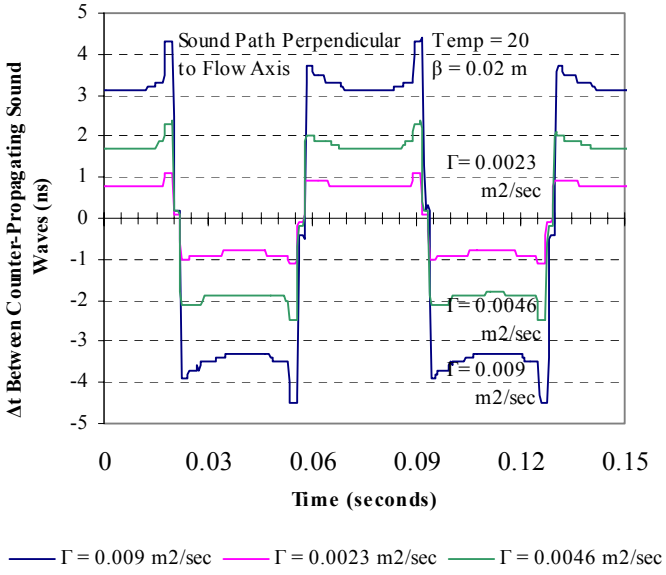

Figure 8-7 Results of the Modified Ray Trace Method in which Sound Waves Propagate Perpendicular to the Flow Axis. This Figure Compares to Figure 8-4.

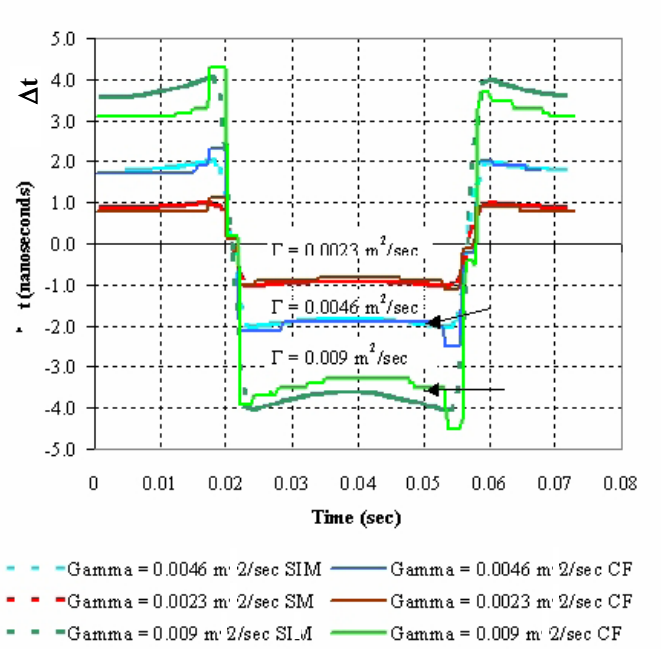

Figure 8-8 Comparison of Piece-wise Numerical Integration with Ray Trace Simulation for Perpendicular Paths

8.3.2 Effect of Circulation On Computation of ΔT

The effect of the strength of vortices in a vortex street on individual Δt realizations for perpendicularly propagating sound pulses was discussed in Sections 8.2 and 8.3.1.2. As was shown, when the sound waves were launched perpendicularly to the direction of uniform flow, a vortex affected the individual Δt realizations for counter-propagating sound waves depending on where the vortex was in relation to the sound path. However, having the sound path perpendicular to the flow path, does not allow the average velocity in a system to be computed, this is because the average flow velocity, $\bar{u}$, does not appreciably affect the time of flight of the sound waves. The actual sound paths are bent slightly off the perpendicular paths by the flow, however, there will be no difference in

time of flight due to average velocity between the contra-propagating waves since the sound path changes are nearly identical. There will be no Δt change due to the bending of the sound paths because the average flow will affect both sets of sound waves equally.

Equation 3 is the governing equation for a system in which the sound path is aligned perpendicularly to the flow. As discussed in Section 2.3.3, when sound waves propagate at an angle to the flow, θ, the average velocity along the sound path can be computed using Equation 13 -16, and 20. Additionally, as vortices cross the sound path, the integrated velocity and therefore the individual Δt realization should vary, just as vortices crossing the perpendicular sound path caused the individual Δt realizations to differ from zero. Figures 8-9 to 8-11 are time series plots showing the effects of vortex strengths and sound path angles on the measured Δt, where a sound path angle of 45°was chosen in

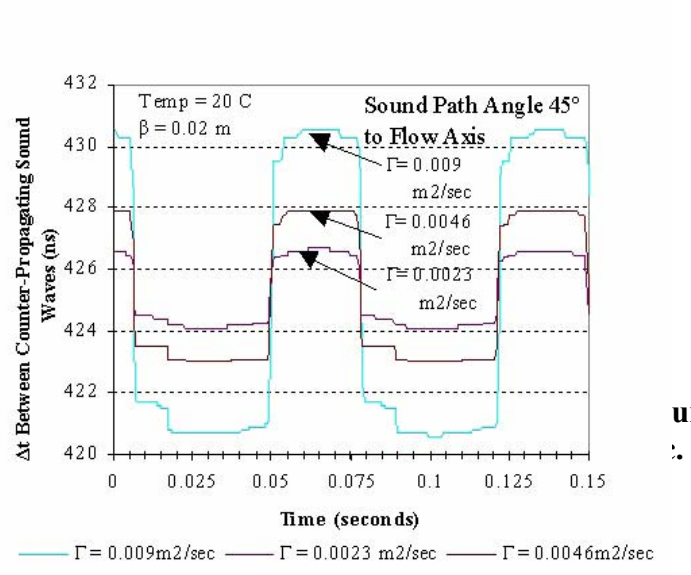

Figure 8-9 Result **und Waves Cross at an Angle of 45°.**

Figure 8-9. For Figures 8-10 and 8-11, the sound path angle was chosen to be 60° and 80° respectively. Table 8-1 is a compilation of the effects of Γ =0.0023, 0.0046, 0.009 m^2/sec and θ = 45°, 60°, 80° and, 90° corresponding to Figures 8-7, and 8-9 to 8-11.

Comparisons of the time series data in Figures 8-7 and 8-9 to 8-11, show that the mean of the Δt realizations remained approximately the same for each Γ and specific angle when a full cycle of vortex passing was examined, which is depicted in Figure 8-12 and in Table 8-1. The Δt realizations varied as the cosecant of the angle of the sound path to the flow, as the sound path turned parallel to the flow the effective Δt would go to infinity because the path does not intersect the wall. As the sound path angle goes to 90°, the Δt goes to near zero since there is no average velocity in the 'y' direction. The fact that the mean of the Δt realizations is the same at a specific angle regardless of the vortex strength

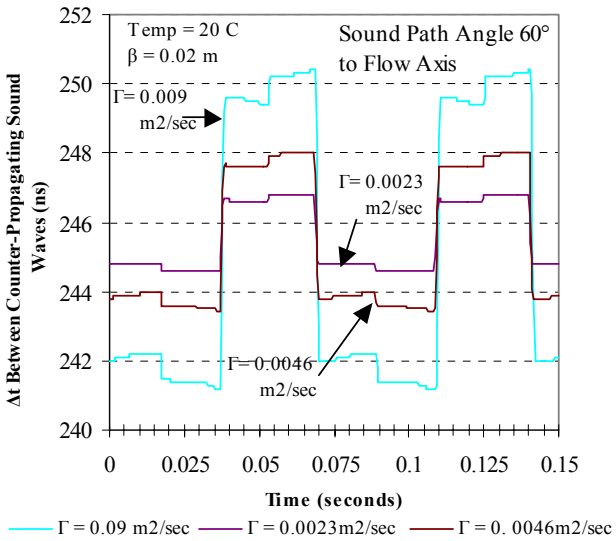

Figure 8-10 Results of the Modified Ray Trace Method in which Sound Waves Cross at an Angle of 60° to the Flow Axis; Γ = 0.0023, 0.0046, 0.009 m^2/sec.

indicates that the correct velocity can be computed. However, the dispersion about the mean, typically called standard deviation, of the individual Δt realizations varies as the vortex strength varies, that is, the standard deviation decreases as Γ decreases and vice versa as can be seen in Figure 8-14 and Table 8-1. Standard deviation is the square root of the variance and is calculated via the relation[6]

$$\sigma = \sqrt{\frac{\sum(\chi - \Upsilon)^2}{(n-1)}}. \qquad \textbf{(74)}$$

where :

$\sigma \equiv$ standard deviation

$\Upsilon \equiv$ population mean; or overall mean

$\chi \equiv$ individual measurement.

The reduction of the standard deviation follows the same pattern seen previously in Sections 8.2 and 8.3.1.2 for the individual Δt realization variations for the perpendicular sound path case. That is, as Γ is reduced by half, the Δt change is reduced by half. Standard deviation is a measure used to describe the variance in data. From the standard deviation, it is then possible to compute the number of individual measurements required to achieve a desired confidence interval, and the maximum percentage error in the mean.[6] Since the standard deviation changes with respect to the Γ, the number of Δt realizations required to compute an accurate mean velocity also decreases. [6] The number of points required to obtain the mean of the Δt time series such that there is a 95% confidence and this mean has a 1% accuracy can be computed from:[6]

$$n = \left(\frac{\text{Confidence}}{\text{percentage error}}\right)^2 = \left(\frac{2\sigma}{\chi - \Upsilon}\right)^2, \qquad \textbf{(75)}$$

where $2\sigma \equiv$ standard deviation for 95% confidence.

If an average of a set of independent population numbers is 10 with a $\sigma = 2.0$, the number of sample points required, n, is 1,600 to compute the average to within a 1% accuracy. This approach is predicated on each data point being independent of others. Such independence is a reasonable assumption for turbulent flow fields in which the temporal correlation of the turbulence between each measurement cycle is nearly zero.[66]

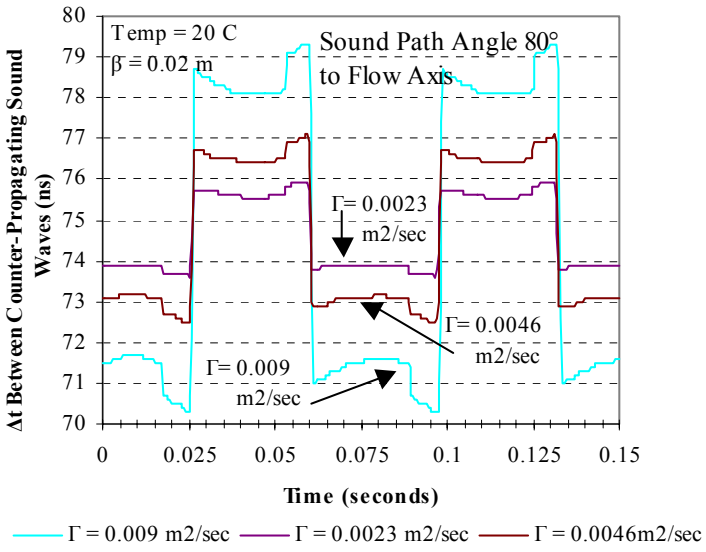

Figure 8-11 Results of the Modified Ray Trace Method in which Sound Waves Cross at an Angle of 80° to the Flow Axis. Γ =0.0023, 0.0046, 0.009m^2/sec.

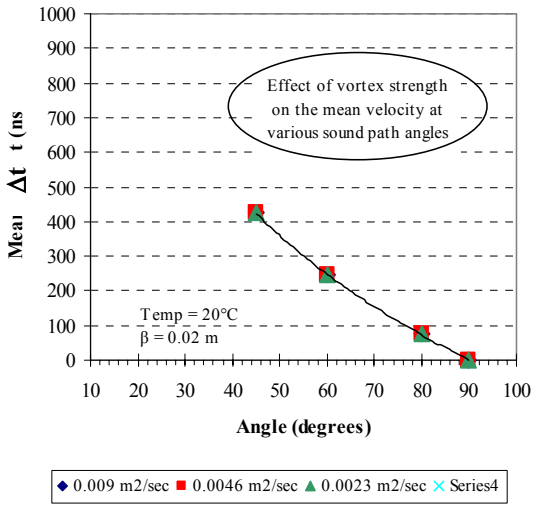

Figure 8-12 Effect of Changing Γ on Mean Δt Realizations.

For the cases in which large scale correlated flow structures are present, such as the vortex street superimposed on a uniform flow, the independence assumption appears to fail. In this case an autocovariance must be computed for the data set and used to modify Equation 74.[6] If one could average the velocities over exactly one cycle of the vortex street superimposed on a uniform flow, the average would be exactly the flow velocity. Additionally, as Γ goes to zero, the average velocity will also go to the uniform flow velocity. The problem with attempting to average over exactly one cycle is that there is no way to know what specific period should be used for the averaging. However, the data shown to this point is a continuous stream of Δt measurements on the uniform flow with a superimposed vortex street. As discussed in Section 5.2, typical flowmeters measure flow at approximately 15 Hz. Figure 8-13 shows the Δt data over 2 seconds taken continuously and then sampled at 15 Hz as a flowmeter would do. Because the data acquired by a flowmeter is typically at a rate of 15 Hz, each Δt realization can be thought of as independent of one another. As was discussed in Section 6.5.3, if the fluid particles

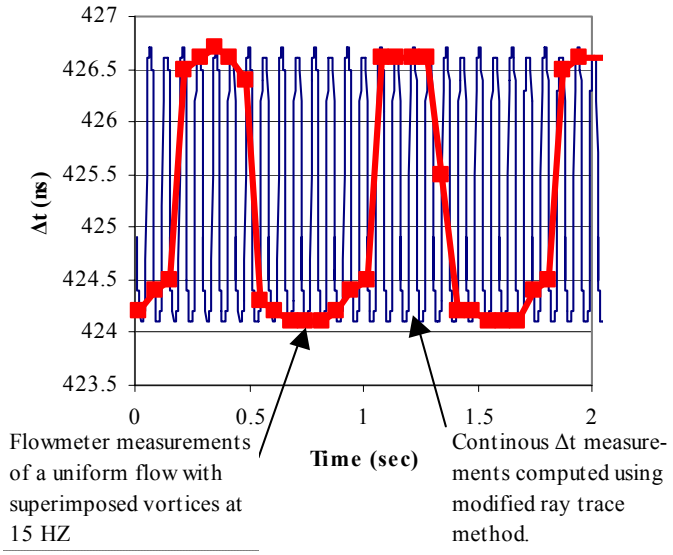

Figure 8-13 Δt Measurements Made Continuously and at 15 Hz on a Uniform Flow with Superimposed Vortex Street.

in the sound path are completely changed when different sets of sound waves propagate over the sound path, the Δt realizations are independent. This independence can be seen in Figure 8-13 because between each flowmeter realization at 15 Hz, several vortices cross the sound path as shown by the continuous data time series. Now, although the data sampled at 15 Hz appears to follow a pattern, the law of large numbers from probability mathematics[6] may be applied to show independence. The law of large numbers indicates even if a series appears in a population of independent data, and a large enough population is sampled, the average will reduce to the average of the population, and therefore Equation 75 still is valid, allowing computation of the number of points needed to reach a valid average based on the standard deviation of the data and the desired accuracy.

Returning to Figures 8-7 and 8-9 to 8-11, spikes were noted on all of the graphs near where the signs change. These spikes correspond to the cores of the vortices crossing the sound path volume. Since Δt effectively measures the integrated velocity over the sound wave path, and the upstream and downstream sound waves are propagating over fluid structures with differing velocity fields, the Δt realization may not be a true representation of the integrated velocity. As the vortex core passed across the sound paths, the velocities in the core of the vortex itself were changing rapidly. Since the sound waves were not launched from both transducers simultaneously, as each sound wave pulse crossed the vortex core, there was enough of a change in the core velocities between the upstream and downstream crossings to cause slight instabilities, which showed up as spikes on the graphs.

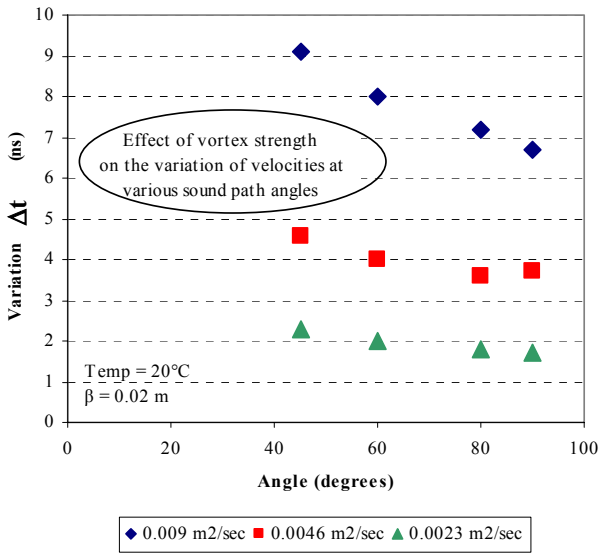

Figure 8-14 Effect of Changing Γ on the Standard Deviation of Δt Realizations

Table 8-1 Data from Ray Trace Method Comparing Effect of Vortex Strengths, Γ, and Sound Path Angles on the Average Δt and Standard Deviation

Angle To Flow θ	Vortex Strength Γ	Mean Computed Δt	Standard Deviation of Computed Δt
(Degrees)	(m^2/sec)	(ns)	(ns)
90	0.009	0.01	6.7
80	0.009	74.6	7.2
60	0.009	245.2	8
45	0.009	424.9	3.1
90	0.0046	-0.02	3.7
80	0.0046	74.6	3.6
60	0.0046	245.4	4
45	0.0046	425.1	4.57
90	0.0023	0	1.7
80	0.0023	74.7	1.8
60	0.0023	245.5	2
45	0.0023	425.2	2.3

8.3.3 Effect of Beam Width

In earlier discussions about beam width, β, in Section 6.3, it was pointed out that the wider the beam width in comparison to the vortex spacing, the less sensitive individual Δt realizations would be to the effects of individual vortices. This hypothesis was investigated using the Modified Ray Trace program with the vortex street in a uniform flow field and showed a very slight dependence of Δt on β. Figures 8-15 to 8-21 are graphs showing the results of the calculations. These graphs are similar to those in

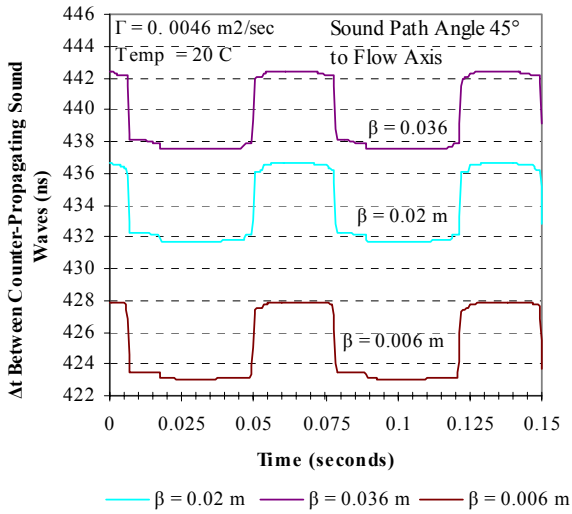

Figure 8-15 Δt Results of the Modified Ray Trace Method in which the Sound Waves Cross at an Angle of 45° to the Flow Axis; β= 0.006, 0.02, 0.036m.

Section 8.3.2 except the Γ was held constant for these while β was varied. While Figure 8-15 appears to show a dependence of Δt on β, Figure 8-16 shows that the velocity error for a sound path angle appears negligible for an angle of 45°. Figures 8-17 and 18 show the same result for a sound path angle of 60°, and finally Figures 8-19 and 20 show the same results for a sound path angle of 80°. Figure 8-21 shows what happens as the sound path becomes perpendicular to the flow field. It is noted in the following graphs where Δt variations versus time are plotted for varying β that as β increases, the Δt increases. However, the computed velocity error remains nearly the same regardless of β. The reason the Δt increases without the velocity error increasing is because the sound path lengthens as β increases. This indicates that the centers of the acoustic transducers grow apart as the sound path broadens.

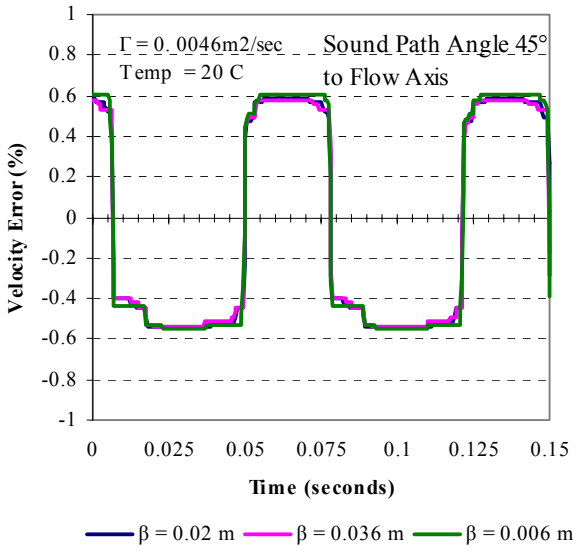

Figure 8-16 Velocity Error Results of the Modified Ray Trace Method in which the Sound Waves Cross at an Angle 0f 45° to the Flow Axis; β=0.006, 0.02, 0.036m.

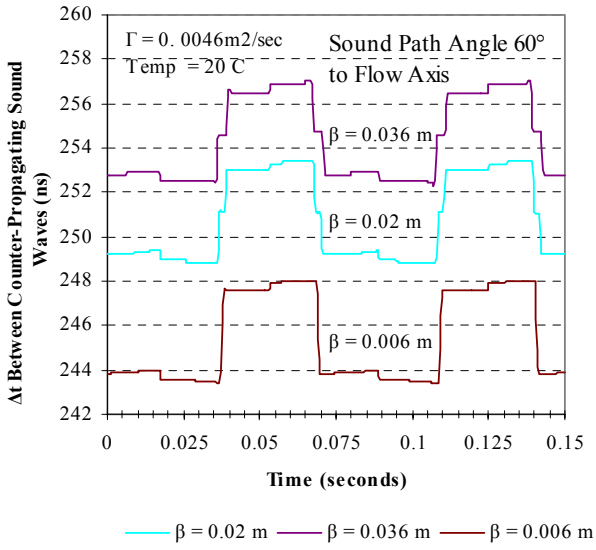

Figure 8-17 Δt Results of the Modified Ray Trace Method in which Sound Waves Cross at an Angle of 60° to Flow Axis; β =0.006, 0.02, 0.036 m.

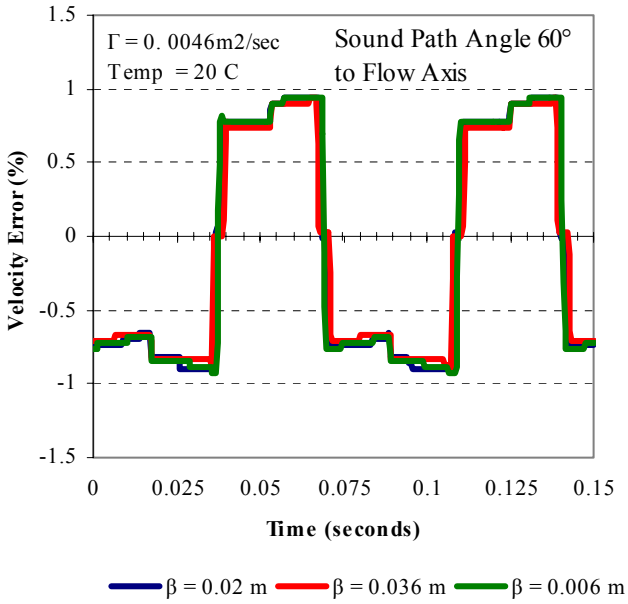

Figure 8-18 Velocity Error Results of the Modified Ray Trace Method in which the Sound Waves Cross at an Angle of 60° to the Flow Axis; β = 0.006, 0.02, 0.036 m.

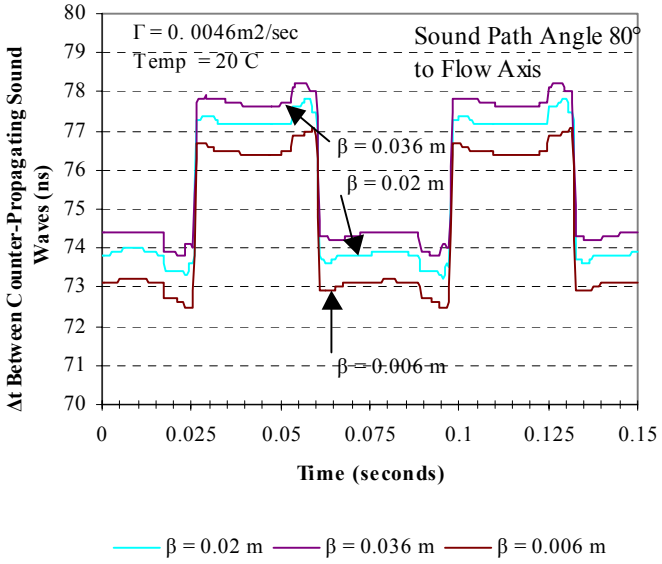

Figure 8-19 Δt Results of the Modified Ray Trace Method in which the Sound Waves Cross at an Angle of 80° to the Flow Axis; β = 0.006, 0.02, 0.036 m.

Compilations of these data are shown in Figures 8-22 and 23, and Table 8-2. Again, as in Section 8.3.2, the mean length of time for the sound waves to cross the flow varies as a function of the cosecant of the angle. Careful examination of the computed standard deviations shows that as β increases, the standard deviation decreases slightly, and this decrease results in the reduced time to produce a statistically meaningful average. For sound path angles of 45° to 80°, the standard deviation was reduced approximately 2.5% as β was increased from 0.006 to 0.02 m, and reduced approximately another 2% as β increased from 0.02 to 0.036 m. For the perpendicular case, the standard deviation was reduced 15% as β increased from 0.006 to 0.02 m, and 21% as β increased from 0.02 to 0.036 m.

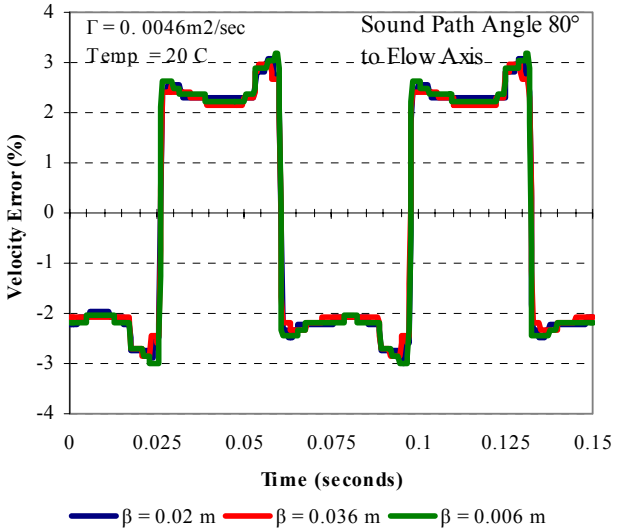

Figure 8-20 Velocity Error Results of the Modified Ray Trace Method in which the Sound Waves Cross at an Angle of 80° to the Flow Axis; β = 0.006, 0.02, 0.036m.

A close examination of Figure 8-21 shows the behavior of the standard deviation of Δt versus sound path angle and beam width graphically. The reason the beam width affects the standard deviation is that as the vortex core crosses the sound beam, the individual Δt realizations tended toward zero. The length of time the Δt realizations remains near zero increases as β was increased as seen in Figure 8-21. As the center of the vortex crossed the sound path, one side of the other beam was sped up while the other was slowed down. This altering of beam front velocities caused the sound front to be warped. The warping was symmetric, and therefore, the upstream and downstream propagation times were equal. But, even without this symmetry (that is the vortex core not centered in the sound path) one side of the sound wave front would reach the receiving transducer in a shorter period of time. When this occurred, the individual Δt realizations would be near zero but not exactly zero. The wider the sound beam, the longer period of time the Δt realizations were near zero. Conceptually, if the sound beam width were to be widened so that at any point in time a vortex core is crossing, the observed error for individual Δt realization would decrease from approximately +/-2% to less than +/-0.5%. This would result in a more accurate flow measurement in a shorter period of time, because the effect of vortices convecting across the measurement volume would be cancelled out. In the situations discussed in this section, anytime a Δt measurement was taken, the likelihood was that it would deviate approximately 2% from the average measurement.

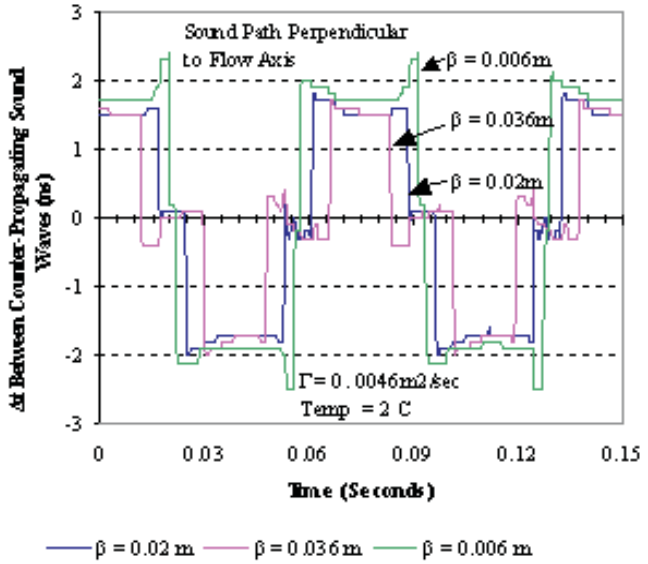

Figure 8-21 Results of the Modified Ray Trace Method in which Sound Waves Cross Perpendicularly to the Flow Axis; β - 0.006, 0.02, 0.036 m

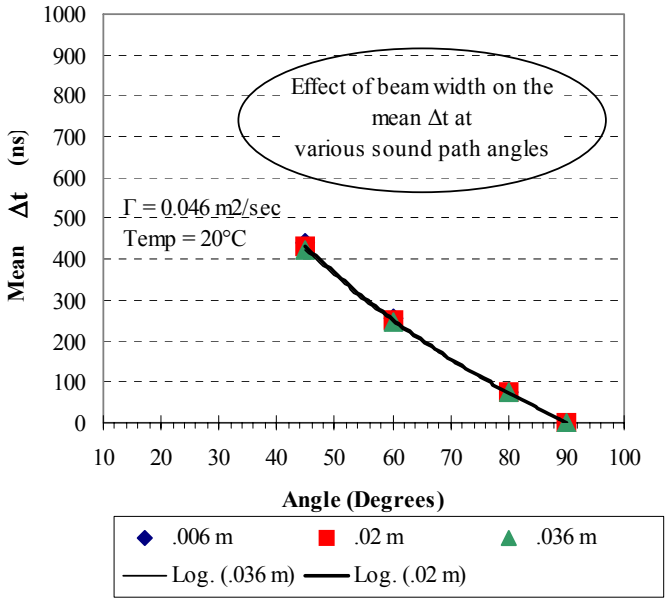

Figure 8-22 Effect of Changing Beam Width, β, on Mean Computed Δt.

Table 8-2 Data from Ray Trace Method Comparing Effect of Beam Width, β,and Sound Path Angles on the Average Δt and Standard Deviation. Γ = 0.046 m^2/sec

Angle To Flow θ	Beam Width β	Mean Computed Δt	Standard Deviation of Computed Δt
(Degrees)	(mm)	(ns)	(ns)
90	6.1	-0.05	2.4
80	6.1	75.9	3.5
60	6.1	254.4	3.8
45	6.1	439.6	4.6
90	24.4	-0.03	2.9
80	24.4	75.4	3.6
60	24.4	250.8	3.9
45	24.4	433.8	4.5
90	36.6	-0.02	3.7
80	36.6	74.6	3.6
60	36.6	245.4	4
45	36.6	425.1	4.6

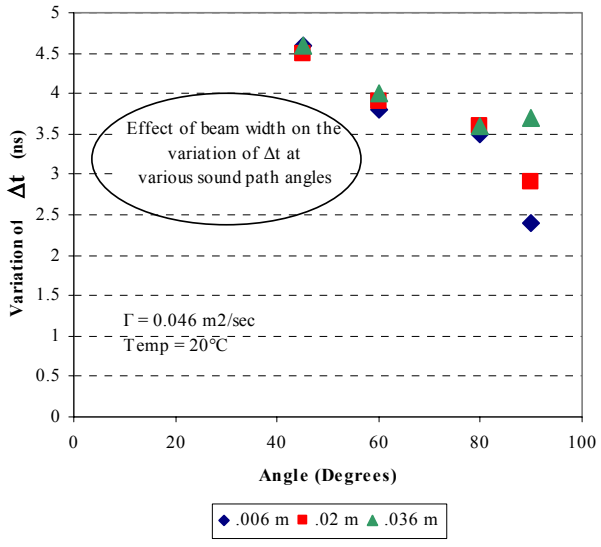

Figure 8-23 Effect of Changing Beam Width, β, on Standard Deviation of Computed Δt.

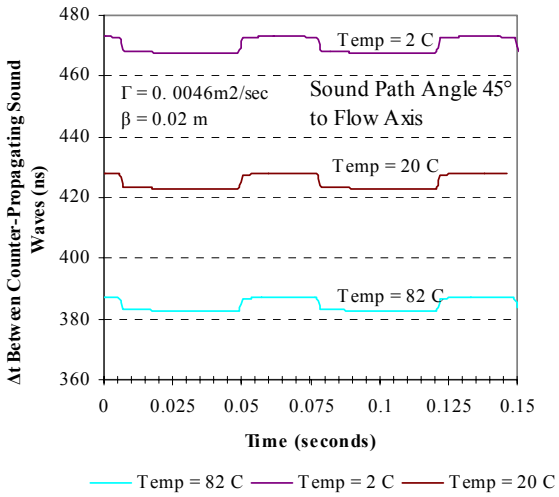

Figure 8-24 Results of the Modified Ray Trace Method in which the Sound Waves Cross at an Angle of 45° to the Flow Axis; Temp = 2°, 20°, 82° C.

8.3.4 Effect of Temperature

The Modified Ray Trace Method was used to determine the effect of changing the average temperature of the fluid on individual Δt realizations. Changing the temperature of a fluid changes the speed of sound, c, meaning that the ratio of the sound speed to the mean flow speed changes. Figures 8-24 to 8-27 contain results from simulations of sound waves propagating across a flow uniform flow field with a superimposed vortex street at angles of 45°, 60°, 80° and 90° using the Modified Ray Trace program. Each graph represents data at varying temperatures while holding Γ, and β constant and varying the θ of the sound path.

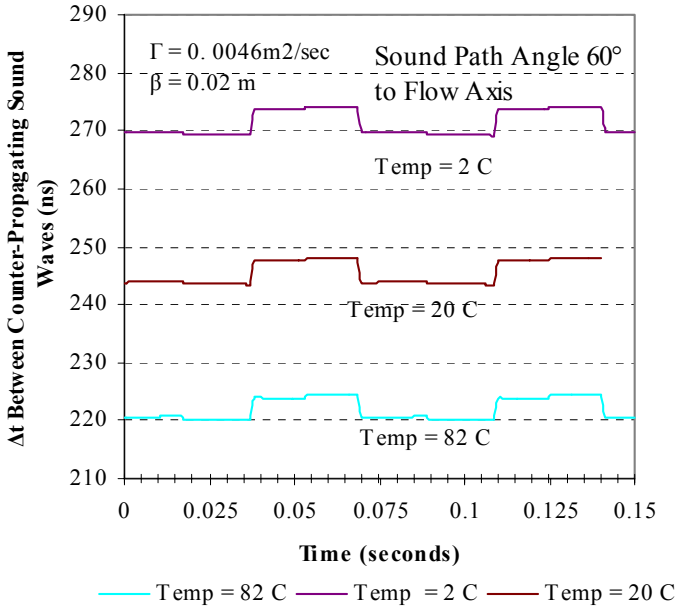

Figure 8-25 Results of the Modified Ray Trace Method in which Sound Waves Cross at an Angle of 60° to the Flow Axis; Temperature = 2°, 20°, 82°C.

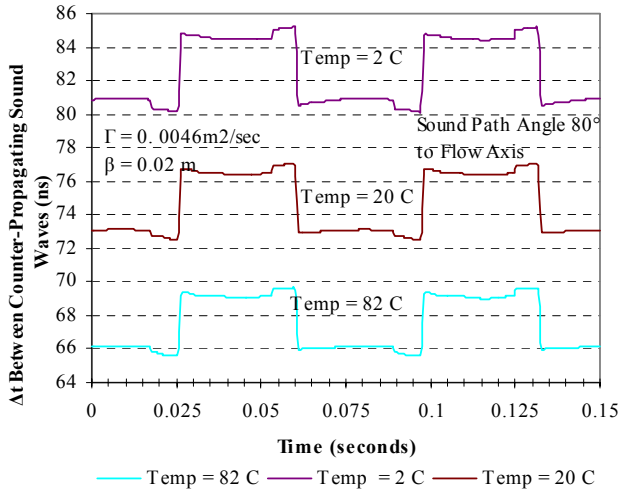

Figure 8-26 Results of the Modified Ray Trace Method in which the Sound Waves Cross at an Angle of 80° to the Flow Axis; Temperature = 2°, 20°, 82° C.

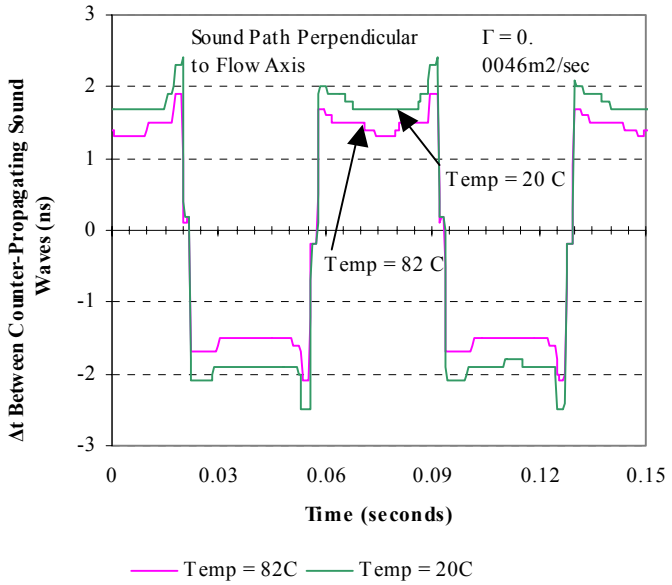

Figure 8-27 Results of the Modified Ray Trace Method in which Sound Waves Cross Perpendicularly to the Flow Axis; Temperature = 20°, 82°C.

Figures 8-24 to 8-27 show two patterns of behavior, the first is as the sound path angle varied from 90° to 45°, the mean Δt increased, and, as in the last two sections, the Δt increased as a function of the cosecant of the angle, Figure 8-28. The second pattern is that as the temperature decreases, the mean Δt increases for a particular angle, this can also be seen in Figure 8-28 as 3 distinct lines, one for each temperature, and in Table 8-3. This variation in mean Δt with temperature change is caused by the decrease in relative speed between the sound wave and the fluid. As the speed of sound decreases, the average fluid flow speed over the sound path has more of an effect on the travel time of sound waves, increasing the Δt. While the relationship of c with Δt can be demonstrated with temperature, the effect is greatly magnified when the type of fluid is changed such that c is significantly changed, as occurs when changing from water to air. The net result

of these simulations indicates that an independent temperature measurement should be taken when using ultrasonic systems for flow measurement. The reason for this is to independently verify c in the fluid, rather than computing it via sound propagation time in the fluid. By independently determining sound velocity, one eliminates the unknown sound velocity in the equations for flow velocity.

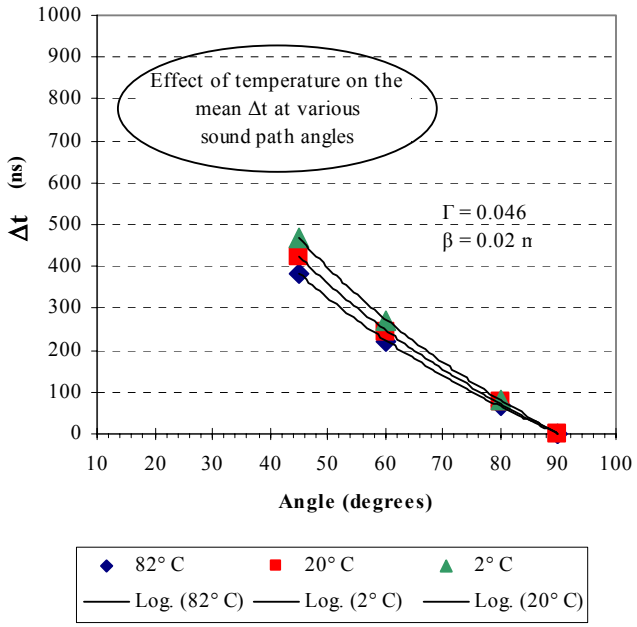

Figure 8-28 Effect of Changing Temperature on the Mean Computed Δt.

Finally, Figure 8-29 and Table 8-3 show the behavior of the standard deviation of Δt with temperature and angle. Generally, as the angle increases the standard deviation decreases. This occurs because the sound waves are in the fluid for a shorter period of time and have less time to be affected by flow disturbances such as vortices. Also, as temperature increases the standard deviation decreases, which occurs because as the temperature increases so does the speed of sound, and the time the sound wave is in the fluid is decreased; this lessens the affect the fluid has on the sound wave propagation.

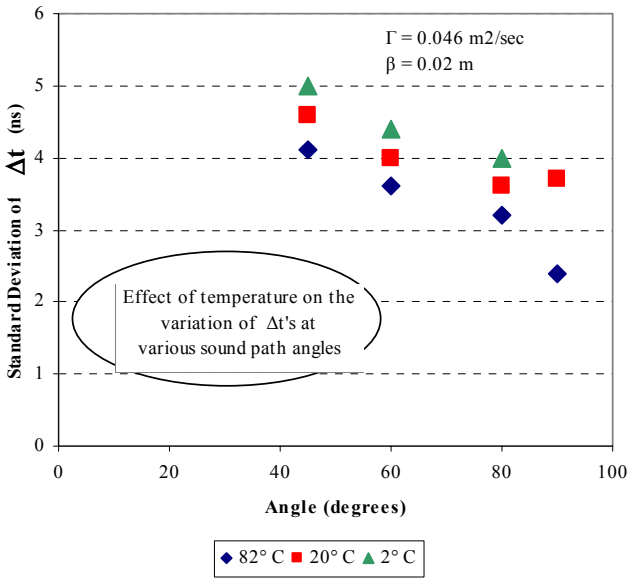

Figure 8-29 Effect of Temperature on the Standard Deviation of Δt.

Table 8-3 Data from Ray Trace Method Comparing Effect of Temperature or Speed of Sound, c, and θ on the Average and Standard Deviation of Δt Realizations. Γ = 0.005m^2/sec

Angle To Flow θ	Temperature	Mean Computed Δt	Standard Deviation of Computed Δt
(Degrees)	(Degree C)	(ns)	(ns)
90	82	-0.01	2.4
80	82	67.5	3.2
60	82	222	3.6
45	82	384.5	4.1
90	20	-0.02	3.7
80	20	74.6	3.6
60	20	245.4	4
45	20	425.1	4.6
80	2	82.5	4
60	2	271.3	4.4
45	2	469.9	5

8.3.5 Effect of Varying the Angle across the Fluid

Minor variation of the uniform flow with respect to the centerline axis was studied by adding "y" direction velocities of 0.06 m/sec and 0.15 m/sec. These additions correspond to 1.13°, and 2.8° flow angles for the baseline, 3.05 m/sec, flow. While the resulting Δt time series remained similar to time series produced by the perpendicular case, the entire time series for each effective angle was displaced below the origin, Figure 8-30. In effect, the sound wave front was being launched at a slight angle to the flow. In general, the absolute displacement from the origin will be increased as the 'y' velocity is increased. The plots in Figure 8-31 were useful in determining the relative error introduced by an inaccurate angle measurement. In this case, by changing the effective angles between the

fluid flow path and sound path from 45° to approximately 43.9° and 42.2°, the errors in average Δt realizations are approximately 2.5% and 5 %. Alternatively, if the transducers were out of alignment by 1.13°, the measurements of the flow would be in error by approximately 2.5%, and for 2.8°, the measurement error becomes 5%.

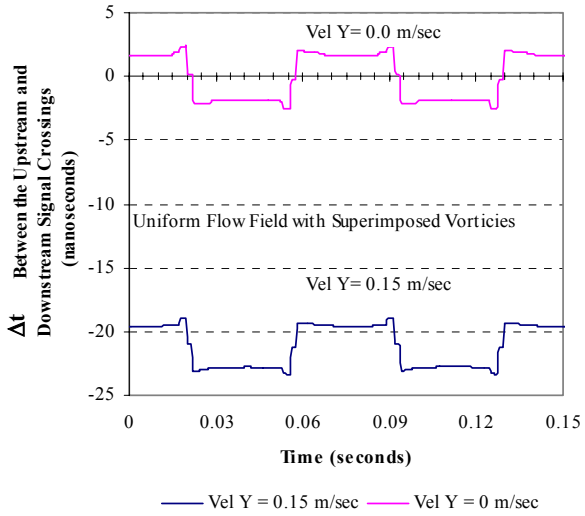

Figure 8-30 Results of the Modified Ray Trace Program in which Simulated Sound Waves Cross Nearly Perpendicularly to a Uniform Water Flow with a Superimposed Vortex Street. These Plots Compare the Resultant Δt when the Uniform Flow is Perpendicular to the Sound Path to when the Uniform Flow is Slightly off the Perpendicular.

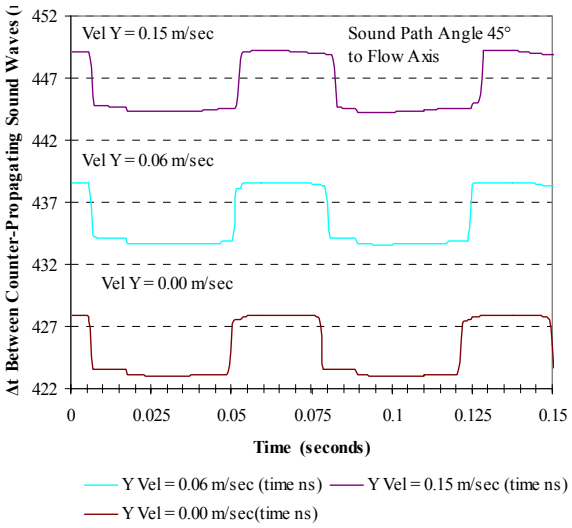

Figure 8-31 Results of the Modified Ray Trace Program in which Sound Waves Propagate at Approximately 45° to the Centerline of the Pipe. The Uniform Flow, in Addition to the Vortex Street, had 'y' velocities of 0.0, 0.06, and 0.15 m/sec added to it. These 'y' velocities add 1.5° and 3.0° to the Angle Between the Measurement volume and the Flow Direction.

8.4 Effect of Uniform Flow on Sound Path

A source of error when determining mean flow velocity is due to the effect of the sound path shape assumption, discussed previously in Section 6.5.4. To determine the error due to sound path, the Modified Ray Trace Method was used in a uniform flow alone. Since the velocity was constant, the ray trace simulation results in a constant velocity, which allows for direct computation of the velocity error by comparison of the simulation velocity result with the input velocity. Figure 8-32 shows the integrated flow velocity in a sound path angled at 45° to a uniform water velocity of 3.05 m/sec. Three sound paths were used to compute the velocity from the Modified Ray Trace data, a straight line path

between the two transducers was first, next a path curved by the action of the flow, and finally the exact path as computed by the simulation. Figure 8-32 contains three sets of plotted data, each set represents the same uniform flow input, but the integrated velocity across the flow was computed using the three different described sound paths. The data in Figure 8-32 were the computed integrated velocities along the sound path across the flow field. The data in Figure 8-33 show percent error or deviation from actual velocities. It may be noted that each error was relatively large considering the uniform nature of the flow being simulated, but as the path varied from straight to curved to exact, the error was reduced. Table 8-4 details the relationship of the computed velocity and the effect of the sound path shape. The velocities shown here were all computed using Equation 20, but used the different paths as detailed in Table 8-4. The comparison of magnitudes of the errors computed using the straight path versus a curved path in these two cases are comparable to the approximately 4% difference in errors found by Yeh and Mattingly in their 1998 paper.[73]

Table 8-4 Comparison of Computed Flow Velocities and Computed Error from Actual Flow Velocity and Shape of the Sound Path Used to Calculate the Velocity

Path Shape	Velocity (m/sec)	Path Length (m)	Error Comparing to actual 3.048 velocity (%)	Error Comparing to actual calculated by MRTP (%)
Straight between transducers	2.99	0.2216	-2.03	2.13
Sound Path Adjusted for Velocity	3.01	0.2195	-1.09	1.16
Exact as Calculated by MRT Program	3.045	0.2170	-0.1	-

To determine the exact path lengths using the Modified Ray Trace program, the path

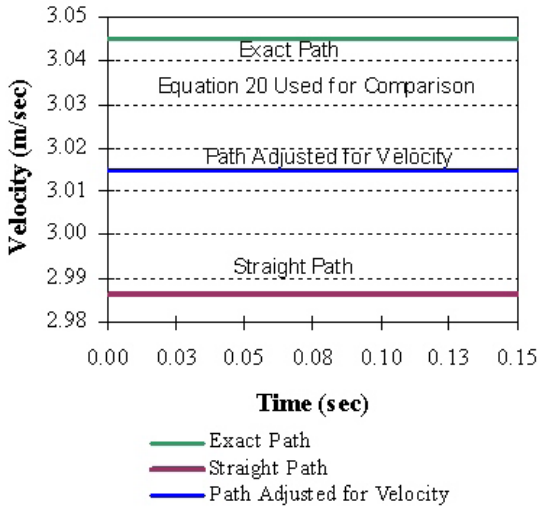

Figure 8-32 Comparison of Three Sound Paths: Straight Path, Path Adjusted for Velocity and the Exact Path. Equation 20 was used for the Comparison. The Velocity was Computed Using the Modified Ray Trace Method on a Uniform Flow of Velocity 3.048 m/sec.

length was the distance traveled by the sound wave in each time step, summed over all the time steps required to reach the opposite transducer. The magnitude of the errors was dramatically lower using this method, and was less than 0.1%. These errors indicate that

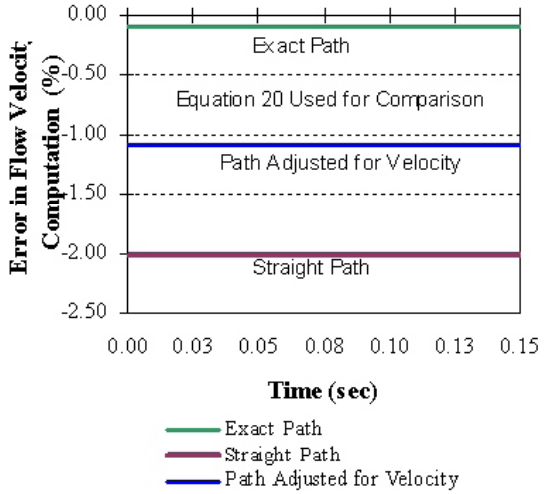

Figure 8-33 Comparison of the Error in Computing the Flow Velocity using the Modified Ray Trace Method on a Uniform Flow Velocity Using 3 Sound Path Assumptions: Straight Path, Path Adjusted for the Velocity, and Exact Path.

the error associated with flow computation will have a dependence on the exact path taken, and therefore, be dependent on the "turbulence" in the flow. The exact path in a turbulent flow field would include all the "wiggles" as the local turbulent velocity fluctuations move the sound wave back and forth, see sketch in Figure 2-7. This dependence on turbulence will cause the measurement error to depend to some extent on the Reynolds number of the flow. In Table 8-4, the comparison of path length is shown.

The path is the longest for the straight path between the two transducers. This happens because as the path is pushed downstream, the sound will cross the receive transducer earlier. Finally, the shortest path for this case is the exact path, see Figure 8-34 for a

diagram of the paths. The reason for the exact path to be the shortest path seems to have to do with the interaction of the wave shape and angle of the sound pulse with the receiving transducer, combined with the asymmetric nature of the send and receive transducer pair when one examines the effect of the flow on the sound wave. The error

Table 8-5 Comparisons of Model Velocity and Velocity Computed Using Equations 20 and 62 from Data Computed via the Modified Ray Trace Method Computed using the Exact Path

Equation	Δt	Model Velocity	Computed Velocity
	sec	m/sec	m/sec
20	0	3.048	3.045
62	0	3.048	3.052

due to the path length, assuming the one calculated by the Modified Ray Trace Method is correct, is slightly over 2% for the straight path and slightly over 1% for the calculated path. So, for a uniform flow alone, the path length is the cause of the majority of the error in computing a velocity.

Finally, the data computed via the modified Ray Trace Method was examined using Equation 62, the equation derived in Section 5.4 to include effects of turbulence. In this case there is no turbulence so the equation should have the same results as Equations 13 - 17, and 20. Table 8-5 compares the results of Equations 20 and 62 of the simulated data computed based on the three paths discussed in this section, a straight path, a curved path, and the exact path. These results indicate that the form of the equation used does not have

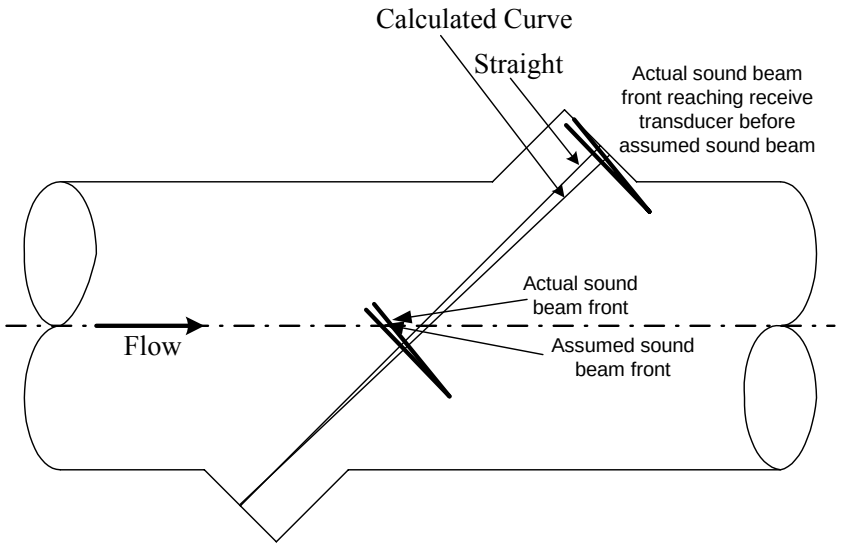

Figure 8-34 How Sound Paths Vary from Straight to Exact

a substantial effect on the size of error; however, the type of path assumed does have an effect on the final outcome of the computation of the velocity.

9 Results From the PIV Measured Velocity Data

As discussed in Section 7.3.2, the PIV technique uses an asynchronous laser sheet and cameras to determine the magnitude and direction of a velocity field. The technique produces an instantaneous two-dimensional grid of velocity vectors in a plane. In this way, a flow field can be frozen in time and various analyses can be performed on the field. Typically, PIV systems sample at rates nearing 15 Hz for as long as the storage systems can keep pace. Since the PIV data were taken at 15 Hz, each individual data set was used for a single realization of back and forth crossings of sound waves. By performing the analysis in this way, frozen flow was assumed. To determine the validity of the frozen flow assumption, the distance the fluid would move while the ultrasonic wave is moving between the two transducers must be calculated. Based on a channel width of 2.2 cm, the fluid would move less than 25 micrometers while the ultrasonic wave is in the fluid. The beam diameter used in this analysis was on the order of 0.3 to 5 millimeters diameter, which means the beam diameter was 12 to 200 times larger than the movement of the fluid particles. Therefore, the assumption of frozen flow is valid since the fluid would move far less than half of the beam width.

9.1 Analysis of Sound Crossing a PIV Measured Velocity Field

The PIV velocity data were read into the Modified Ray Trace program, providing the velocity field information in a discrete data tabular format, which differs from the work in previous chapters (Chapter 8) in which the velocity field was a continuous field

computed using superposition principles. Since the velocity was discretized, the ray-tracing program was modified with a two-dimensional interpolation scheme so that the resolution needed to examine the Δt realizations between the forward and reverse propagating acoustic waves could be obtained. The interpolation was necessary to determine the velocities between grid points because the PIV data grid was not fine enough to allow the Modified Ray Trace program to resolve the individual Δt realizations between the upstream and downstream propagating sound waves. The interpolation method used was a linear spatial interpolation between the surrounding four grid data points. No temporal interpolation was performed because each individual PIV realization was far enough apart in time to be considered independent.

The expected time differences for each of the individual realizations were on the order of 1.0 ns. Therefore, the time steps used were as small as 100 picoseconds. In addition, since the PIV data for the flow were only measured over half the channel width, the analysis was only performed over that portion of the channel.

Initially the PIV data set was used to examine mean and fluctuating streamwise velocities using a method similar to a single Ray Trace Method rather than multiple rays. For this computation, each 'x' direction velocity along a single row was summed along with the sound velocity in each direction, upstream and downstream. The row of fluid velocities was parallel to the flow, and by performing this summation a single ray moving parallel to the flow was simulated, producing a spatially averaged velocity for the row. After

producing a spatially averaged velocity for each time step in the PIV data set, the summed velocities at each time step were then averaged along this same row, producing a single temporally, and spatially averaged velocity for the point. This process was repeated along each row parallel to the channel axis from the near wall region to the last row of the PIV data near the center of the channel, thereby producing the 51 second time-averaged velocity profile in the channel on a line perpendicular to the flow axis. Figure 9-1 shows this average velocity profile along with the standard deviation profile. The mean velocity profile graph starts at approximately 0.22 m/sec and rises to approximately 0.60 m/sec, these values are shown on the left axis of the graph. This plot represents data as if it were taken using a long time constant velocity measurement device at a series of points in flow field. This graph, in fact, matches the typical shape of a turbulent channel flow profile.[43] The second set of data in Figure 9-1 is the turbulence intensity of the

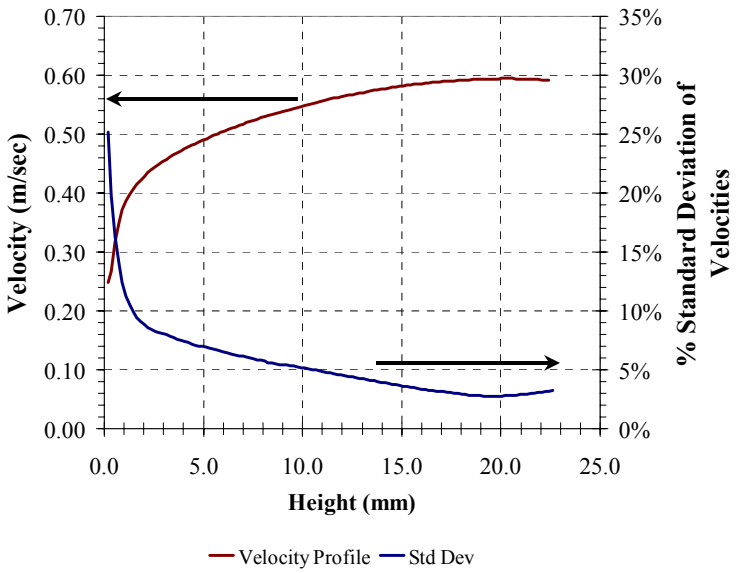

Figure 9-1 Velocity Profile versus Height in Channel and Standard Deviation versus Height in Channel as Computed Using a 1-D Analysis Similar to an Ultrasonic Flowmeter. Data Courtesy of Dr. Kenneth Kiger of the University of Maryland.

velocity field and is the root mean square of the turbulence in a pipe or channel. The major difference between the PIV generated data shown in Figure 9-1 and typical pipe turbulence data [57] is that the scatter of the calculated data does not include a near wall decrease to zero. However, PIV data were not available close enough to the wall to actually show the decrease.

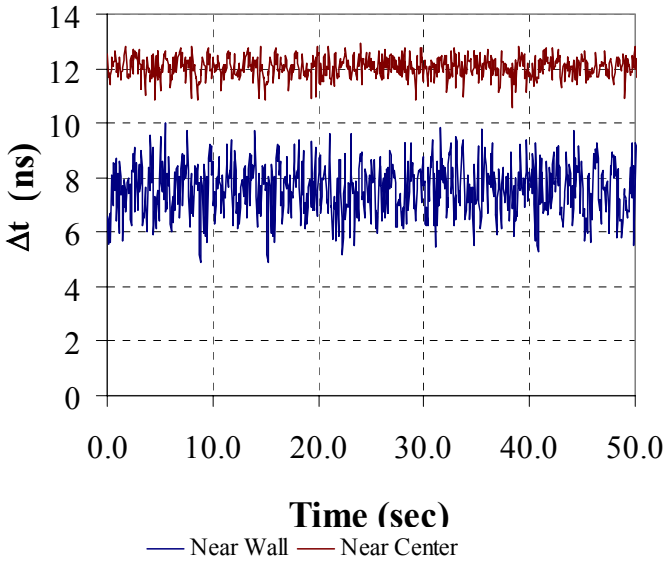

Figure 9-2 Δt versus Time Calculated from Channel PIV Data using a 1-D Analysis; Sound Path Parallel to Flow; Upper Plot Near Center, Lower Plot Near Wall. Data Courtesy of Dr. Kenneth Kiger of the University of Maryland.

Figure 9-2 shows data depicting the instantaneous Δt realizations versus time using the single ray trace analysis technique. Each graph in the figure is at a different location in the channel, near the wall and near the center. These two plots show not only the Δt fluctuations with time, but also that the average Δt realizations, and therefore average velocities, vary as a function of distance from the wall as expected. The temporal

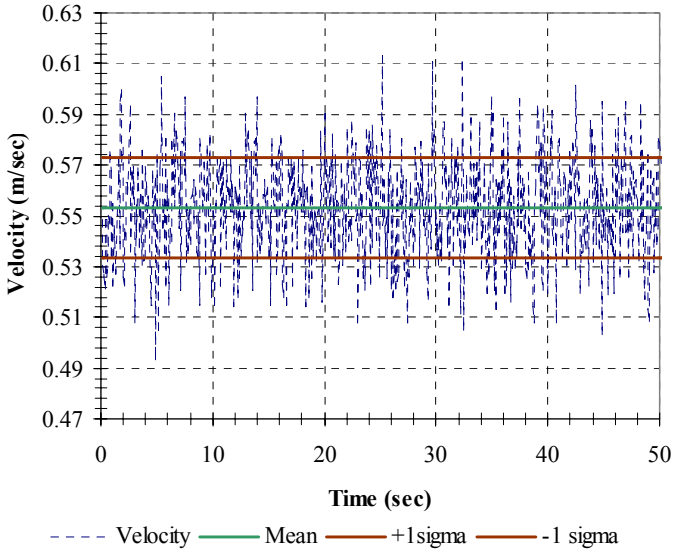

Figure 9-3 Instantaneous Average Velocity Computed using the Modified Ray Trace Method versus Time; Straight Lines Represent the Mean and Standard Deviation of Data. Data Courtesy of Dr. Kenneth Kiger of the University of Maryland.

variation, of course, represents the expected output of a theoretical ultrasonic flowmeter with a very fast time constant and a narrow beam parallel to the channel axis.

While using a single Ray Trace Method along with what amounts to a thin line provides interesting information, simulating a finite width beam and turning it to an angle to the flow field, providing a more realistic simulation of the ultrasonic flowmeter. The Modified Ray Trace program described previously was used for these calculations. By placing the sound path at an angle to the flow field, the integrated velocity of the flow can be determined.

Figure 9-3 is a plot of the computed velocity integrated along a 60° ultrasonic path as computed by the Modified Ray Trace program versus time. These path-averaged

velocities are the instantaneous ultrasonic flowmeter output and are equivalent to Δt. Two types of information are plotted in the graph. The first comprises the computed instantaneous path average velocities, which are the individual points plotted with the dashed lines. The second set of data is made up of the arithmetic mean and the upper and lower standard deviations represented by the 3 straight horizontal lines. The standard deviation of the instantaneous data in this case was approximately 3.5% of the population mean. The mean for this data was the sum of all the individual velocity vectors in the x direction divided by the total number of vectors,

$$\bar{\vartheta} = \frac{\sum_{N} \vartheta_i}{N}. \qquad \textbf{(76)}$$

Initially, the data on this graph, in Figure 9-3, might seem slightly misleading. Ultrasonic flowmeters routinely provide a much smoother and less scattered signal, as shown, for example, in Figure 5-3 courtesy of NIST.[38] The reason for the difference is the electronic averaging used by manufacturers. For example, if a meter averages 15 individual Δt realizations prior to reporting a data point, each of the individual data points will be 1 second apart, and the scatter will be reduced by an amount reflective of the standard deviation and the average of the 15 Δt realizations. The tradeoff is that short-term information such as data through large turbulent structures like vortex streets, may be lost due to the averaging technique. In addition, the averaging must be performed such that the statistical characteristics, data correlation for example, of the data being measured are being properly accounted for, or a misinterpretation of the velocities may result. This

appears to have occurred in Figure 5-3 for the unit under calibration, because the average determined velocity, as shown, was approximately half a percent higher than the flow velocity at the time of measurement. Close scrutiny of the graph shows that the velocity of this particular flowmeter jumps suddenly near the beginning of the time period and at the end of the time period, indicating that there was a strong change of the velocity as measured by the unit under calibration. However, this was not borne out by the average velocity during the calibration time.

9.2 Turbulence Data

9.2.1 Discussion

As discussed in Section 6.5.1, an important factor in making ultrasonic flow measurements is the desirability of the same or nearly the same fluid particles to be in the measuring volume when the two waves are sent back and forth across the flow. This ensures that the same velocity fields are integrated by the passage of each ultrasonic beam moving in opposite directions. If the waves can be sent back and forth through the same flow field, then the measured Δt realization is proportional to the velocity as shown in Equations 13 -16, and 20. Therefore, if a velocity field is measurable, then the Δt realizations should have statistics similar to the velocity field being measured.

Qualitative results were achieved using statistical analysis of the calculated individual Δt realizations for the PIV measured turbulent flows. In this way, the required averaging

technique necessary to produce a velocity within a defined error band can be found. For example, in any of the vortex street cases, if the length of time of the measurement is too short, the mean calculated velocity would be too high or low depending on the relative position of the vortex to the sound travel path. If in these cases, the measurements could be made such that determination for the crossing time of the cores of two different vortices, of the same sign Γ, could be achieved, then a true mean velocity could be calculated. However, this would require very fast signal processing and may not be possible due to the geometry of the flow system, or the actual speed of the flow.

9.2.2 Statistical Evaluation of Turbulent Velocity Measurement

As discussed in Section 8.3.2, standard deviation is a measure used to describe variance in data. From standard deviation, it is then possible to compute the number of individual measurements required to achieve a desired confidence interval, and the maximum percentage error in the mean is specified.[6] Using the results obtained from the channel PIV velocity data parallel to the flow, shown in the plot in Figure 9-2 and Equation 75, the number of Δt realizations necessary to acquire an average within a desired confidence limit at different parts of the pipe can be determined. Furthermore, the length of time required to obtain a mean within specified tolerances, assuming a sample rate of 15 Hz, may be calculated. The results are listed in Table 9-1 for various parameters. It can be seen that the level of turbulence intensity in the measurement volume directly influences the number of measurements needed.

Using Equation 75, with the data generated using the Modified Ray Trace program on a 60° angle across the flow channel, it is possible to determine the length of time required needed to determine an average within prescribed parameters. If the computed average is to be within 1% of the mean, the number of points required prior to reporting a result is 51. If the desired accuracy is 0.5%, the number of data points required increases to 204. At a data rate of 15 Hz, these values translate to a time of 3.4 and 13.6 seconds respectively. To gain an accuracy of 0.25%, the number of data points required increases to 817 points requiring 54 seconds of data, more than is available in this data set. Figures 9-4 and 9-5 are of the same data used in Figure 9-3, however, running 51 and 204 point averages were computed for 1% and 0.5% accuracies respectively. The heavy black lines on each graph represent the computed running averages at the desired accuracy. The standard deviation and mean lines are plotted as in Figure 9-3. In addition, lines

Table 9-1 Compilation of Number of Points Required and Time Required at a 15 Hz Sample Rate to Determine a Mean Velocity, which is in a 95% Confidence Interval and 1% and 0.25% Accurate

		0.25% Accuracy 95% Confidence		1.0% Accuracy 95% Confidence	
Position in Channel	**2σ**	**Number of Points**	**Time Required at 15 Hz**	**Number of Points**	**Time Required at 15 Hz**
Overlap Flow Layer	1.89	616	41.0 sec	9849	10.9 min
Outer Flow Layer	0.77	41	2.7 sec	657	43.8 sec

representing the desired accuracy are plotted on the respective graphs. In general, if a data set is not sampled long enough, the error bands for the computed mean will be larger than expected. The size of this error band can be computed using Equation 75, by solving for error and substituting for the number of points measured. Therefore, by computing the standard deviation of the individual Δt realizations being measured, two important conclusions were drawn. First, the relative level of turbulence in a flow system can be measured by measuring the Δt versus time series as was discussed in Section 9.2.1 and shown using the channel PIV velocity data plots in Figure 9-2. Second, the error bands of the computed mean may be determined and are directly related to the turbulence level in the flow measurement volume.

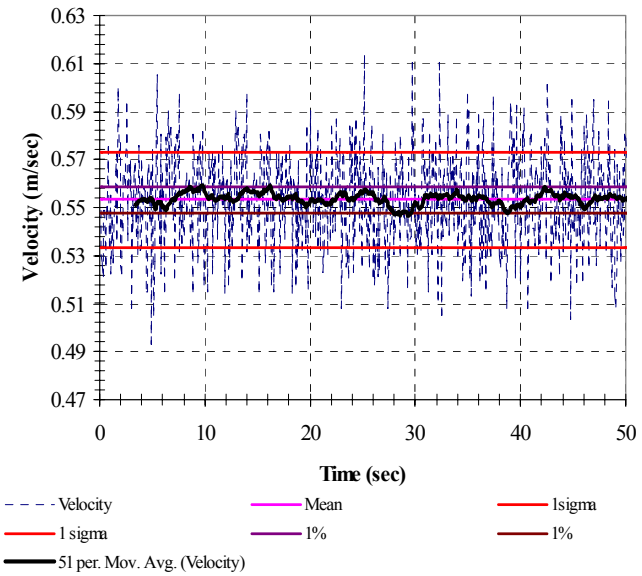

Figure 9-4 Instantaneous Average Velocities Computed versus Time; 1% Running Average Plotted as Heavy Line on Graph. Data Courtesy of Dr. Kenneth Kiger of the University of Maryland.

When actual flow measurements are acquired using an ultrasonic flowmeter system, in addition to flow noise due to turbulence, there is also electronic noise. Presumably, this electronic noise can be independently measured without flow, and this noise can be assumed to be distributed normally with each measurement independent of the previous measurement. By using the "law of large numbers" from statistics,[36] these two independent sets of normally distributed data can then be added together resulting in a single set of normally distributed data. Therefore, if the standard deviation of electronic noise can be measured without flow, it can then be separated out of the total data noise and direct information on the relative turbulence levels within the flow measurement volume can be determined.

Understanding the effect of turbulence on ultrasonic flowmeter system measurements directly leads to the realization that a detailed description of the flow field being measured is needed to properly evaluate the accuracy of a flowmeter. Without such characterization of the turbulence in a pipe flow, an ultrasonic flowmeter system may potentially have an error band about the computed mean that is much larger than expected. If the flow in the system being measured has a higher turbulence level than that in the calibration system, the error band will be larger due to the increased standard deviation of the measured data scatter. This will be true unless the flowmeter system accounts, in some way, for the relative difference between the actual system and the calibration system. Additionally, if large scale coherent flows such as a vortex street are being convected through the measurement volume, the standard deviation of the data measurements will be increased, and the number of Δt realizations required to compute

the mean to within a certain error band will increase. These are important issues which must be considered when using ultrasound to make measurements of a flow field as no two flow fields can be predictably the same. Turbulence within the flow field depends a great deal on the entire flow structure upstream of the measurement location.

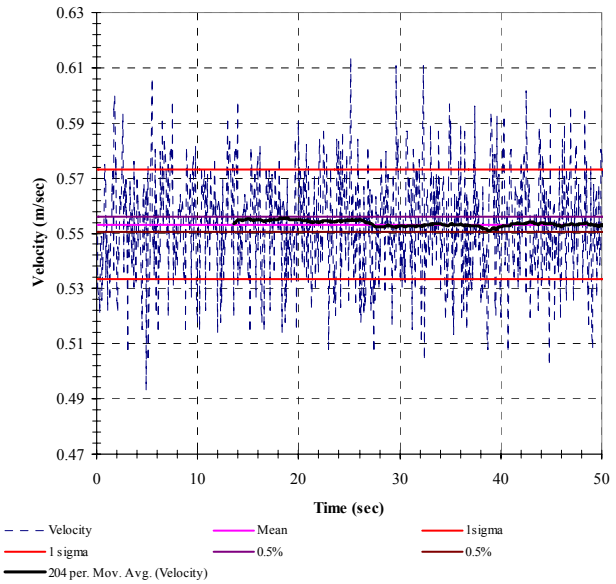

Figure 9-5 Instantaneous Average Velocities Computed Versus Time; 0.5% Running Average Plotted as Heavy Line on Plot. Data Courtesy of Dr. Kenneth Kiger of the University of Maryland.

9.3 Parametric Studies Using PIV Data

A parametric study was conducted using the PIV turbulence data to determine the effects of the beam width, sound velocity, and sound path angle on the velocity measurements in a turbulent flow. The effects on the individual Δt realizations and standard deviation were observed. These parametric studies were performed using the same PIV data and

Modified Ray Trace program, except, that beam diameter, β, path angle, θ, and sound speed c were varied. The speed of sound was altered by changing the temperature of the fluid flow. It was assumed that this change in temperature had no effect on the velocity field, only on the sound speed. This, of course, is not entirely correct, as the temperature changes so does the viscosity of the fluid, therefore changing the Reynolds Number and the turbulence intensity in the fluid. The change in turbulence intensity could make the actual sound paths longer or shorter depending on the change in Reynolds Number, as was shown in a simplified manner using the uniform flow with superimposed vortex street earlier in section 8.3. However, due to the extremely limited range of Reynolds Numbers, in this research, this effect is expected to have only second order effects on the results.

9.3.1 Effect of Path Angle

The angle at which the sound beam crosses the flow influences the measured Δt since the path length changes with changes in angle. Figure 9-6 shows a graph and data of the mean Δt versus θ. As expected, $\Delta t \approx 0$ at 90° because the streamwise velocities had little effect on the propagation of sound. As seen in Chapter 8, the Δt's increase as a function of the cosecant of a decreasing angle for sound path angles down to 50°, which was the minimum angle able to be evaluated with the existing PIV data set. No angles less than 50° were evaluated because the data set was square, so when the angle was less than 50° there was not enough room to propagate a finite sized sound beam across the PIV data.

At $\theta = 0°$, or parallel to the channel walls the Δt will reach mathematical infinity, since the transducers are no longer constrained by the walls of the channel and can be infinitely far apart.

Figure 9-7 is the standard deviation of the Δt measurements, and clearly shows a minimum at approximately 75°. Therefore to make a more accurate measurement in the shortest amount of time, one could design the sound path in the ultrasonic flowmeter to be 75°.

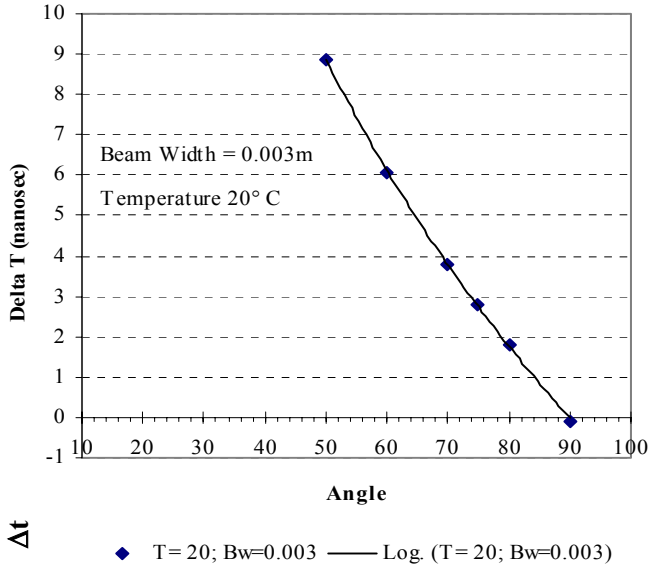

Figure 9-6 Effect of the Angle of the Sound Path Relative to the Flow on Δt. Data Courtesy of Dr. Kenneth Kiger of the University of Maryland.

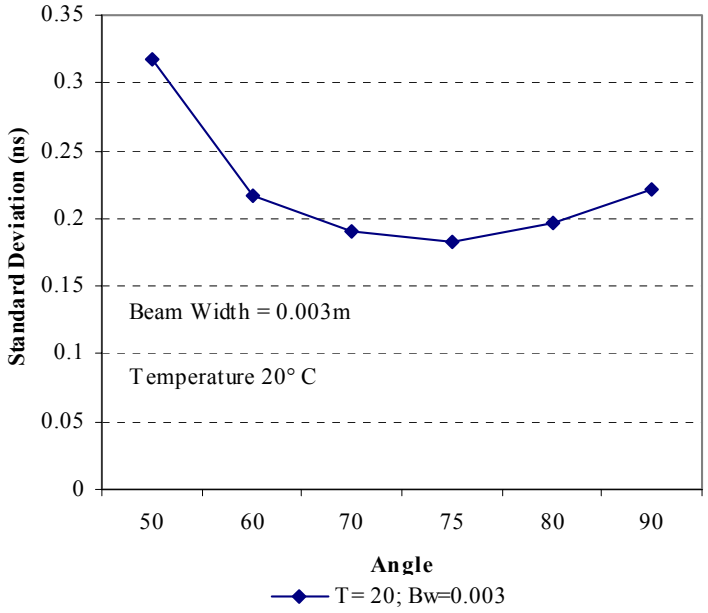

Figure 9-7 Standard Deviation of Δt Data vs Sound Path Angle Relative to the Flow. Data Courtesy of Dr. Kenneth Kiger of the University of Maryland.

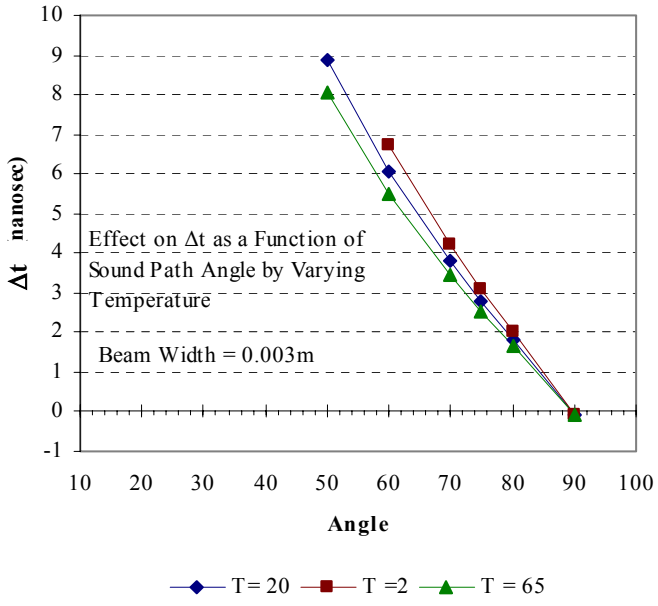

Figure 9-8 Effect of Water Temperature and Sound Path Angle on Δt. Data Courtesy of Dr. Kenneth Kiger of the University of Maryland.

9.3.2 Effect of Speed of Sound

The effect speed of sound on the measured Δt realization was examined and the results are plotted in Figure 9-8. As the temperature or speed of sound decreased, the magnitude of the Δt realizations increased slightly for the same θ. In addition, as the angle of the sound path increased, the average Δt's increased. The results plotted here were for 2°C, 20°C, and 65°C. The standard deviation also varied with temperature as can be seen in Figure 9-9. As temperature increased the standard deviation decreased. This decrease, on average, across all the sound path angles was approximately 18.7%. As before, a minimum occurred at 75°. So, all else being equal, a fluid with a higher sound speed relative to the average flow will produce a lower data scatter, and therefore, the average can be found more quickly. In the data presented here, the reduction in time to achieve a desired accuracy is not as large as the reduction in standard deviation, because the measured Δt realizations also change with temperature. The reduction in the number of points necessary to achieve a desired accuracy is approximately 2.2%, Tables 9-2, 9-3, 9-4, present this data in numerical format.

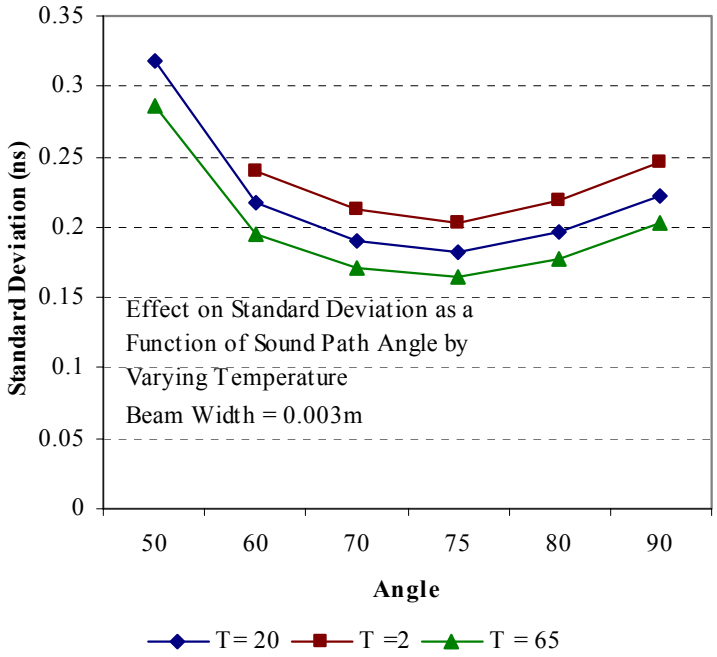

Figure 9-9 Standard Deviation of Δt Data at Individual Sound Path Angles and Sound Speeds. Data Courtesy of Dr. Kenneth Kiger of the University of Maryland.

9.3.3 Effect of Beam Width

As was described earlier in this work, the width of the sound beam was thought to have some influence on the accuracy of the measurements by averaging subtle velocity differences over the width of the beam. Figure 9-10 shows there were no significant effects on the mean Δt realization as the beam width changed, agreeing with earlier qualitative results shown in Section 8.3.3. Figure 9-11, however, does show that the standard deviation of the Δt realizations did change with beam width, β. As β increased, the standard deviation decreased. The decrease in standard deviation averages out to be 14.6%. The effect of the angle remains the same as in previous sections, that is a

minimum standard deviation occurs at approximately 75°. The effect of the sound path angle remained the same for all cases. This information, therefore, shows that β does seem to average the locally high and low velocities along the width of the beam to produce a more stable average. The end result of this reduction in standard deviation with β, without a change in average Δt realizations, was an average of 27.4% reduction in the number of points required to obtain a desired average accuracy, Tables 9-2, 9-3, and 9-4 present the data in numerical format.

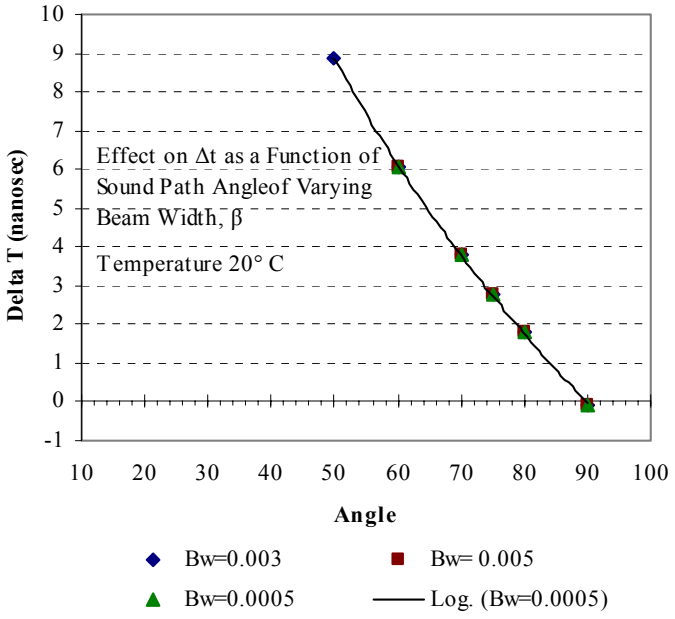

Figure 9-10 Effect of Beam Width and Sound Path Angles on Measured Δt. Data Courtesy of Dr. Kenneth Kiger of the University of Maryland.

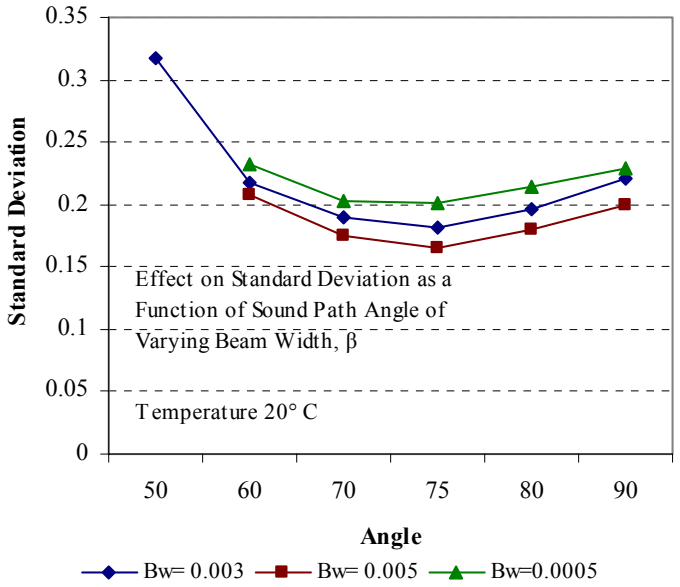

Figure 9-11 Standard Deviation of Δt Data at Individual Sound Path Angles and Beam Widths. Data Courtesy of Dr. Kenneth Kiger of the University of Maryland.

Table 9-2 Measured Mean Δt Realizations in Nanoseconds for Various θ, c, and β.

Angle	T= 20 C, Bw=0.003 m	T =2 C, Bw = 0.003m	T = 65 C, Bw = 0.003m	T= 20C, Bw= 0.005 m	T= 20C, Bw=0.0005 m
50	8.864	-	8.044	-	-
60	6.080	6.720	5.520	6.089	6.072
70	3.801	4.200	3.452	3.806	3.797
75	2.780	3.073	2.525	2.783	2.776
80	1.809	1.997	1.643	1.813	1.803
90	-0.082	-0.091	-0.071	-0.079	-0.089

Table 9-3 Number of Points Required to Achieve a 0.5% Accuracy at Various θ, c, and β. Calculations of the Percentage Reduction of the Number Points Required to Achieve Accuracy Desired Due to c Differences and β Differences

Angle	T= 20 C; Bw=0.003 m	T =2 C; Bw=0.003 m	T = 65 C; Bw=0.003 m	T= 20 C; Bw= 0.005 m	T= 20 C; Bw=0.0005 m	Percent Reduction of Number of Points Required from T = 2 C to T = 65.5 C	Percent Reduction of Number of Points Required from Bw = 0.005 m to Bw = 0.0005 m
50	206.0	-	203.4	-	-	-	-
60	204.2	202.8	200.7	186.7	235.2	1.0%	20.6%
70	399.5	406.9	395.7	339.2	458.5	2.7%	26.0%
75	686.3	697.0	684.3	565.4	838.5	1.8%	32.6%
80	1879.6	1930.3	1871.6	1572.9	2262.2	3.0%	30.5%
90	1168149.4	1158549.6	1318413.2	1019907.6	1071622.1	-13.8%	4.8%
					Average Reduction (not including Perpendicular Sound Path)	2.2%	27.4%

Table 9-4 Standard Deviation of Individual Δt Realizations in Nanoseconds for Various θ, c, and β. Calculations of Percent Reduction of Standard Deviation Due to c Differences and β Differences

Angle	T= 20 C; Bw=0.003m	T =2 C; Bw=0.003m	T = 65 C; Bw=0.003m	T= 20 C; Bw= 0.005m	T= 20 C; Bw=0.0005m	Percent Reduction of Standard Deviation from T = 2 C to T = 65.5 C	Percent Reduction of Standard Deviation Bw = 0.005m to Bw = 0.0005m
50	0.318	-	0.287	-	-	-	-
60	0.217	0.239	0.196	0.208	0.233	18.3%	10.7%
70	0.190	0.212	0.172	0.175	0.203	18.9%	13.8%
75	0.182	0.203	0.165	0.165	0.201	18.6%	17.7%
80	0.196	0.219	0.178	0.180	0.214	19.0%	16.2%
90	0.221	0.246	0.203	0.199	0.229	17.5%	13.0%
					Percent Average Reduction (not including Perpendicular Sound Path)	18.7%	14.6%

10 Summary, Conclusions, Recommendations

A numerical and analytic study was performed to investigate the effect of turbulent flow on the propagation of sound waves. Specifically, the effect of turbulence on the difference in propagation times between a wave moving with a flow and a second wave moving against the flow along approximately the same path, otherwise referred to as Δt, was calculated. Significant effort was put into the development of the Modified Ray Trace Method that allows numerical modeling of the propagation of acoustic waves through a turbulent fluid. Below the findings are summarized and directions for the future research are outlined.

10.1 Summary and Conclusions

In Chapter 1 the motivations leading to the research work were outlined. Chapter 2 provided a review of past research on acoustic flowmeter development. A brief synopsis was given of mathematical formulation of ultrasonic flowmeter work. Accuracy issues of ultrasonic devices were addressed and prospects for improving of flowmeters performance were evaluated. The overview was followed up by the problem statement and a list of objectives in Chapter 3.

The basis of the ray trace method was reviewed in Chapter 4. Derivation and analysis of the equations describing the propagation of acoustical waves in inhomogeneous moving

media was provided. Review of numerical modeling using ray trace method was presented.

The Chapter 5 was devoted to the derivation of the modified ultrasonic flowmeter equation that accounts for the flow velocity fluctuations. Output data of ultrasonic flowmeters collected from different setups were presented in order to demonstrate qualitatively the effect of the turbulence on acoustic wave propagation.

Chapter 6 discussed the assumptions used during this research and an estimation of their range of viability.

Chapter 7 was devoted to the development of the new, Modified Ray Trace Method and its application to the problem of waves propagation in inhomogeneous moving medium. Two flow models (vortex street in a uniform flow and experimentally obtained PIV data) employed by the numerical code were discussed.

Chapters 8 and 9 presented and discussed the results obtained from the Modified Ray Trace Method. The piece-wise numerical integration method was used for the code validation and provided results used as a benchmark. Corresponding comparisons were performed in Chapter 8. Numerical and analytical studies lead to the following conclusions:

1. It was shown that computed Δt can be used to determine mean flow velocity along the sound path, and finally the flow in the flow system can be determined.

Two different types of flow fields were used in the study; first, a uniform flow field with superimposed large fluid structures, such as a vortex street, second, a flow field of PIV measured channel flow. Parametric studies were performed on these flow fields using a single ray trace method, and a Modified Ray Trace Method, using multiple rays, examining variables which included beam width, vortex strength, sound speed, and sound path angle.

2. Using the Modified Ray Trace Method on a uniform flow field with a superimposed vortex street, a number of observations were made regarding the effect of the flow field on the sound waves.

   a. Changing sound path angles affected Δt and its standard deviation between the two contra-propagating sound waves as the angle varied from perpendicular, 90°, to 45°. Changing sound path angles caused the Δt to increase as the inverse function of the cosecant of the angle.

   b. As flow temperature, or sound speed increased the measured mean Δt and standard deviation of the Δt realizations decreased.

   c. Changes in sound beam width, when the sound path was perpendicular to the flow, showed that as a vortex core passed through the sound path, there was a region where the mean error dropped by an order of magnitude for a short period of time. This period of time for the reduced error during vortex core passage lengthened as the beam width increased. The reason for reduced error while the vortex core passed through the sound beam

was that velocities on both sides of the vortex core center were averaged as the core passed through the sound beam. It was shown that as the sound beam width increased, there was no effect on the Δt; however, as the beam width increases the standard deviation of the Δt's decreased. This behavior directly reduces the number of individual realizations needed to determine the average flow to within a predetermined certainty.

d. Using the uniform flow with superimposed vortex model, the effect of changing the vortex strength, Γ, and the cross-stream velocity was examined. Results showed that when the Γ of the vortices in the vortex street was changed, the mean Δt did not change; however, the standard deviation of the data changed nearly proportional to the change in Γ. So, by doubling of the magnitude of Γ, the corresponding standard deviation also nearly doubled. This change in standard deviation with varying Γ indicates that off axis velocity conditions, such as a velocity induced in the 'y' direction by a vortex, can have a real effect on the output of an ultrasonic flowmeter, and the stronger the disturbances, the greater the variation of Δt.

e. The effect of adding cross-stream velocities to the uniform flow field, a velocity in the 'y' direction was added to the uniform flow model and resulted in an offset of the mean Δt. In the case where cross-stream velocities of 0.06 m/sec and 0.15 m/sec were added to the 3.05 m/sec

uniform flow field with superimposed vortex street, Δt offsets of 2.5% and 5% were recorded. Interpreting the cross-stream velocities into sound path angle misalignments, the 0.06 and 0.15 m/sec cross-stream velocities caused a 1.1° and 2.8° respectively misalignment in the sound path angle.

3. The instantaneous Δt time series shape depended on the type of coherent structures in the fluid flow, as demonstrated using the Modified Ray Trace Method with a uniform flow model and a large scale flow structure superimposed. A full vortex street had a square wave time series shape.

4. Channel flow fields with PIV measured data allowed analysis of sound wave propagation in a turbulent channel flow. Using the single ray trace method with the ray parallel with the flow, showed that the long term average of Δt resulted in average velocity and standard deviation measurements similar to results obtained in literature by Moser.[43] Single ray trace measurements were taken parallel to the channel wall extending from the wall to near the center of the channel. Using the data from these single ray trace methods, it was seen that the region of typically higher root mean square (rms) velocity scatter near the wall of the channel caused the standard deviation of the computed velocity data to also be higher. Correspondingly, the area of typically reduced rms velocity scatter in the center of the channel resulted in a reduction of standard deviation in the same area.

5. Using the PIV measured data field, but utilizing a sound path at an angle to the flow field, as found in industrial applications in conjunction with the Modified

Ray Trace Method, resulted in standard deviations comparable to those found in industrial flowmeter applications. Near the center of a pipe, a 3.5% standard deviation in the angled simulation was observed which is comparable to the 3.0 to 3.5% standard deviations observed in industrial flowmeters. This result indicated that much of the data scatter observed in an ultrasonic flowmeter system is due to turbulent fluctuations in the velocity field. Based on these observed fluctuations, it was determined that to achieve a 0.5% measurement accuracy would require a 13 second sequence of Δt realizations if an ultrasonic measurement system was used in the particular flow field described by the PIV data used. The length of time to achieve a desired level of accuracy depends on the standard deviation of the measured data, temporal correlation of the data, and the data rate of the measurement technique. An important consideration is whether or not the forward and reverse propagating sound passes through similar instantaneous flow fields.

6. Other observations using the Modified Ray Trace Method on a sound path angled across the PIV measured data set and uniform flow field with superimposed vortex street resulted in the following conclusions.

   a. Variation of the angle of the sound path relative to the flow direction from perpendicular to 50° to the flow field, resulted in a cosecant function of the angle with an increasing magnitude of the Δt between the counter-propagating sound waves. Understanding this relationship between sound

path angle and Δt is important, as the length of the Δt is indicative of the precision of the timing device needed to measure the mean flowrate. Since the magnitude of Δt increases with the cosecant with decreasing sound path angle, as the sound path angle varies from parallel to the flow axis, the Δt goes to infinity. However, the standard deviation of the measured data indicates that while the Δt continually increases as the sound path angle decreases, the standard deviation has a minimum for a sound path of 75°. The importance of this minimum is that the length of time required to obtain an average velocity within a desired accuracy is minimized at this angle because the number of individual Δt realizations needed to determine the average flow velocity within a confidence level.

b. Using the Modified Ray Trace Method and simulating a temperature change of the fluid, with all other factors remaining the same, it was possible to study the effect of sound speed changes. As the speed of sound increased, the Δt and its standard deviation decreased. The importance of this observation is that higher precision timing devices will be required as the fluid sound speed increases because of the smaller Δt to be measured. As the sound speed in the flow increased, the Δt standard deviation was reduced by an average of 18%, thereby reducing the number of points required to achieve an 0.5% accuracy by approximately 2%.

c. Adjusting the beam width in the Modified Ray Trace Method used in conjunction with both the PIV data set, and uniform flow field with superimposed vortex street, there was no discernable effect on the mean Δt. However, as the beam width increased, the measured Δt data scatter was reduced. When the beam width was increased by 5 times, the standard deviation decreased 18%. Since the beam width did not appreciably affect the measured Δt, the number of data points required to achieve an average velocity accuracy within a 0.5% band was reduced by 27%. This reduction in data required would result in a considerable savings of data acquisition time.

7. In summary, not accounting for the turbulence of the flow field as well as the mean velocity profile of the field, causes an ultrasonic flow system to incorrectly compute the mean flowrate in a pipe or channel. The flowrate miscalculation can be mitigated by performing a calibration of the meter and associated instrumentation. However, the calibration must account for the turbulence and sound speeds at different flow Reynolds numbers. In addition, in order to obtain a average flowrate within a prescribed accuracy band, proper statistical averaging techniques must be employed and the standard deviation of the instantaneous realizations must be examined. Finally, in order to reduce the time required to determine the mean to within a proscribed accuracy band, physical characteristics of the flowmeter such as the beam width and the angle of the sound path should be examined in an attempt to ensure that the optimal meter is developed.

8. An equation can be developed to account for the turbulence in a flow system when using an ultrasonic flowmeter. This equation is similar to those found in literature, but is modified by the integration of the fluctuating velocities in each direction.

10.2 Recommendations

It has long been known that the mean velocity profiles in a pipe duct or duct have a significant influence on indicated flow rate. In response, elaborate quadrature techniques have evolved so as to minimize sensitivity to mean profiles. It has been shown here that the time varying components of a flow field, whether eddy structures or turbulence, similarly affect measurement accuracy. It is almost certain that turbulent temperature fluctuations will also be found to have substantial effects on flow measurement. Continuation of experimental work is currently under way. A better understanding of the effects of the temperature fluctuations is needed. Experimental apparatus consisting of two high-speed data acquisition cards installed in a PC allows to collect and analyze propagation time data with extremely high precision. This apparatus will be expanded to include high performance temperature indicators and fast thermocouples to monitor temperature fluctuations of up to 0.2°C in the mean flow to promote increased accuracy in speed of sound computations. Measurements provided by the updated experimental apparatus may lead to a better understanding of the effects of the temperature fluctuations on ultrasonic flowmeter performance.

BIBLIOGRAPHY

1. Anwer, M. and So, R. M. C., “Rotation Effects on a Fully-Developed Turbulent Pipe Flow,” Experiments in Fluids, 8, pp.33-40, 1989.

2. Anwer, M. and So, R. M. C., “Swirling Turbulent Flow Through a Curved Pipe,” Experiments in Fluids, 14, pp.85-96, 1993.

3. Botma, H. C., "Acoustic Flowmeter For Use With Hydraulic Models", Flow Measurement of Fluids, pp.385-390, 1978.

4. Brassier, P., Hosten, B., Vulovic, F., "High-Frequency Transducers and Correlation Method to Enhance Ultrasonic Gas Flowmetering", Flow Measurement and Instrumentation, Volume 12, pp. 201-211, 2001.

5. Brockwell, P. J. and Davis, R. A., Time Series: Theory and Methods, 2nd edition, Springer-Verlag, 1991.

6. Byrkit, D. R. Elements of Statistics, Van Nostrand Reinhold Company, 1972.

7. Dane, H. J., “Ultrasonic Measurement of Unsteady Gas Flow”, Flow Measurement and Instrumentation, Volume 8, pp.183-90, 1997.

8. Desabrais, K. J., 1997, "Direct Measurement of Wing Tip Vortex Circulation Using Ultrasound," M. S. Thesis, Worcester Polytechnic Institute, Worcester, MA.

9. Fisher, S. G. and Spink, P. G., "Ultrasonics as a Standard for Volumetric Flow Measurement," September, 1971.

10. Fouche, D. G., Higgs, C., and Pearson, C. F., "Scaled Atmospheric Blooming Experiments (SABLE)," The Lincoln Laboratory Journal, Volume 5, Number 2, pp. 273-292, 1992.

11. Gatke, J., "Non Invasive Acoustical Flow Measurement at Pipes with Disturbed Profiles," Flowmeko'98 Conference, pp. 155-60, 1998.

12. Gurevich, Y., Lopez, A., Flemons, R. , and Zobin, D., "Theory and Application of a Non-Invasive Ultrasonic Cross-Correlation Flowmeter," Flowmeko'98 Conference, pp.347-51, 1998.

13. Heller, G. S., "Reflection of Acoustic Waves from an Inhomogeneous Medium. I," The Journal of the Acoustical Society of America, Volume 25, Number 6, pp. 1104-06, November, 1953.

14. Hemp, J., "A Review of the Weight Vector Theory of Transit Time Ultrasonic Flowmeters," Flowmeko'98 Conference, pp.375-80, 1998.

15. Hooker, S. G., "On the Action of Viscosity in Increasing the Spacing Ratio of a Vortex Street," Proc. Roy, Soc. A, Vol. 154, pp. 67-89, 1936.

16. Hughes, A. and Grawoig, D., Statistics: A Foundation for Analysis, Addison-Wesley Publishing Company, 1971.

17. Ishikawa, H., Takaamoto, M., Shimizu, K., and Matsui, G., "The Effect of Beam Width on Ultrasonic Flowmeter Performance," Flowmeko'98 Conference, pp. 137-42, 1998.

18. Johari, H. and Durgin, W. W., "Direct Measurement of Circulation using Ultrasonic Methods," (Proceedings of the ASME Fluids Engineering Summer Meeting Conference Chair), Book No. H01075, pp 379-84, 1996.

19. Karal, F. C. , Jr and Keller, J. B., "Elastic Wave Propagation in Homogeneous and Inhomogeneous Media," The Journal of the Acoustical Society of America, Volume 31, Number 6, pp.694-705, June, 1959.

20. Keller, J. B.., "Reflection and Transmission of Sound by a Moving Medium," The Journal of the Acoustical Society of America, Volume 27, Number 6, pp. 1044-1047, November, 1955.

21. Kim, J., Moin, P., and Moser, R., "Turbulence Statistics in Fully Developed Channel Flow at Low Reynolds Number," Journal of Fluid Mechanics, Volume 177, pp. 133-166, 1987.

22. Kochnert, H., Melling, A., and Baumgartnert, M., "Optical Flow Field Investigations for Design Improvements of an Ultrasonic Gas Meter," Flow Measurement and Instrumentation, pp.133-40, 1996.

23. Kornhauser, E.T., "Ray Theory for Moving Fluids," The Journal of the Acoustical Society of America, Volume 25, Number 5, pp. 945-49, September, 1953.

24. Lanning, C. and Ehrhart, R. W., "Application of Acoustic Velocity Flowmeters",Journal AWWA, pp.102-105, February 1977.

25. Landau, L.D., Lifshitz, E.M., "Course of Theoretical Physics, Fluid Mechanics," Volume 6, 2nd Edition, 1973.

26. Laufer, J., “The Structure of Turbulence in Fully Developed Pipe Flow”, Report 1174- National Advisory Committee for Aeronautics,1952.

27. L'Esperance, A., Herzog, P., Diagel, G.A., Nicolas, J.R.,"Heuristic Model of Outdoor Sound Propagation Based on an Extension of the Geometrical Ray Theory in the Case of a Linear Sound Speed Profile", Applied Acoustics, Volume 37, pp.111-139, 1992.

28. Leslie, D.C., Developments int the Theory of Turbulence, Clarendon Press, Oxford, 1973

29. Lipkens, B. and Blackstock, D. T., "Model Experiment to Study Sonic Boom Propagation Through Turbulence. Part II. Effect of Turbulence Intensity and Propagation Distance Through Turbulence", Journal of Acoustical Society of America, Volume 104, No. 3, Part 1, pp.1301-1309, September 1998.

30. Loland, T., Saetran, L. R., Olsen, R., Gran, I. R., and Sakariassen, R., “Cavity Flow Correction for the Ultrasonic Flowmeter,” Flowmeko’98 Conference, pp.127-31, 1998.

31. Lowell Jr., F. C., "Acoustic Flowmeters For Pipeline Flowrate", Water Power and Dam Construction, pp.39-46, June 1979.

32. Lowell Jr., F. C., "The Design of Open Channel Acoustic Flowmeters for Specified Accuracy: Sources of Error and Calibration Test Results", National Bureau of Standards Special Publication 484, Proceedings of the Symposium on Flow in Open Channels and Closed Conduits held at NBS, (Gaithersburg,MD, Feb 23-25, 1977),pp.243-266, October 1977.

33. Lowell Jr., F. C., "Acoustic Flowmeters For Open Channels: Designing to Meet a Specified Accuracy", Flow Measurement of Fluids, pp.371-378, 1978.

34. Luntta, E. and Halttunen, J., "Neural Network Approach to Ultrasonic Flow Measurements," Flow Measurement and Instrumentation, 10, pp. 35-43, 1999.

35. Lynnworth, L.C., "Ultrasonic Measurements for Process Control", Academic Press, San Diego CA, 1989

36. Miller, R.B., and Wichern, D.W., Analysis of Variance, Regression and Time Series, Holt Rinehar, and Winston, 1977.

37. Mattingly, G. E., Private Communication

38. Mattingly, G. E. and Yeh, T. T., "NIST's Ultrasonic Technology Assessment Program to Improve Flow Measurements." NIST TN-1429, 2000.

39. Mintzer, D., "Wave Propagation in a Randomly Inhomogeneous Medium. I," The Journal of the Acoustical Society of America, Volume 25, Number 5, pp. 922-27, September, 1953.

40. Mintzer, D., "Wave Propagation in a Randomly Inhomogeneous Medium. II," The Journal of the Acoustical Society of America, Volume 25, Number 6, pp. 1107-11, November, 1953.

41. Mintzer, D., "Wave Propagation in a Randomly Inhomogeneous Medium. III," The Journal of the Acoustical Society of America, Volume 26, Number 2, pp. 186-90, March, 1954.

42. Montgomery, D. C., Design and Analysis of Experiments, 3rd edition, John Wiley & Sons, 1991.

43. Moser, R. D., Kim, J., Mansour, N. N., "Direct Numerical Simulation of Turbulent Channel Flow Up to Re = 590," Physics of Fluids, Volume 11, Number 4, pp.943-45, April, 1999.

44. Munk, W., "Acoustic Monitoring of Ocean Gyres," The Journal of Fluid Mechanics, Volume 173, pp.43-53, 1986.

45. Nakamura, S., Applied Methods with Software, Prentice Hall, 1991.

46. Nakamura, S., Computational Methods in Engineering and Science with Application to Fluid Dynamics and Nuclear Systems, John Wiley & Sons, New York, 1977.

47. Nystrom, J. B. and Padmanabhan, M., "Swirl Due to Combined Pipe Bends," International Conference on the Hydraulics of Pumping Stations Manchester, England 17-19 September, 1985, Paper 2, pp. 9-24,1985.

48. Paik, J. S. , Kim, C. H., and Lee, D. K., "Effects of Variation of Pipe Velocity Profile on the Ultrasonic Cross Correlation Flowmeters."

49. Park, K., Paik, J. S., Choi, H., Choi, Y., and Tyan, K.S., "Error Verification of the Multi-Path Ultrasonic Flowmeter," Flowmeko'98 Conference, pp. 133-36, 1998.

50. Pedersen, N., Lynnworth, L., "Nonintrusive Dynamic Flowmeter", Ultrasonics Symposium Proceedings, IEEE, 1973.

51. Potter, M. C, Mechanics of Fluids, Prentice Hall, Englewood Cliffs, NJ, 1991.

52. Ralston, A., A First Course in Numerical Analysis, McGrawHill Book Company, New York, 1965.

53. Rayleigh, J. W., The Theory of Sound, Dover Press 2nd edition, New York, 1945.

54. Raspet, R., L'Esperance, A., Daigle, G. A., "The Effect of Realsistic Ground Impedance on the Accuracy of Ray Tracing", Journal of Acoustical Society of America, 97, pp.154-158, January 1995.

55. Raspet, R. and Wu, W., "Calculation of Average Turbulence Effects on Sound Propagation Based on the Fast Field Program Formulation", Journal of Acoustical Society of America, 97, pp.147-153, January 1995.

56. Schaefer, J. W., Eskinazi, S., "An Analysis of the Vortex Street Generated in a Viscous Fluid," Journal of Fluid Mechanics, Vol. 6 [2], pp. 241-60, 1959.

57. Schlicting,H., Boundary Layer Theory, McGrawHill Book Company, New York, 1965.

58. Schuster, J. C., "Measuring Water Velocity by Ultrasonic Flowmeter", Journal of the Hydraulics Division, pp.1503-1517, December, 1975.

59. Schmit, D. W., Tilman, P. M., "Experimental Study of Sound-Wave Phase Fluctuations Caused by Turbulent Wakes", Journal of the Acoustical Society of America, Volume 47, Number 5 (part 2), pp.1310-1324, 1970.

60. Sielschott, H., "Measurement of Horizontal Flow in a Large Scale Furnace Using Acoustic Vector Tomography," Flow Measurement and Instrumentation, Volume 8, pp.191-97, 1997.

61. Shen, C. and Lemmin, U., "A New Method for Probing the Turbulence Scalar Spectrum by Ultrasonic Sonar Scanning," Experiments in Fluids, 24, pp. 90-92, 1998.

62. Skwarek, V. and Hans, V., "Influence of Disturbances on Correlative Ultrasound-Flow-Measurement," Flowmeko'98 Conference, pp.343-46, 1998.

63. Sofialidis, D. and Prinos, P., "Wall Suction Effects on the Structure of Fully Developed Turbulent Pipe Flow," Transactions of the ASME Journal of Fluids Engineering, Volume 118, pp. 33-39, March, 1996.

64. Streeter, V. L., Fluid Mechanics, 2nd edition, McGraw-Hill, 1958.

65. Suzuki, H., Nakaborik H., Kitajima, A., "New Applications of Ultrasonic Flowmeters", Conference on Fluid Flow Measurement in the Mid 1970's, pp.162-173, April, 1975.

66. Tennekes, H., Lumley,J.L., A First Course in Turbulence, The MIT Press, 1999.

67. Vassallo, P.F., "An Experimental Study of High Reynolds Number Flow in a Multiple Bend Piping System."

68. Weber, F. J., Jr., 1994, "Ultrasonic Circulation-Meter For Determining the Magnitude of Circulation about a Rapidly Pitching Airfoil," M. S. Thesis, Worcester Polytechnic Institute, Worcester, MA.

69. Wenzel, A., Keller, J., "Propagation of Acoustic Waves in a Turbulent Medium" , The Journal of the Acoustical Society of America, Vol 50, Number 3, 1971.

70. White, F. M., Viscous Fluid Flow, McGraw Hill Companies, 1974

71. White, F. M., Fluid Mechanics, McGraw Hill Companies, 1999.

72. Worch, A., "A Clamp-On Ultrasonic Cross-Correlation Flowmeter for Two-Phase Flow," Flowmeko'98 Conference, pp. 121-26, 1998.

73. Yeh, T. T. and Mattingly, G. E., "Ultrasonic Flow Measurement Technology: Prospects for Transfer and Primary Standards," Flowmeko'98 Conference, pp. 161-66, 1998.

74. Yeh, T., Mattingly, G., "Computer Simulations of Ultrasonic Flowmeter Performance in Ideal and Non-ideal Pipe Flows", FEDSM97-3012, 1997 ASME Fluids Engineering Division Summer Meeting, 1997.

75. Yeh, T.T., and Mattingly, G.E., "Ultrasonic Technology Prospects for Improving Flow Measurements and Standards," Proceedings of the 4th International Symposium on Fluid Flow Measurement, Denver, CO: NAFFMC 1999 and Proceedings FLOMEKO, 2000.